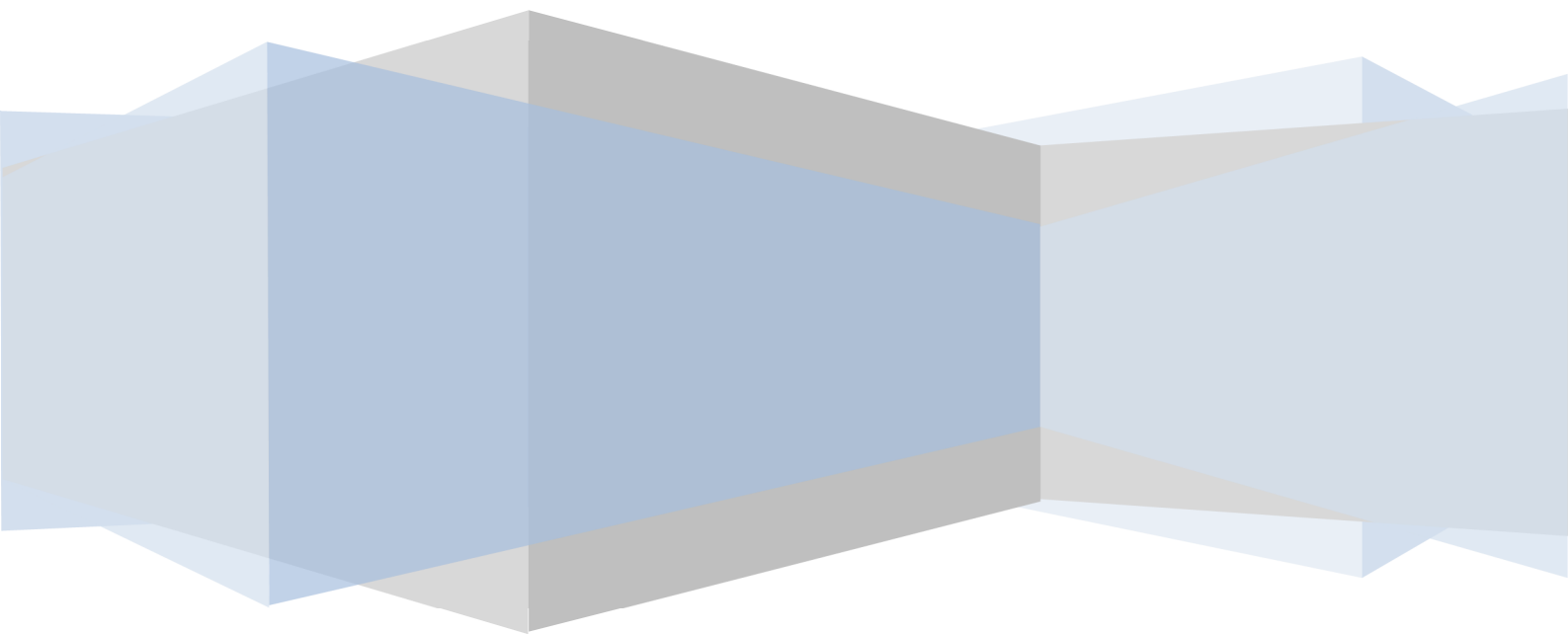


MSc Thesis

Modular cross-laminated timber buildings

Richard Gijzen



Author

R.P.T. Gijzen
richardgijzen@gmail.com
+31 6 12338102
4021355

Graduation committee

Prof.dr.ir. J.W.G. van de Kuilen	Delft University of Technology, Chairman
Dr.ir. G.J.P. Ravenshorst	Delft University of Technology
Dr.ir. M.A.N. Hendriks	Delft University of Technology
Ir. H.M.C. Kuijpers	Pieters Bouwtechniek Amsterdam

*“Of course there is no formula for success, except perhaps
an unconditional acceptance of life, and what it brings”*

- Arthur Rubinstein -

Preface and acknowledgements

This report presents the results of my master thesis research project into modular cross-laminated timber buildings. The research project concludes the Master of Science program of Structural Engineering with specialization Steel, Timber and Composite Structures at the faculty of Civil Engineering and Geosciences at Delft University of Technology.

First and foremost, I would like to express my gratitude to the members of my graduation committee: Prof.dr.ir. J.W.G. van de Kuilen, Dr.ir. G.J.P. Ravenshorst, Dr.ir. M.A.N. Hendriks and ir. H.M.C. Kuijpers. Thank you for sharing the experience and knowledge in assisting me to conduct my research.

A special thanks to Hubert Kuijpers in providing me a professional environment with all the resources at Pieters Bouwtechniek Amsterdam. I will never forget your positivity and enthusiasm about timber buildings and the times you walked up to me and cheered me up. Thank you for allowing me to have such great design of the cross-laminated timber modules as a basis for my graduation project.

I would like to thank my parents Wim Gijzen and Ingrid Gijzen - van Warmerdam, for always believing in me and supporting me in everything I do.

Last but not least, my beloved girlfriend Emily Lannon, thank you so much for your love and support, even when an ocean in between, you were right next to me. Thank you for your patience and encouragement when times were tough.

Richard Gijzen

Amsterdam, February 2017

Summary

Multi-storey timber buildings are becoming internationally more and more common. The thriving forces behind this trend involve the sustainable aspects of the material and the rapid development of innovative engineered timber elements. An example of an engineered timber element are cross-laminated timber (CLT) panels. CLT panels consist of cross-wise glued layers of timber to obtain panels that can be used as wall and floor elements.

Another innovative trend is the modular construction method. This method is based on the prefabrication of modules as building compartments, which can be stacked on-site to form a cellular building type. Reasons for this trend, are the increased building speed and the benefits of repetitive fabrication in a controlled environment.

The first application of a modular multi-storey timber building is Hotel Jakarta in Amsterdam, for which construction started in 2016. This building was the reason for this master thesis, in which the following question was formulated. What is the structural behaviour of a cross-laminated timber module system, how can it be designed and is it possible to construct a 'self-supporting' system of modules for a tall timber building?

In order to answer the research question, a literature research has been done to investigate the aspects involved with tall timber buildings, modular construction, the material cross-laminated timber and the connections. Then a universally applicable module with a concrete floor slab and CLT side walls, stabilization wall and ceiling elements was specified. A design case of 8 modules in height and 8 modules in width, placed onto a concrete podium structure, has been investigated.

To examine the structural behaviour of the modular assembly in terms of deformations and force distribution a 3D finite element model was made. Then, resistance verifications have been done to find the critical limits for this design case.

For this design case it was proven that a multi-storey modular cross-laminated timber building composition is a structurally viable solution. The limiting factors found for maximum building height and minimum slenderness are the fire situation in relation to buckling of a side wall, the connection strength and the maximum deformation due to rotation of a stabilization wall involving bending of the floor and ceiling element.

Table of contents

Preface and acknowledgements.....	3
Summary	4
List of figures	9
List of tables	11
1 Introduction	12
1.1 Background information	12
1.1.1 Interest in timber buildings	12
1.1.2 Hotel Jakarta	12
1.1.3 Cross laminated timber (CLT)	13
1.2 Specification research.....	14
1.2.1 Problem definition	14
1.2.2 Goals	14
1.2.3 Research questions.....	15
1.3 Work approach.....	16
1.3.1 Literature research	16
1.3.2 Structural design – connections	16
1.4 Finite element modelling.....	18
1.4.1 Module	18
1.4.2 Stacking	19
2 Tall timber buildings.....	20
2.1 Why timber?	20
2.1.1 Sustainability and the forest.....	20
2.1.2 Structural aspects	21
2.2 Types of timber construction systems.....	22
2.2.1 Timber framing construction.....	22
2.2.2 Post and beam construction.....	23
2.2.3 Panelised construction.....	23
2.2.4 Hybrid construction	23
2.2.5 Review on current tall timber and cross-laminated timber buildings	24
2.3 Fire safety aspects	28
2.3.1 Introduction.....	28
2.3.2 Reaction to fire	29
2.3.3 Fire resistance.....	29

2.3.4	Legislation	30
2.3.5	Detection and suppression.....	31
2.3.6	Fire safety engineering.....	31
3	Modular construction.....	32
3.1	Why modular?.....	32
3.1.1	Speed of construction	33
3.1.2	Improved quality and safety.....	33
3.1.3	Sustainability	33
3.2	Types and applications of modular construction	35
3.3	Structural aspects	36
3.3.1	Inaccuracies and imperfections.....	36
3.3.2	Second-order effects.....	38
3.3.3	Robustness	39
3.3.4	Lifting and transportation	41
4	Cross-laminated timber.....	42
4.1	Introduction	42
4.2	Product	42
4.3	Chances for multi-storey buildings from cross-laminated timber	42
4.3.1	Benefits of CLT	43
4.3.2	Drawbacks	43
4.3.3	Global production of CLT.....	44
4.4	Regulations and guidelines	44
4.5	Material properties.....	45
4.6	Cross-sectional values.....	46
4.6.1	Net cross-sectional values.....	46
4.6.2	Effective cross-sectional values	47
4.7	Ultimate limit state verifications.....	49
4.7.1	Loading in plane.....	51
4.7.2	Loading out of plane	54
4.7.3	Buckling.....	56
4.8	Serviceability limit state.....	57
4.8.1	Stiffness and deformation.....	57
4.8.2	Time dependent deformation	58
4.9	Fire Safety	59

4.9.1	Charring.....	59
4.9.2	Delamination	59
4.9.3	Verification	60
4.10	Connections	61
4.10.1	Glued-in rods	62
4.10.2	Screws in CLT	67
5	Structural design	72
5.1	Introduction	72
5.2	General assumptions	72
5.3	Module.....	73
5.3.1	Dimensions	73
5.3.2	Detailing	73
5.4	Modular building structure	76
5.4.1	Modular assembly	76
5.4.2	Inter-modular detailing.....	77
6	Loads	79
6.1	Load cases	79
6.1.1	Permanent loads.....	79
6.1.2	Imposed loads.....	80
6.1.3	Wind load	81
6.2	Load combinations	86
6.2.1	Ultimate limit state	86
6.2.2	Serviceability limit state	86
6.2.3	Combination factors	86
7	Verifications.....	88
7.1	SLS – FEM modelling.....	88
7.1.1	Introduction.....	88
7.1.2	Element discretization	88
7.1.3	Loads and boundary conditions.....	96
7.1.4	Finite element analysis results	98
7.1.5	Conclusions FEM.....	105
7.1.6	Discussion.....	106
7.2	Second order effects.....	107
7.3	ULS verifications	109

7.3.1	Parallel wind direction – stabilization wall.....	109
7.3.2	Perpendicular wind direction – side wall	113
8	Conclusions and recommendations.....	119
	Recommendations	123
9	References	124

List of figures

Figure 1 - Architectural design of Hotel Jakarta, left: exterior, right: natural interior (Search 2014) ...	12
Figure 2 - 5-layered cross-laminated timber element (A. Thiel 2010)	13
Figure 3 - Modular CLT residential unit (Thompson 2013)	13
Figure 4 - Glued-in rod in glued-laminated timber (Gonzales, Tannert and Vallee 2016)	16
Figure 5 - X-RAD connection (Rothoblaas 2014)	17
Figure 6 - Traditional CLT connectors	18
Figure 7 - Work approach diagram	19
Figure 8 - The timber life cycle (Tropical Timber 2011)	20
Figure 9 - Savings of carbon-dioxide by using wood as a building material (Frühwald 2002)	21
Figure 10 - Left: Platform type, right: Balloon type timber framing (American Wood Council 2001)...	22
Figure 11 - Murray Grove London (Trada 2009)	24
Figure 12 - Limnologen block with weather protection system (Serrano 2009)	24
Figure 13 - Life Cycle Tower, prefabricated floor slabs and facade elements (Will+Perkins 2014)	25
Figure 14 - Forte building (Will+Perkins 2014)	25
Figure 15 - Treet: Structural model without modules (R.B. Abrahamsen 2014)	26
Figure 16 - HoHo Tower Vienna (Moneo 2015)	27
Figure 17 - Principles for fire safety considerations	28
Figure 18 - Stages of a typical fire development (A. Buchanan 2000)	28
Figure 19 - Nominal and parametrical temperature-fire curves (Ravenshorst 2014)	29
Figure 20 - Comparison of construction speed (Lawson, Ogden and Goodier 2014)	32
Figure 21 - Modular building with a podium structure (Lawson, Ogden and Goodier 2014)	35
Figure 22 - Permitted maximum dimensional tolerances (Lawson and Richards 2010)	36
Figure 23 - Eccentric loadings (Lawson and Richards 2010)	36
Figure 24 - Displacement components (adjusted from Hoenderkamp 2002)	38
Figure 25 - Load distribution and tying action in modules for localization of damage route (Lawson, Byfield, et al. 2008)	40
Figure 26 - Lifting of module by main beam and crossbeams (M. Lawson 2014)	41
Figure 27 - 5-layered Cross-Laminated timber element (Karacabeyli and Douglas 2013)	42
Figure 28 - Global production of CLT (Espinoza, et al. 2016)	43
Figure 29 - CLT cross-section with designations and out-of-plane stresses (Wallner-Novak, Koppelhuber and Pock 2014)	46
Figure 30 - Cross section of CLT element with designations (KLH Massivholz GmbH 2012)	48
Figure 31 - Relation between number of boards parallel and system coefficient	50
Figure 32 - Failure modes I, II and III for CLT loaded in in-plane shear (Flaig and Blaß 2013)	52
Figure 33 - Specimen failed net-shear (left) and gross-shear (right) (Brandner, Dietsch, et al. 2015) ..	53
Figure 34 - Point supported CLT panels (left) and line supported CLT panels (right) (Brandner and Schickhofer 2014)	54
Figure 35 - Mechanism I: Shearing deformation (Bogensperger, Moosbrugger and Silly 2010)	57
Figure 36 - Mechanism II: Torsional deformation (Bogensperger, Moosbrugger and Silly 2010)	57
Figure 37 - RVE and RVSE elements for CLT elements (Bogensperger, Moosbrugger and Silly 2010) ..	57
Figure 38 - Residual cross section, char layer and zero-strength layer (SP 2010)	59
Figure 39 - Load slip curves for connections in timber-concrete composite floors (Dias 2005)	61
Figure 40 - Determination of K_{ser} (EN 26891)	61

Figure 41 - Gluing the rods (Steiger, et al. 2015)	62
Figure 42 - Parameters influencing a Glued-in rod connection.....	63
Figure 43 - Failure mechanisms for a single glued-in rod (Steiger, et al. 2015)	63
Figure 44 - Springs representing the Glued-in rod connection	66
Figure 45 - designation for screw positions (Ringhofer, Brandner and Flatscher, et al. 2015)	67
Figure 46 - Tested screwed connection configurations with axial- and lateral load (Flatscher, Bratulic and Schickhofer 2014)	68
Figure 47 - Minimum spacing, end and edge distances (MERK Timber GmbH 2013)	70
Figure 48 - Determination of the effective cross section in fire for timber-concrete composites (Frangi, Knobloch and Fontana 2010).....	71
Figure 49 - Strength reduction of screws in case of fire (Frangi, Knobloch and Fontana 2010)	71
Figure 50 - Representation and dimensions of module with concrete (left) and CLT (right) floor	73
Figure 51 - Transverse cross-section of module (concrete floor)	74
Figure 52 - Cross section wall-floor concrete (left) and CLT (right)	75
Figure 53 - Cross section wall-ceiling-stabilization wall	75
Figure 54 - Modular building structure (8 x 8)	76
Figure 55 - Concrete podium structure.....	76
Figure 56 - Visualisation of Inter-modular connections.....	77
Figure 57 - Sylomer elastomeric bearing strips.....	78
Figure 58 - Peak velocity pressure profiles over building height (EN 1991-1-4)	82
Figure 59 - Wind directions applied to modules	84
Figure 60 - Plane stress element	88
Figure 61 - Plate element	88
Figure 62 - Shell element	88
Figure 63 - CLT side wall with arch effect.....	91
Figure 64 - Loads on concrete floor strip	93
Figure 65 - Graphical representation of a line-to-line interface element.....	94
Figure 66 - Representation of modelled connections.....	95
Figure 67 - Graphical representation of load and boundary conditions application.....	97
Figure 68 - Max horizontal parallel y- (left) and perpendicular x-direction (right) displacements	98
Figure 69 - Deformation contributions of stabilizing wall.....	100
Figure 70 - Horizontal deformation of lower modules	101
Figure 71 - Vertical normal stresses in side walls	102
Figure 72 - Axial force in line-to-line connections	103
Figure 73 - Shear stresses in side walls, podium beam stiffness infinite (left) and effective (right) ...	104
Figure 74 – Hor. Normal stresses in side walls, infinite- (left) and effective (right) podium stiffness.	104
Figure 75 - Shear deformation profile	107
Figure 76 - ULS checks for stabilization wall	109
Figure 77 - Lateral failure mechanisms for glued-in rod.....	112
Figure 78 - Maximum number of modules in height (n) for a given modular width (m).....	112
Figure 79 - Design loads for bottom module side wall	113
Figure 80 - Unity check for buckling of side wall with increasing building height.....	118

List of tables

Table 1- Strength to weight ratio of building materials.....	21
Table 2 - Overview on tall timber projects.....	24
Table 3 - Fire resistance requirements for the main load bearing structure	30
Table 4 - Sustainability benefits for off-site manufacture (Lawson, Ogden and Goodier 2014).....	34
Table 5 - Displacement components for second-order considerations.....	38
Table 6 - Categorisation in consequence classes and provisions	39
Table 7 - Indication dynamic acceleration factors f.....	41
Table 8 - Main European suppliers of cross-laminated timber (Porteous and Kermani 2013).....	44
Table 9 - Density material properties of CLT	45
Table 10 - Strength properties for CLT	45
Table 11 - Stiffness properties for CLT	45
Table 12 - Modification factor for CLT	49
Table 13 - Definition of load duration classes	49
Table 14 - CLT in-plane strength verifications figures from (Wallner-Novak 2014)	51
Table 15 - CLT out-of-plane compression verification figure from (Wallner-Novak 2014)	55
Table 16 - CLT out-of-plane bending and shear verifications figures from (Wallner-Novak 2014)	55
Table 17 - Deformation coefficients for CLT.....	58
Table 18 - Designations of minimum spacing, end and edge distances for glued-in rods (DIN 1052) ..	65
Table 19 - Minimum spacing, end and edge distances for glued-in rods	65
Table 20 - Performance parameters for glued-in rod connections in CLT (Koets 2012).....	66
Table 21 - Test results of screwed connections (Flatscher, Bratulic and Schickhofer 2014)	68
Table 22 - $k_{sys,k}$ values in dependence of N (Ringhofer, Brandner and Schickhofer 2013).....	69
Table 23 - Minimum spacing, end and edge distances of screws in CLT (Uibel and Blaß 2007)	70
Table 24 - Effective number of screws for different configurations.....	70
Table 25 - Modification factor for screwed connection strength in fire.....	71
Table 26 - Input of building dimensions for wind load calculations	81
Table 27 - Method to calculate the peak velocity pressure	82
Table 28 - Method to calculate the structural factor	83
Table 29 - External pressure coefficients for facades (EN 1991-1-4 Table NB.6 - 7.1)	83
Table 30 - Horizontal wind forces perpendicular on the building ($n \times m = 8 \times 8$).....	84
Table 31 - Horizontal wind forces parallel on the building ($n \times m = 8 \times 8$).....	85
Table 32 - Load combinations for ultimate limit state.....	86
Table 33 - Load combinations for serviceability limit state	86
Table 34 - Corresponding ψ factors for buildings.....	86
Table 35 - Load combinations for the ultimate limit state.....	87
Table 36 - Load combinations for the serviceability limit state	87
Table 37 - Load combination for the accidental fire limit state	87
Table 38 - Real mean stiffness properties of used CLT panels in N/mm^2	89
Table 39 - Modelling input shell elements.....	93
Table 40 - Modelling input line-to-line link elements.....	95
Table 41 - Calculation of gamma factors.....	116
Table 42 - Calculation of instability factor k_c	117
Table 43 - Verification of wall against buckling for $n=8$	118

1 Introduction

1.1 Background information

1.1.1 Interest in timber buildings

When I started my study at the Delft University of Technology, I found out that the courses I liked most were mainly about timber structures. At the beginning of the master programme I joined a study trip to London, where we visited several impressive timber buildings under construction. I was surprised by the appearance of the timber structures and the fact that timber construction is being used more frequently in a leading city like London.

At first I had some doubts about graduating with a focus on a timber project. I believed that being specialised in timber structures, might imply some restrictions for a future career as a structural engineer. After I saw the possibilities and the potential of the material, I realised that timber might be even more interesting than (for example) steel, because of its complex properties. In my opinion, this can be even more beneficial for a structural engineer in practice.

1.1.2 Hotel Jakarta

The inspiration for this master thesis is 'hotel Jakarta'. Construction of this hotel started in 2016 and the structural engineering is done at Pieters Bouwtechniek. The original architectural design was based on a complete bearing structure of timber. Mainly due to practical issues, the decision was made to build a substructure, as a sort of table structure from concrete and a superstructure of CLT modules. The CLT modules are the hotel rooms which will form building blocks on top of the concrete table structure. The hotel consists of a part which will be 9 storeys and a part of 5 storeys.

For the modules it was decided that the floor should be made out of concrete and the walls and ceilings out of cross-laminated timber. The idea behind the architectural design is to make the timber as visible as possible to highlight its natural character. These modules will be completely prefabricated, with all technical contents included. The surface of the cross-laminated timber is part of the final finishing in the hotel rooms.

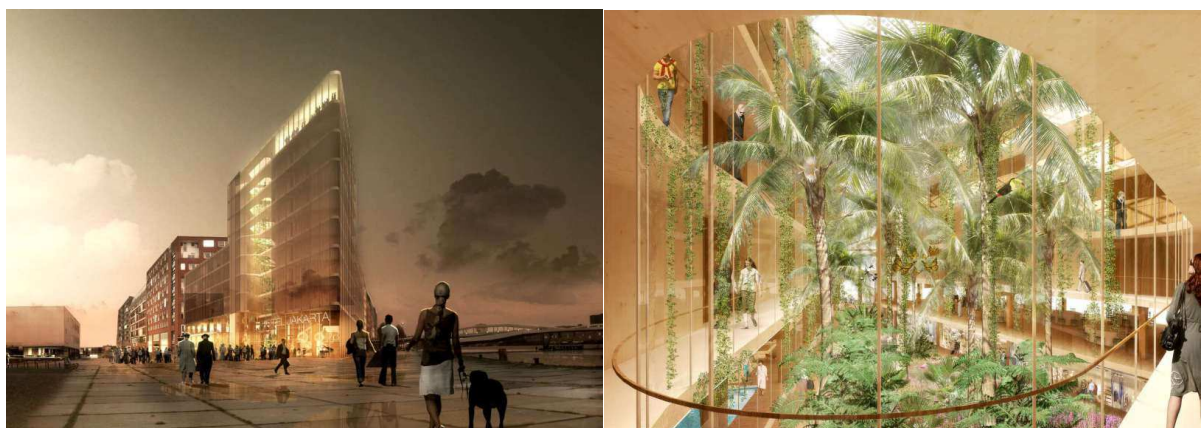


Figure 1 - Architectural design of Hotel Jakarta, left: exterior, right: natural interior (Search 2014)

1.1.3 Cross laminated timber (CLT)

While attending lectures on timber structures, I noticed that cross laminated timber can offer a lot of new possibilities for buildings. Especially the possibility of adequate force transfer in more than one direction to achieve diaphragm action is advantageous for a new timber building element. For low-rise buildings, timber frame method has proven to be very sufficient. For high-rise buildings CLT has a lot of potential because the solid panels are able to transfer bigger forces. CLT panels are made out of cross-wise glued lamellas with an uneven number of layers. The thickness of each layer ranges between 6 and 45mm.

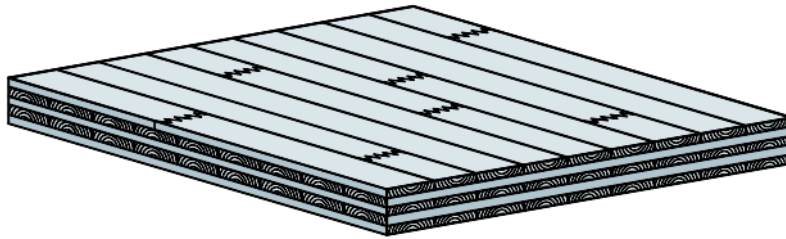


Figure 2 - 5-layered cross-laminated timber element (A. Thiel 2010)

The ideal building configuration when using CLT elements, would be a cell-based type of building. When there are a lot of large open spaces, beam elements would be more suitable to enable large spans. This is why it's interesting to look for the potential to use CLT modules for high-rise buildings. Next to this, the modular type of building is a trend due to its fast building speed and the benefits of constructing a part of a building, with all of its final installations, in an assembly facility where all external conditions can be controlled.



Figure 3 - Modular CLT residential unit (Thompson 2013)

The concept of modular CLT buildings is a very promising building solution. The figure above shows a conceptual case study.

1.2 Specification research

In order to set the framework for this thesis, this chapter will specify the research as initiated at the start phase. The problem will be defined and the research questions will be formulated and then used to strive towards the goal as specified below.

1.2.1 Problem definition

Hotel Jakarta will be the highest timber building in the Netherlands. Both common sense as well as building regulations require careful design for such a large timber building. The lack of experience and practical issues like fire safety, acoustics and dynamic behaviour in wind conditions. Apart from the issues of timber buildings in general, cross laminated timber and modular construction are relatively new building solutions.

When designing a timber building, special attention is always necessary for the connections. Not only the structural behaviour but also aesthetics are important when constructing hotel rooms with a visible and transparent CLT character. To connect CLT elements, glued-in-rods can possibly be a solution to this aspect.

In general, for timber buildings, the displacements and the connections are the governing design criteria. When calculating the horizontal displacements in the serviceability limit state, the extreme wind loads can cause a change from compression to tension in the vertical connection. This phenomenon is typical for timber structures because of the relatively low weight of a timber structure. However this makes it a challenge to design a good connection. Another challenge is the fact that timber is weak in the direction perpendicular to the grain.

1.2.2 Goals

The main goal of this thesis is divided in the following sub-goals.

1.2.2.1 Connections

For the connections, the goal is to investigate different connection types and to find a way which enables the modules to act as a system for the overall stability.

1.2.2.2 Stacking

Using the obtained strength and stiffness properties of the modules, the next goal is to find a way to connect the individual modules to each other, bearing in mind the practicalities involving construction execution. When stacked, the investigation into the behaviour of the modular building. Verification of horizontal stability and prevention of tension between the modules.

1.2.2.3 Modelling

In order to be able to investigate the structural behaviour of a modular CLT timber building, the goal is to obtain a linear 3D finite element model. The model has to be well suited to verify against maximum horizontal displacements.

1.2.2.4 Main goal

The main goal of this thesis is to investigate the aspects and limits for stacking CLT modules to prove the structural feasibility of an innovative multi-storey building solution that has a multi-purpose applicability.

1.2.3 Research questions

To reach the goal and provide a solution to the problem, the following research questions are formulated.

1.2.3.1 Main question

- What is the structural behaviour of a cross-laminated timber module system, how can it be designed and is it possible to construct a 'self-supporting' system of modules for a tall timber building?

1.2.3.2 Sub questions

- Which structural and practical aspects play a role in multi-storey modular buildings made from timber?
- What are the properties and calculation methods of cross-laminated timber elements?
- Which connection types are suitable for an application in the CLT modules and how can the modules be connected to each other?
 - What practical issues are of importance for the connections?
 - What is the strength and stiffness of the connections when they are applied in CLT?
- How can a universally applicable cross-laminated timber module be designed for which the stability can be guaranteed in order to ensure a self-supporting system of modules?
- What are the forces that will be exerted on a modular building configuration?
- What are the properties and what is a suitable modelling design to set up a useful finite element model of a building configuration consisting of CLT modules?
- What is the force distribution in a modular CLT building and what are the deformations that result from wind forces?
- What is the resistance capacity of CLT modules and which maximum height and minimum slenderness ratio can be achieved for the designed modules?

1.3 Work approach

To answer the research questions, the following work approach will be carried out. This approach will mainly follow the research questions set out in the previous chapter.

The research will be focused on the configuration and the structural behaviour of a cross laminated timber modules. First a literature research will be carried out, then the structural design of the modules will be specified and modelled in a finite element model. Finally the total system of stacked modules will be analysed.

1.3.1 Literature research

To gain information the current state of development in (modular) tall timber buildings and the material cross laminated timber a literature research will be carried out. The regulations for tall timber buildings will be investigated. The fire safety regulations and sprinkler possibilities will be clarified. Also an investigation into connection types will be performed in order to find information on failure mechanisms and on the strength and stiffness properties.

1.3.2 Structural design – connections

In this master thesis different connection types will be investigated. The strength, stiffness, aesthetical and practical properties of the connections will determine the optimal structural and practical behaviour of the modules. Also the influence on fire safety of the connection type will be determined. The following three different connection types will be examined.

1.3.2.1 Glued-in rods

Currently glued-in rods are often used for renovating and-/or strengthening existing timber structures. Also for application in tall timber buildings glued-in-rods seem to be a promising solution, because the high bearing capacity and the benefits of being able to coop with load variations. The idea is to develop an analogy between glued-in rods in CLT and common used connections to connect prefabricated concrete elements.

In order to find out the properties of a glued-in-rod joint the different failure mechanisms shown below have to be investigated. The influence factors will be deduced from literature, because the procedure is no longer in the Eurocode, let alone the influence when using this joint in CLT elements.



Figure 4 - Glued-in rod in glued-laminated timber (Gonzales, Tannert and Vallee 2016)

1.3.2.2 X-RAD

The company Rothoblaas from Italy is a manufacturer of timber connections. At the moment they are introducing a new CLT connection which is called the X-Rad connection.

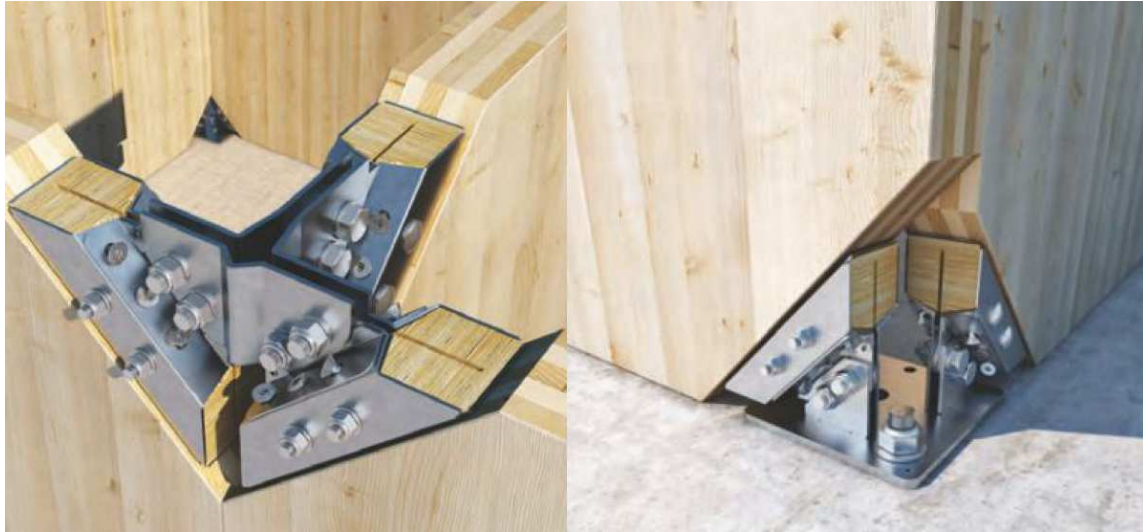


Figure 5 - X-RAD connection (Rothoblaas 2014)

This innovative connection consists of pre-mounted boxes which are screwed on the CLT element. These boxes are connected to each other by means of metal plates and bolts.

Benefits:

- Ductile behaviour
- Fast assembly
- Minimization of production errors
- High strength and stiffness properties

The metal boxes are composed of a metal casing that contains a hardwood (Beech) internal element that allows accurate screwing thanks to the predrilled holes in the hardwood. The box distributes the forces on the contact surface of the CLT element. The ductile behaviour is guaranteed by the metal plates with the bolts, because that is where the governing failure mechanism occurs.

Note: this connection type was originally part of the work approach, but has not been used or further elaborated in the scope of this thesis.

1.3.2.3 Traditional CLT connections

The traditional way of connecting CLT elements is by using hold-down anchors, shear connectors and screws or nails as shown below.

These connectors are advantageous because of their simplicity, but the disadvantage is primarily because of visibility issues. Nevertheless, at places where the visibility of connections isn't that important, traditional CLT connections can be an option. That's why these connections are incorporated in the work approach.

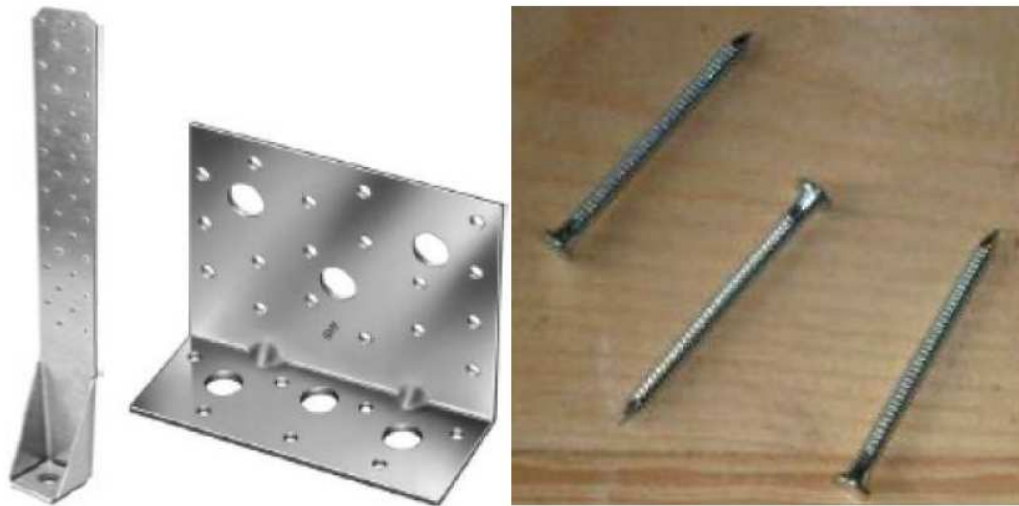


Figure 6 - Traditional CLT connectors

1.4 Finite element modelling

1.4.1 Module

The program that's being used at Pieters Bouwtechniek is AxisVM. The approach to design the finite element model will be discussed here.

Once the properties are investigated, choices must be made for the most appropriate way to model the connection with the right stiffness and possibility for adjusting. Before modelling the modules, preliminary designs of the modules with a reasonable amount of connections, will form a starting point. Strength and stiffness calculations will be made as hand calculations, to be able to verify the finite element model. This will be done for modules with concrete floors. Once the preliminary design is finished, the module will be translated to a finite element model. Choices will be made to select the element types, which will represent the floors, walls and ceilings of the modules. The finite element mesh will be chosen, which suits the analysis for a single module. After the loads and constraints are applied, a first analysis can be made.

1.4.2 Stacking

After the alternatives of modules are modelled the obtained structural properties can be used to stack the modules like container elements. The inter-modular connections will be specified. A model will be produced in which the building blocks as modules are simplified.

The possibility of progressive collapse can be investigated by removing one module out of the building model. Also the horizontal displacements are checked to see whether the stacked modules can provide their own stability in both directions. If the horizontal stability will cause problems, it can be interesting to see what happens when the stability in the transverse direction of the module is replaced by a beech wall. In this way iterations can be made between the modelling of the module and the stacking of the modules.

Investigations can be done to obtain force distributions for modular buildings with CLT modules with concrete floors. A qualitative comparison will be made to show the difference for the properties concerning acoustics and vibrations.

Several basic building configurations will be investigated to optimize the building and the model for the most preferable force distribution. Eventually, the relation between the maximum height of the building compared to the required width of the building can be determined, and a slenderness ratio can be derived.

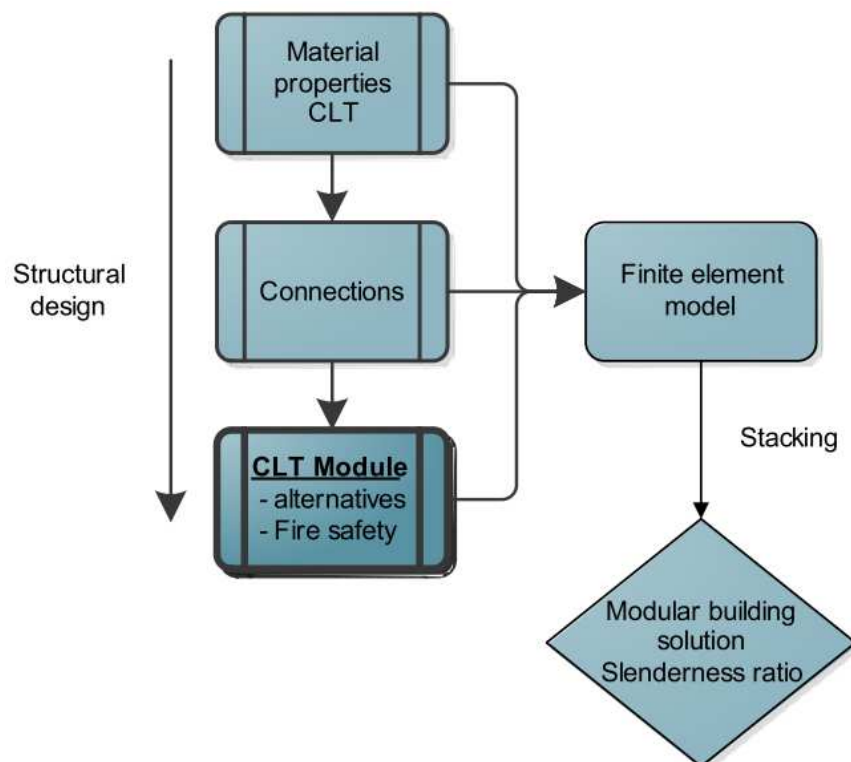


Figure 7 - Work approach diagram

2 Tall timber buildings

In this chapter, emphasis is made on (tall) timber structures in general. The main reasons for the decision makers to choose for a timber structure, the different types of timber building method, several reference projects and the fire safety aspects that characterize tall timber buildings will be considered. Structural (fire) design aspects are dealt with in chapter 4, which relates these aspects to the building method using CLT.

Especially in the last ten years timber is gaining more and more interest for an application in construction of tall buildings. Next to the favourable sustainability effects concerning timber construction, new engineered (composite) wood products and systems are reasons for this trend.

2.1 Why timber?

2.1.1 Sustainability and the forest

The use of wood instead of conventional building materials like masonry, concrete or steel, for structural purposes results in a reduction of the environmental impact. The following aspects are of importance concerning sustainability considerations.

- Life cycle

The timber that is used for structural purposes is produced using rapidly growing and young trees, from sustainably managed forests. These trees consume water, sunlight and carbon-dioxide. Well managed forests can produce structural timber every 10 or 12 years (Brinck 2013). Also there is a high degree of recycling and reuse of timber residue and timber from demolition of buildings. When the timber cannot be recycled it is still very valuable when it's used to produce biomass energy.

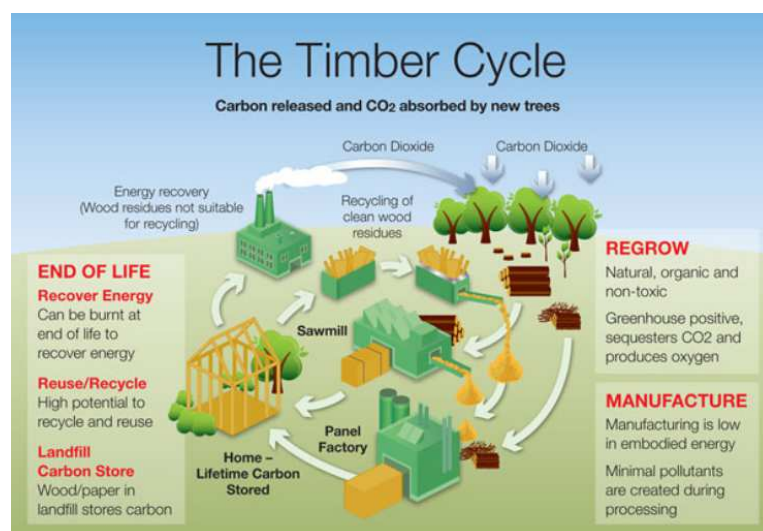


Figure 8 - The timber life cycle (Tropical Timber 2011)

- Embodied carbon value

First of all, the forests sequester carbon-dioxide from the atmosphere by means of photosynthesis. In 1 m³ of harvested wood, 0,9 ton of carbon-dioxide is stored. Apart from the carbon storage, wood usage contributes to a reduction in carbon-dioxide emissions through so-called substitution effects.

The substitution effect is based on fuel substitution and material substitution and results in a reduction of 1,1 ton of carbon-dioxide compared to conventional building materials. Fuel substitution considers the positive effect of using wood instead of fossil fuels to produce energy. Material substitution considers the emission-savings effect from using wood instead of non-wood products. The savings in emission are the result of the fact that non-wood products require more energy for their production and disposal (Knauf, et al. 2015). Combining these effects, results in a total saving of 2 ton CO₂, for each cubic metre of wood.

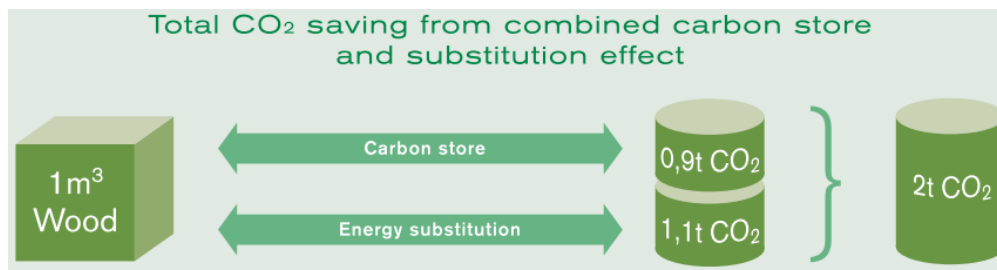


Figure 9 - Savings of carbon-dioxide by using wood as a building material (Frühwald 2002)

A common misconception of mass timber construction type can be that one might think that it is not good for the environment since many trees have to be cut down to obtain the building material (Spickler 2014). In fact, according to the sustainable forestry agency in North America, less than 2% of the trees in the U.S. has been cut down during the last 50 years, while the net growth of trees was 3%. Additionally, if these trees are not used for construction or other purposes, they decay in the forest, which means they emit carbon-dioxide back into the atmosphere.

- Thermal performance

The cellular structure of wood contains air pockets, which makes timber a naturally insulating material. Next to that, the contact-temperature of timber is relatively high.

2.1.2 Structural aspects

The most important advantage of timber, in terms of structural performance, has to be the low weight to strength ratio of timber compares to e.g. steel and reinforced concrete. This implies that timber has higher structural efficiency, because of the carried load per unit weight.

Material	Bending strength f_m [N/mm ²]	Density ρ [kg/m ³]	Ratio ρ/f_m
Timber	20	400	20
Steel	300	7850	26
Reinforced concrete	40	2400	60

Table 1- Strength to weight ratio of building materials

Another aspect is the ductile behaviour of timber structures. When using the well-engineered connection systems, timber can have excellent seismic-resistant properties.

Thanks to new innovations in the timber industry, the limitations in dimensions of regular timber are dissolved. By making use of adhesives to glue thin strips of wood, from which all flaws have been cut out, larger sections can be produced. This product is called engineered timber and is also more dimensionally stable in terms of swelling and shrinkage.

2.2 Types of timber construction systems

The use of timber for the load-bearing system of buildings has evolved over time, which results in different construction methods. A distinction can be made for three types of main load-bearing structural systems. First the conventional timber framing method, considered as light timber construction. This method is often used for low- and mid-rise residential buildings up to five- and six storeys. For heavy timber construction the post and beam and panelised construction method is considered. Combinations of the different systems can also be a design solution.

2.2.1 Timber framing construction

Typically, the timber framing construction system consists of timber stud members that are enclosed within thin plates to form wall and floor elements. The open spaces between the studs are generally filled with insulation material. Timber framing can be divided into platform frame construction and balloon frame construction. The difference is that by using the platform framing method, the walls are completely covered by the sub-floors forming a platform. In the balloon frame construction the load-bearing walls do not interfere with the floors. The two basic configurations of the timber framing construction method are shown below. In the Netherlands, a high degree of prefabrication of timber framing elements is present.

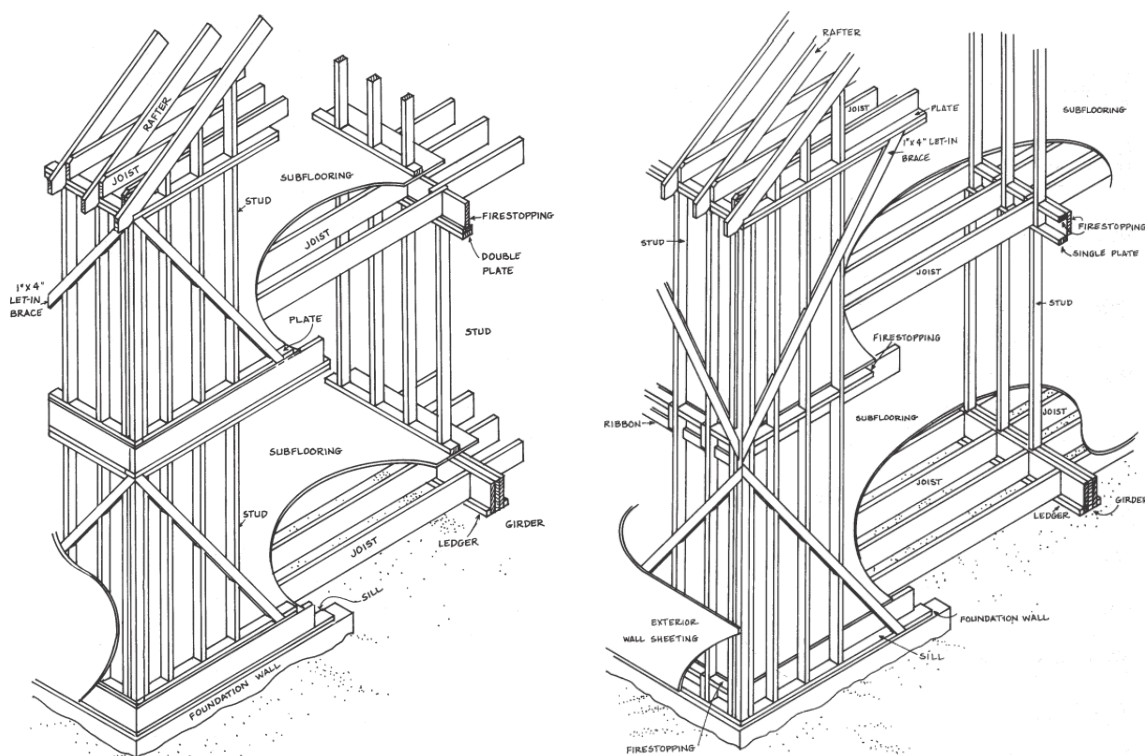


Figure 10 - Left: Platform type, right: Balloon type timber framing (American Wood Council 2001)

2.2.2 Post and beam construction

The post and beam construction method consists of vertically load-bearing columns and horizontally load-bearing beams. This method allows for larger spans and more open spaces, unlike the light timber framing method. Mechanical fasteners are used to connect the different elements. The elements can be heavy sawn timber members, but more typical are engineered timber products like glued laminated timber members. The availability of larger cross-sections when using engineered timber products opens the possibility to construct tall timber buildings.

2.2.3 Panelised construction

Panelised construction consists of solid timber panels as primary structural elements. These panels are made of engineered timber, namely CLT. The vertically oriented CLT elements act as load-bearing and shear walls. The horizontally oriented CLT elements are load-bearing floors and roofs, which also have to provide the diaphragm action. Because large open spaces are not common for this method, its use is mainly for residential buildings.

2.2.4 Hybrid construction

The hybrid construction system consists of a main load-carrying system that is a combination of two materials. The core of the building is erected from concrete and/or a composite floor system is used. Often the use of concrete for particular structural elements is driven by the positive effect of the selfweight, for stability considerations of the building.

Whether or not a building with such a structural system can be called a timber building, is left open for discussion. However, due to the presence of innovative solutions for the use of timber as part of the load-bearing structure, the hybrid system is incorporated as well.

2.2.5 Review on current tall timber and cross-laminated timber buildings

It is clear that tall timber buildings have become more popular due to sustainability aspects and new product innovations. Below, a selection of current tall timber buildings is shown, for which the structural system and characteristics will be described.

Project	Location	Structural system	Storeys	Completion date
Murray Grove	London, England	CLT Panel system	9	2009
Limnologen	Växjö, Sweden	CLT Panel system with tension bars	8	2009
Life Cycle Tower	Dornbirn, Austria	Hybrid: Reinforced concrete slabs on glulam beams and columns	8	2012
Forte Building	Melbourne, Australia	CLT Panel system	10	2012
Treet	Bergen, Norway	Load-carrying glulam trusses, prefabricated building modules	14	2015
HoHo Tower	Vienna, Austria	Hybrid: Concrete core with a self-supporting timber shell	24	2017

Table 2 - Overview on tall timber projects

Murray Grove

Probably the most well-known, tall cross-laminated timber building is Murray Grove (Trada 2009). Cross-laminated timber panels are used as load-bearing internal and external walls, floor slabs, lift and stair cores. In the total structure there are no beams or columns, just panels in a cellular configuration which allowed for openings to be cut out. The total nine-storey structure was assembled in nine weeks. This project was an eye-opener for designers of multi-storey buildings, because the potential of the material CLT was demonstrated in a large-scale project.



Figure 11 - Murray Grove London (Trada 2009)



Figure 12 - Limnologen block with weather protection system (Serrano 2009)

Limnologen

Project Limnologen is part of the Välle Broar programme, which is intended to stimulate the local and national use of timber or wood based products in the construction industry (Serrano 2009).

Limnologen consists of four eight-storey houses, with a structure of seven timber storeys on a concrete foundation and concrete first floor. The seven timber storeys have a load-bearing structure of Cross-Laminated timber walls and floors, with some additional timber frame walls. To prevent tension forces between the elements as a result of wind loading, 48 prestressing tie rods have been mounted in every building. In this way, the forces in the connections between the elements are not alternating in direction, which implies much less complex connection behaviour.

Life Cycle Tower

The Life Cycle Tower (One) project is an exceptional timber project as it is built to serve as a living educational laboratory. It was specifically designed to build industry capacity and transfer knowledge about the benefits of mass timber building (Will+Perkins 2014). It is a prototype project to develop and test a prefabricated construction system, which consists of hybrid wood-concrete slabs supported by glued-laminated timber posts connected through a system of pins and cones. The system is supported by a central concrete core. A very open floor plan is created because the composite slabs span 9m. In terms of building speed and sustainability, this building system has proven to be a more than viable solution. Therefore the system is now proposed to be used in a resource efficient, prefabricated, 20-storey building.



Figure 13 - Life Cycle Tower, prefabricated floor slabs and facade elements (Will+Perkins 2014)

Forté Building

Formally the world's tallest Cross-laminated timber building is the Forté Building in Melbourne, Australia. Forté is also the first residential building in Australia with CLT as a structural solution. Only the first storey is made of concrete, the remaining nine storeys are constructed with CLT panels in only nine weeks, including the walls, floors, stair shafts and the elevator core. All the CLT elements were shipped from a factory in Austria towards Melbourne. Fire-safety tests have been done to prove the required fire performance. The project was financed, designed and constructed by Lend Lease as a pilot. Lend Lease has a long history of landmark innovations in sustainable construction. The company concluded that this structural wood solution can be cost competitive compared with more conventional building materials such as concrete or steel which then by default address negative industry preconceptions about timber construction.



Figure 14 - Forté building (Will+Perkins 2014)

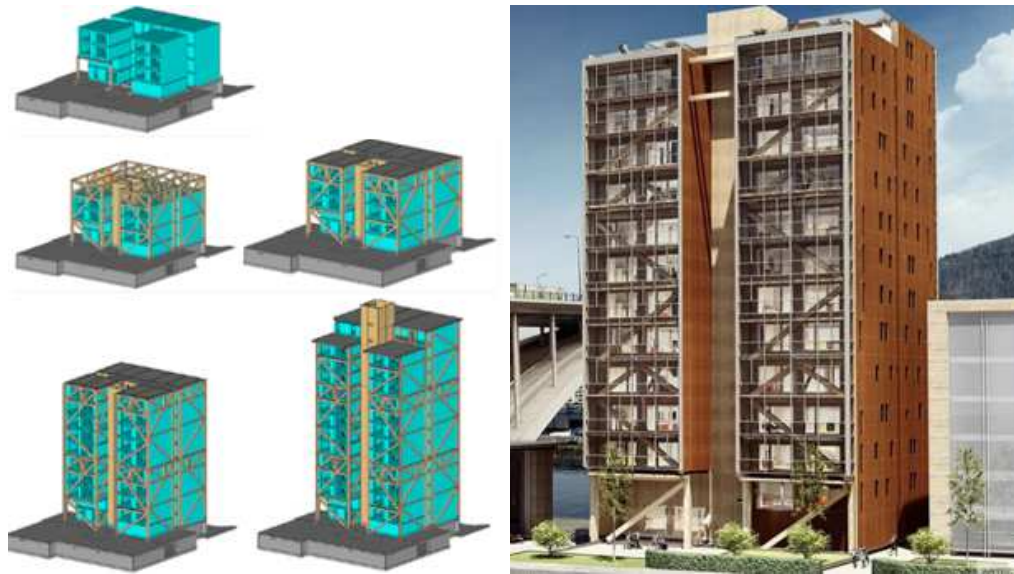
Treet

Figure 15 - Treet: Structural model without modules (R.B. Abrahamsen 2014)

The Forté Building enjoyed its place as the tallest timber building of the world for a short period only due to the 2015 construction of a 14-storey residential building called “Treet” in the city of Bergen, Norway (Abrahamsen and Malo 2014). The load-bearing structure of the building consists of a system of glued-laminated timber trusses, in which two intermediate levels are strengthened. Prefabricated CLT building modules are stacked on top of a concrete garage and on top of the strengthened levels. The structural system is generally explained by an analogy to a cabinet rack filled with drawers. The timber framed modules on top of the strengthened levels do not rest on the building modules below, but on a concrete slab which is incorporated to connect the trusses. The additional function of the concrete slabs is to increase the mass of the building. CLT is also used for the elevator shaft and internal walls, but are not part of the main load bearing system.

HoHo Tower

Figure 16 - HoHo Tower Vienna (Moneo 2015)

The 14-storey timber tower in Norway will not hold the title of the world's tallest timber building very long. In 2016 the construction of a 24-storey timber building in Vienna has started. The hybrid structure of the HoHo tower consists of supporting concrete cores, with a self-supporting timber structural system secured to these cores (Moneo 2015). The timber system is made from prefabricated composite floor panels and prefabricated external wall modules (comparable to the system of the Life Cycle Tower). The floor panels will be supported by a wooden column system around the outline of the building and then the prefabricated external wall modules from solid wood panels with a concrete shell will be mounted and supported by the timber structure.

2.3 Fire safety aspects

2.3.1 Introduction

Probably the first aspect that comes to mind when a tall building will be erected in timber, are the fire safety considerations. Because timber is a combustible material, the perception of fire risk is triggered. Nevertheless, properly designed heavy timber construction performs very well in fires because of the protective char layer.

In order to describe the most important principles concerning fire safety for timber buildings, a distinction can be made between the reaction to fire and the fire resistance. The reaction to fire, is related to the effects of the material timber on the fire and smoke development. As a result, the building must have sufficient fire resistance, which is related to the structure, in order to prevent fire spread and collapse.

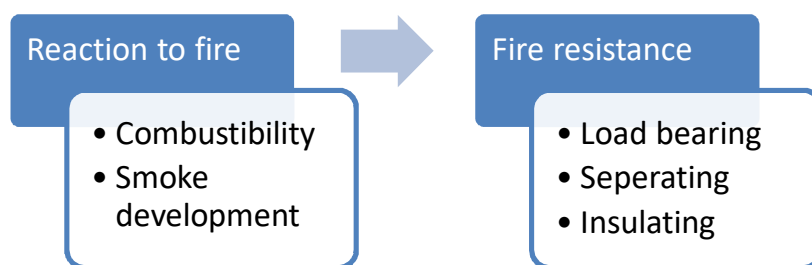


Figure 17 - Principles for fire safety considerations

The figure below shows a typical fire development temperature-time curve. For the development of a fire, different stages can be recognised. After the ignition there is a growth phase in which pyrolysis of the material takes place and hot gasses and smoke are released, called the “reaction to fire”. If this process continues the elevated temperature in a compartment results in “flashover”, meaning the occurrence of a fully developed fire in which all exposed surfaces are burning. The response of a structure during the post-flashover phase determines the fire resistance. After consumption of the available fuel in a compartment the decay phase takes place and the fire extinguishes.

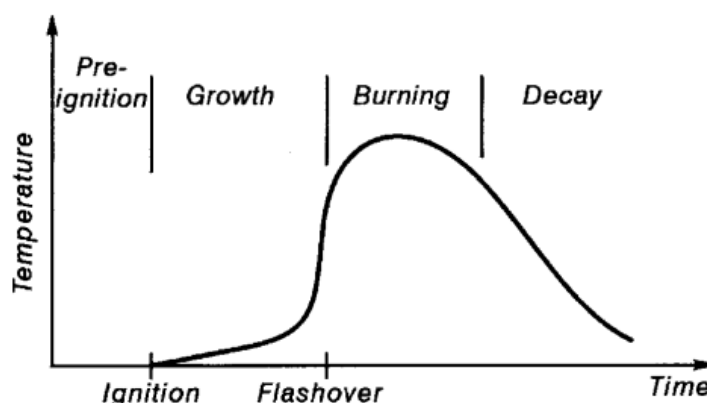


Figure 18 - Stages of a typical fire development (A. Buchanan 2000)

Today, these principles are generally regulated in building codes, by means of ‘performance-based’ requirements. The requirements are demonstrated below for the Dutch building situation. The most important objectives concerning fire safety and the provisions that can be taken are presented.

2.3.2 Reaction to fire

The reaction to fire is defined as the extent to which products (buildings, contents) contribute to the pre flashover fire development (Breunese and Straalen 2014). The reaction to fire describes the ignitability, flame spread, heat and smoke production and falling burning droplets or particles. These factors are depending on the type and arrangement of the materials and the ventilation conditions.

In general, the reaction to fire of a specific material or compartment, the assessment method involves testing. Eventually, the reaction to fire of buildings products after testing and combining test results is expressed in classes. In the pre-flashover phase active measures can be taken to prevent the occurrence of flashover as stated in 2.3.5.

2.3.3 Fire resistance

Fire resistance can be defined as the time during which a building element (system) exposed to fire, can fulfil its anticipated functions under end-use conditions (Breunese and Straalen 2014). The main functions to be considered are the load bearing function, the separating function in terms of integrity and the insulation function. Buildings must have sufficient fire resistance to prevent fire spread and structural collapse for the burning period of a post-flashover fire.

In order to determine the fire resistance, the time-temperature development can be defined by several models. Simplified models are the nominal fire curves, e.g. ISO 834, which represent the phase of the fully developed fire that increases monotonically with time. More realistic failure times can be achieved by using parametrical fire curves. These models incorporate the effects of the available fire load, ventilation conditions, boundaries and fire-fighting action. For this kind of detailed analysis, like fire safety engineering, computer simulations involving fluid dynamic models can be used.

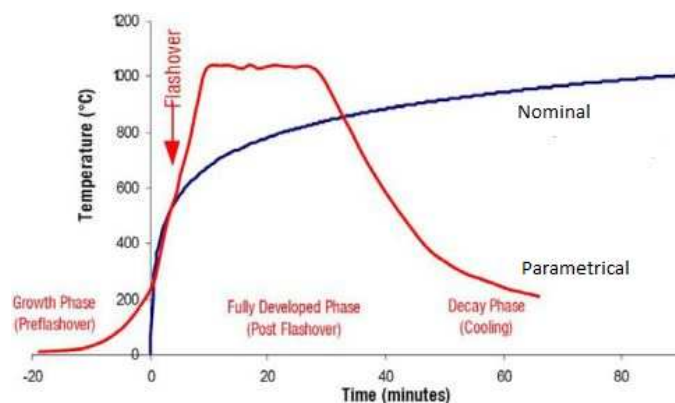


Figure 19 - Nominal and parametrical temperature-fire curves (Ravenshorst 2014)

In calculating the fire resistance of timber structures, the charring of the wood that reduces the cross-section is the main criterion. The charring rate is strongly dependent on the density of the wood. A higher density results in a lower charring rate. Two methods that are commonly used are the reduced cross-section method and the reduced properties method. The reduced cross-section method is further elaborated specifically for CLT in section 0.

2.3.4 Legislation

To achieve an acceptable level of fire safety of a building, a comprehensive fire safety strategy with adequate combination of measures is needed. The following general fire safety objectives have to be considered in this strategy (Frangi, Fontana and Knobloch, Fire Design Concepts for Tall Timber Buildings 2007).

- Safety of occupants and fire brigade
- Safety of neighbours and their property
- Limitation of financial loss (building and contents)
- Protection of the environment in case of fire

The documents that are relevant for timber buildings in the Netherlands are the Dutch building decree and Eurocode 1995-1-2. The building decree is a performance based code, which implies that the objectives and requirements stated in the code, once met allow for any form of construction.

The required fire resistance of the main load bearing structure, according to the building decree, is expressed in minutes (60, 90 or 120 minutes). During this time, the ultimate limit state of the main load-bearing structures must not be exceeded. The main load-bearing structure comprises all parts of the structure whose collapse may result in progressive collapse. This resistance is dependent on the function, height and fire load of the building, according to article 2.10 of the Dutch building decree and is shown below. In certain cases the requirements of the fire resistance of the main load bearing structure may be reduced. This is possible when the compartment has a low fire load density (<500 MJ/m², the same as 25 kg of spruce).

Highest floor height		Fire resistance requirement [min]
Residential	Non-residential	
$h < 7\text{m}$	$h < 5\text{m}$	60
$7\text{m} < h < 13\text{m}$	$5\text{m} < h < 13\text{m}$	90
$h > 13\text{m}$	$h > 13\text{m}$	120

Table 3 - Fire resistance requirements for the main load bearing structure

In Dutch legislation, there is no specific restriction on the maximum number of storeys or building height which can be constructed from wood. The performance based fire safety requirements are only provided for building heights below 70 metres. Article 2.128 of the building decree states that a building with a highest floor height above 70 metres, requires an equal level of fire safety as intended for buildings with a lower highest floor level. This is an example of the principle of equivalence, that gives designers flexibility, allows deviation from the performance requirements, provided that alternative measures are taken that result in an equivalent safety level (Breunese and Straalen 2014). Methods that are used to achieve an equal level of safety are referred to as fire safety engineering.

Furthermore, the Dutch building decree sets out several material related requirements regarding the reaction to fire. Building materials must be tested in order to assign it to a specific European fire class. These tests provide the designer more insight into the fire propagation, smoke development and flame droplets that are the result of the material in fire conditions. The requirements set by the decree are minimum fire classes which are allowed to be applied at certain fire and smoke compartments or escape routes.

Apart from the material related requirements, several fire safety regulations that affect the building's layout are provided by the code. The most important one is that the distance between the entrance of a compartment and the staircase must be within 30 metres according to article 2.102. Additional requirements are considered to be outside the scope of this thesis.

2.3.5 Detection and suppression

To meet the requirements that are set by codes and to achieve fire safety objectives, several measures can be taken. These measures are designed to detect and suppress a fire or even to prevent the possibility of ignition. Active systems are measures that respond actively to the fire, such as detection and alarm systems, extinguishing systems like sprinklers, smoke extraction ventilators and pressurisation systems. Passive systems do not need activation, such as fire insulation of the load bearing structure, compartment walls and escape routes (Breunese and Straalen 2014).

The active system that is generally used in multi-storey timber buildings is the sprinkler system. This system is designed to extinguish a fire in an early stage. There are a lot of different types of sprinkler systems on the market. Often, a wet or dry system is used. The advantage of wet systems is the fast response time, however freezing can occur because the pipes are filled with water. For dry systems, this is the other way around because the pipes are filled with pressurized air. In the Netherlands the reduction of the fire resistance for the main load bearing structure can be 30 or 60 minutes, but is dependent of the local authority.

2.3.6 Fire safety engineering

The conventional fire safety approach is based on the verification of single building components for generalised standard fire curves. Fire safety engineering is a more complex method in order to determine a more realistic approach. Extensive analysis for example with computational fluid dynamic modelling.

3 Modular construction

Today, the building industry is using more and more prefabricated elements. These elements can be e.g. prefabricated concrete beams or prefabricated façade elements. When the prefabrication trend is extended, considering transport restrictions, the modular construction type is born. At first, modular construction was used mainly in portable or temporary buildings, but the benefits of off-site manufacture resulted in a wide range of usage in permanent buildings as well.

Modular construction is a way of building in which prefabricated box-shaped modules are stacked and joined together to make a single building. The inside of the closed box can be provided with all the installations and finished surfaces. Bathroom and kitchen furniture can be installed in the factory. This chapter will describe the benefits, types and most important aspects of this construction method.

3.1 Why modular?

The decision for modular, made by a project's design team generally the result of a highly repetitive layout of the building and site limitations. Cellular-type buildings such as hotels, student residences, prisons and social housing are well-suited for a modular construction method. The benefits of this building method have been assessed by different parties, such as the Modular Building Institute. Below the most important quantifiable economic and sustainability benefits are elaborated.

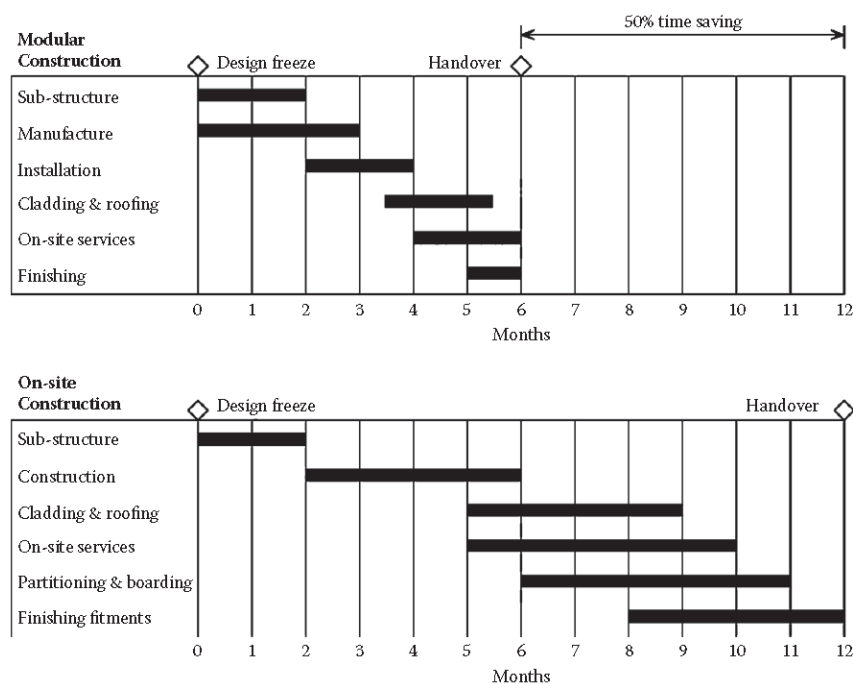


Figure 20 - Comparison of construction speed (Lawson, Ogden and Goodier 2014)

3.1.1 Speed of construction

The off-site fabrication of modules may occur simultaneously with construction at the site. The repetitive character of the production of the modules can be seen as a fast industrialised chain production, without weather delays. This results in increased productivity, as the factory has all of the key players onsite, contracting separate teams is not necessary anymore. The time savings in construction of a modular system compared to a conventional on-site production for a 6-storey building is shown in Figure 20.

3.1.2 Improved quality and safety

The construction process of the modules takes place inside the factory, implying regulated environmental conditions for the modules as well as the workers. The repetitive process is less susceptible to errors in design and execution and allows for higher quality control, which results in higher accuracy, less damage and less waste. The controlled environment inside the factory eliminates the risk of mold, rust and sun damage to the materials.

Modular construction is a safer method, because less people, equipment and traffic is present on the construction site for a shorter period. Inside the factory, workers do not have to deal with extreme temperatures, rain and wind. Additionally, the controlled setting provides each worker an assigned workstation supplied with all the appropriate equipment nearby, ensuring the safest work environment possible. As such the risk for construction hazards is significantly reduced.

3.1.3 Sustainability

The benefits of modular construction in terms of sustainability benefits can be assessed by different procedures. In general, the following key performance indicators have to be assessed and are briefly elaborated:

- Energy and CO₂
- Materials
- Waste
- Pollution
- Management
- Performance improvements
- Adaptability and end of life
- Social responsibility

Energy and CO₂ is about the use of energy of the building and the embodied carbon in its materials over the life span of the building. Modular timber buildings can be designed and manufactured very airtight and the solid timber panels perform very good in terms of insulation and embodied carbon. Modular construction is very efficient in use of materials, which also results in a reduction of waste. When lightweight materials are used, like timber, the savings in foundation dimensions are significant. Additionally, the material maintains its value when the modules are re-usable. Concerning pollution, modular construction is beneficial in two ways. On site much less noise, dust and noxious gases are generated because this can be captured in the manufacturing facility. Next to that, raw materials can be delivered in bulk quantities to the factory of the modules, consisting of accurate quantities, instead of multiple small deliveries the building site.

The management aspect is much improved because of the 'just in time' delivery of the modules and the potential of the modular structure in modern building information modelling (BIM) systems. The performance improvement is satisfied, because the modular units are strong and robust. High levels of acoustic and thermal performance are achieved by the 'double skin' configuration. Modular

buildings can easily suit the user's requirements, are flexible and can later be disassembled and reused. The Health and Safety Executive data show that factory-based processes, including modular manufacture, are five times safer than regular construction processes in terms of reportable accidents (Lawson, Ogden and Goodier 2014). Besides, modular construction contributes to a clean and safe working environment where noise and disruption is minimised to suit social responsibility.

Below the most important sustainability benefits of off-site manufacturing are summarized both for the construction process and the performance during the lifetime. Apart from the social and environmental aspects a sustainable solution should also be economically viable. The biggest driver for modular construction would be the economy of scale. The investment for the modular production factory has to be balanced by the benefits of the faster rate of return for the client, due to the building speed and the benefits of the improvements in quality and safety.

Sustainability benefits for off-site manufacture	
Construction process	In-service performance
Social <ul style="list-style-type: none"> Fewer accidents on site and in manufacture More secure employment and training Better working conditions in the factory Reduced traffic movements to site Less noise and disturbance during construction 	Social <ul style="list-style-type: none"> Acoustic insulation is improved due to sealed double-leaf construction Improved finished quality and reliability Future point of contact to the modular supplier Modular buildings can be extended or adapted
Environmental <ul style="list-style-type: none"> Less pollution, including traffic, dust, noise, and VOC's Less wastage of materials on site and in manufacture More recycling of materials and use of materials with higher recycled content 	Environmental <ul style="list-style-type: none"> Improved energy performance by better airtightness and installation of insulation, hence, reduced CO₂ emissions Renewable energy technologies can be built in and tested off-site Modular buildings can be 'sealed' against gases
Economic <ul style="list-style-type: none"> Faster construction programme Site preliminary costs are reduced Less snagging and rework Economy of scale in production reduces manufacturing cost Higher productivity on-site Less infrastructure and hire charges 	Economic <ul style="list-style-type: none"> Savings in energy bills, including the use of renewable energy systems Longer life and freedom from in-service problems, e.g., cracking Reduced maintenance costs Modular buildings can be extended and adapted Asset value can be maintained if they are reused

Table 4 - Sustainability benefits for off-site manufacture (Lawson, Ogden and Goodier 2014)

3.2 Types and applications of modular construction

There are three basic types of modular construction in terms of structural behaviour.

- Corner supported modules
- Continuously supported modules
- Non-load bearing modules

Corner supported modules are load bearing modules, designed to span between the corner supports by means of edge beams and corner posts. Continuously supported modules have load bearing side walls. Non-load bearing modules (often called 'pods') are modules that deduce their support from the separate load bearing skeleton of the building.

Additionally, a distinction can be made between the supporting principle. The 'self-supporting principle' means that the modules are designed and stacked in such a way, that they provide their own strength and stability. The required capacity against loads in horizontal direction can be achieved by bracings or diaphragm action in the walls. Another supporting principle is the 'Bookcase principle'. The bookcase supporting principle means that the stacked modules are horizontally supported by an additional structure, like a core structure for vertical transport that provides the overall stability. The principle considered in this master thesis is the 'Self-supporting principle', in which diaphragm action in the walls provides the horizontal stability.

In general, 'self-supporting' modules are placed on a so-called 'podium structure'. This podium or platform forms a more open space for the first one or two storeys of the building. This open space is often used for retail, commercial use or below-ground parking areas. In the figure below an example is shown of such a podium structure. The support beams should align with the walls of the modules.



Figure 21 - Modular building with a podium structure (Lawson, Ogden and Goodier 2014)

3.3 Structural aspects

In order to design a structurally safe modular multi-storey building, several aspects are of importance specific only to this type of construction. The structural behaviour of modules is characterized by the capacity to independently withstand the effects of transportation and lifting. To achieve at a 'self-supporting' principle, the modular 'building blocks' must act as a group. To gain insight in the resistance against horizontal forces, the effect of manufacturing and installation tolerances and the robustness aspects for accidental actions are investigated below.

3.3.1 Inaccuracies and imperfections

Tolerances in modular buildings are a result of tolerances of a module in the manufacturing process and tolerances due to misalignment during installation of the modules. Figure 22 shows the maximum tolerances for a single module which are based on the standard for the execution of steel and aluminium structures (EN 1090-2). When a large number of modules are considered, the average value of manufacture may be taken as $h/1000$, which results in a cumulative error over n floors of height h of $nh/1000$ (Lawson and Richards 2010).

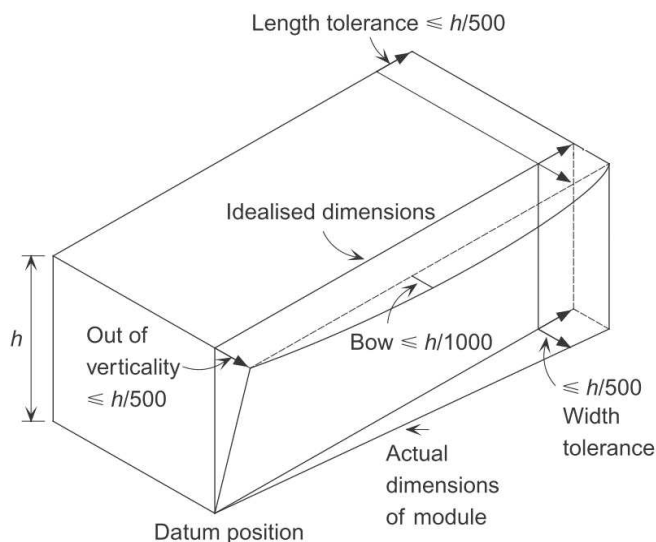


Figure 22 - Permitted maximum dimensional tolerances (Lawson and Richards 2010)

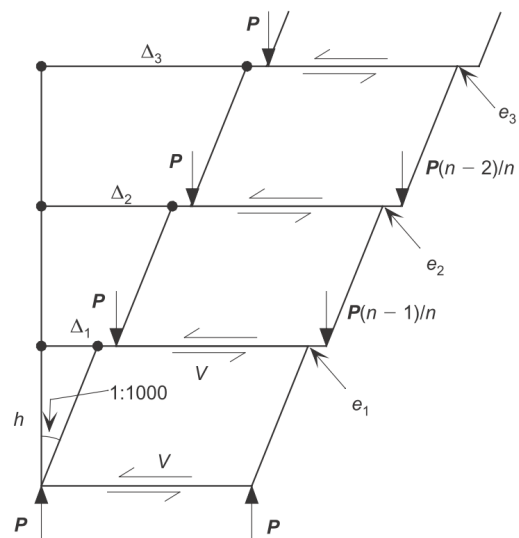


Figure 23 - Eccentric loadings (Lawson and Richards 2010)

During installation of the modules, difficulties in positioning one module on top of another arise and may result in misalignment. This can be controlled on site by for example laser equipment, to limit the cumulative positional error to 5 mm per module. According to (Lawson and Richards 2010), it is recommended and achievable to limit the total out of verticality to 80 mm for 10 or more storeys by good control on installation.

If necessary, gradual adjustments in the positioning of the modules can be made by varying the cavity spacing between the modules. A recommended value for the cavity width is 40 mm, which is incorporated in the design of the modular building. The tolerance in height of the module is not considered here, because this does not have a reasonable effect on the structural behaviour of the building.

The eccentricities, which are caused by manufacturing and installation tolerances on the compression load path, may lead to additional horizontal forces applied to the modules. Because the side walls are unable to resist the resulting moments due to eccentric loading shown in Figure 23, the equivalent horizontal forces required for equilibrium are transferred as shear forces in the ceiling, floor and internal shear wall of the module. To calculate the additional moment that acts on the base module, a good approximation for the effective eccentricity of the vertical group of modules, according to (Lawson, Ogden and Goodier 2014), is given by:

$$\Delta_{eff} = 3 \cdot n^{1,5} \text{ mm}$$

The next step is to convert this eccentricity to a notional horizontal force that acts on each floor level and causes the same equivalent moment in the base module. The following expression is determined for the aforementioned tolerances and varies with the number of storeys.

$$F = 0,2 \cdot n^{0,5} \%$$

This notional horizontal force is expressed as a percentage of the factored vertical load of a module and varies between 0,5 % and 0,8 % for 6 and 16 modules on top of each other respectively. The calculated notional horizontal loads should be applied in combination with the wind loading.

3.3.2 Second-order effects

The wind forces and the notional horizontal forces due to tolerances (initial eccentricities over the building height), cause a horizontal displacement of the building that increases with the height of the building. This horizontal displacement causes a shift of the centre of gravity relative to the foundation. This shift and the vertical load of the building results in an additional bending moment and consequently an additional horizontal displacement. This phenomenon is called the second order effect and is also known as the P-Delta effect. In an extreme case, second-order effects may lead to failure. Usually, these effects are small and may be neglected. When these effects are of influence, they can be incorporated through a second-order calculation or the calculation can be avoided by applying an adjusted cross-section for the individual elements (Hoenderkamp 2002).

The check whether the buildings structure is vulnerable to second-order effects can be performed using the critical load method. In this method, the stabilising elements of the building can be simplified and modelled as a column with a specified bending and shear stiffness uniform over the building height and a rotational spring at the bottom, as can be seen in the outer right sketch of Figure 24. In general, the second-order effects can be the three displacement components shown in Table 5 and Figure 24.

Bending	Shear	Rotation of foundation
$y_b = \frac{ql^4}{8EI}$	$y_s = \frac{ql^2}{2GA}$	$y_f = \frac{ql^3}{2C}$

Table 5 - Displacement components for second-order considerations

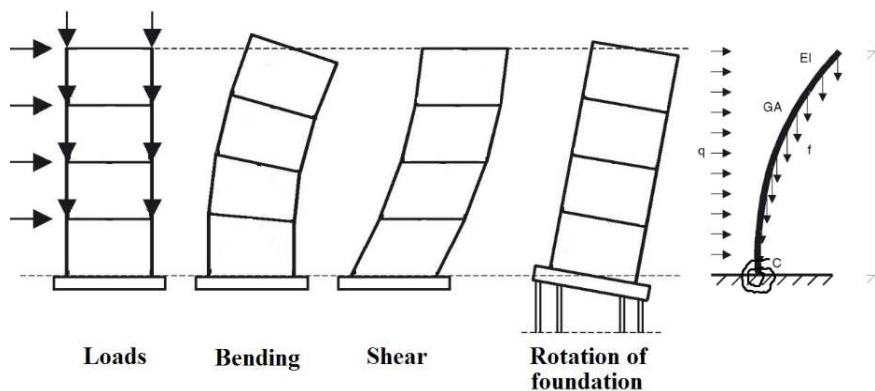


Figure 24 - Displacement components (adjusted from Hoenderkamp 2002)

The key to evaluating for the susceptibility to second-order effects, is to calculate the critical buckling load of the column P_{cr} that contains the stiffness's belonging to each displacement component.

$$\frac{1}{P_{cr}} = \frac{1}{P_{cr,b}} + \frac{1}{P_{cr,s}} + \frac{1}{P_{cr,f}} = \frac{1}{\frac{7,837}{l^2}} + \frac{1}{2GA} + \frac{1}{2C}$$

The critical buckling load can be divided by the total vertical load F of the building that belongs to that stabilising element which results in the ratio n .

$$n = \frac{F_{cr}}{F}$$

Using the ratio n , the following magnification factor for second order effects may be used.

$$\frac{n}{n-1}$$

In general and in Eurocode 2 (concrete structures) art. 5.8.2(6), second order effects can be neglected if they are less than 10% of the corresponding first order effects. $F \leq 0,1 F_{cr}$. If the second-order effects are however significant, these effects have to be incorporated into the ULS and SLS verifications via additional horizontal forces.

3.3.3 Robustness

By increasing the scale and height of a (modular) building, it becomes more and more important to design in a robust manner to withstand accidental actions. The Eurocode (EN 1991-1-7) defines robustness as follows:

- “Robustness is the ability of a structure to withstand events like fire, explosions, impact or the consequences of human error, without being damaged to an extent disproportionate to the original cause.”

It is a basic requirement for any structure to be designed and executed in a robust manner and to have sufficient ‘structural integrity’. In short, it implies that structures should not fail catastrophically if a minor part fails. The Eurocode gives guidance on how to arrive at a structurally robust design. The regulations classify buildings in four categories. Dependent on the type of building and the severity of the consequences of damage, different provisions are presented in Table 6.

Consequence class	Type of building	Provisions
1	Houses maximum 4 storeys	None
2a	Flats, hotels, offices and residential buildings not exceeding 4 storeys in height	Horizontal ties
2b	Flats, hotels, offices and residential buildings exceeding 4 storeys but not exceeding 15 storeys	Horizontal and vertical ties No disproportional damage
3	Large public buildings	Risk assessment

Table 6 - Categorisation in consequence classes and provisions

The following 3 routes of achieving structural robustness can be used to comply with the regulations, however the applicability to modular construction varies:

- Tying force route
- The key element route
- Localization of damage route

The tying force route is characterized by the ability of neighbouring elements to provide the tensile tie capacity to support the damaged element. A precondition is that the connections should have adequate ductility in order to cope with the deflections, that are necessary to develop this tying or catenary action. The key element route is based on the simulation of a blast load on an element that is essential for the load bearing function of the structure. This blast pressure of 34 kN/m² is often problematic for lightweight structures. Lastly is the localization of damage route. This method implies the notional removal of a module from the building.

Modules themselves are inherently robust in their construction, because they are designed with the stability and stiffness required for lifting and transportation. This provides the cellular assembly of modules with a certain redundancy to withstand accidental actions by the natural ability to redistribute loads.

The method that is most suitable for modular construction, to comply with the building regulations, is the combination of the localization of damage route that leads to a specific tie force route. This approach to establish structural integrity is based on selective removal of modules and to realize an alternative load path by means of tying forces through inter-modular connections. Two critical situations are identified:

- Removal of an internal module
- Removal of an edge module

The removal of an internal module causes the modules above to span horizontally over a damaged area by acting as a deep beam. When an edge module is removed, the modules above must be able to cantilever over the damaged module. This last situation tends to be the worst case, because the compression force in the wall of the adjacent module is at least doubled. For this mechanism it may be assumed that each cantilevering module is resisted by its neighbouring module (Lawson, Byfield, et al. 2008).

The design for the inter-modular connections must ensure the possibility to develop these tie forces. The inter-modular connections are made both horizontally and vertically, although the practical installation of connection plates and bolts can be problematical, considering ease of access and the sequence of construction.

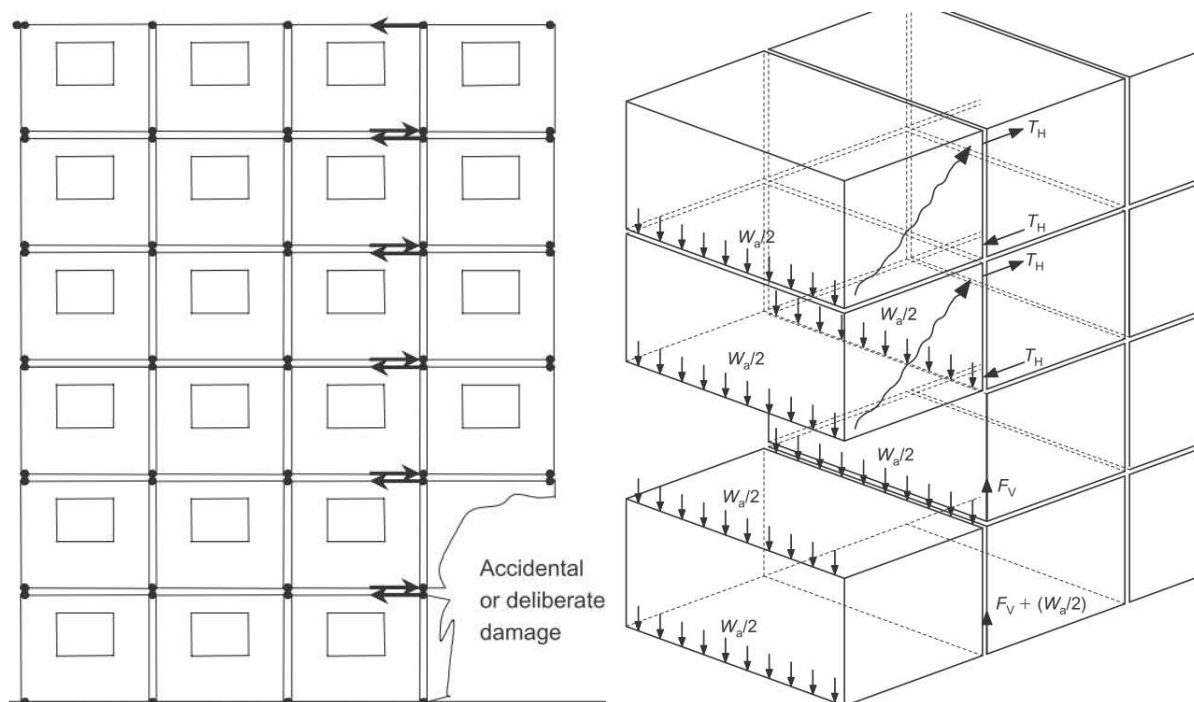


Figure 25 - Load distribution and tying action in modules for localization of damage route (Lawson, Byfield, et al. 2008)

3.3.4 Lifting and transportation

A critical aspect of modular construction is transportation and the lifting of the modules in particular. In the Netherlands, it is required to apply for an exemption in order to transport modules of more than 3 m in width on the road. When the module is more than 3,5 m wide, the transportation has to be escorted by a certified traffic attendant according to the RDW (Dutch national road traffic service).

There are multiple ways of lifting the modules. The modules can be lifted by inclined cables to the corner or edge of the modules, with or without a lifting beam. However, to minimize the internal forces and avoid diagonal pull in the module and to achieve a perfect static weight distribution, usually a lifting frame or a main beam with crossbeams are used (Halfen 2015). This system must be used both in the yard and on site. On site, the modules are generally lifted directly from the lorry into position.

To determine the required design capacity of the lifting points, the weight of the module, the dynamic loads and the effects of the spread angle of the cable must be taken into account according to the following formula.

$$F_z = \frac{F_G \cdot f \cdot z}{n}$$

With: F_z Tension force on the anchor
 F_G Module weight
 f Dynamic acceleration factor
 z Spread angle factor
 n Number of load-bearing
anchors



Figure 26 - Lifting of module by main beam and crossbeams (M. Lawson 2014)

The dynamic factor depends on the lifting equipment and the corresponding accelerations applied on the module being lifted and transported. Below the dynamic lifting factors according to DIN 15018 are shown.



Lifting class		Dynamic acceleration factor f	
		0-90 m/min	90 m/min
H1: Fixed		1,1 - 1,3	1,3
H2: Mobile		1,2 - 1,6	1,6

Table 7 - Indication dynamic acceleration factors f

The spread angle factor z is $1/\cos(\alpha)$, with α as the cable angle which is 2 times the spread angle of the cable. For the resistance side of the lifting point in the module in case of timber, k_{mod} can be chosen short-term.

4 Cross-laminated timber

4.1 Introduction

4.2 Product

Cross-Laminated timber (CLT) is a two-dimensional, solid timber product which can be used for load-bearing applications. CLT panels are made out of cross-wise glued lamellas with an uneven number of layers, which generally results in a symmetrical cross-section. A layer or lamella consists of boards positioned next to each other, with or without gaps of 6mm maximum. In longitudinal direction the boards are connected by means of finger-joints.

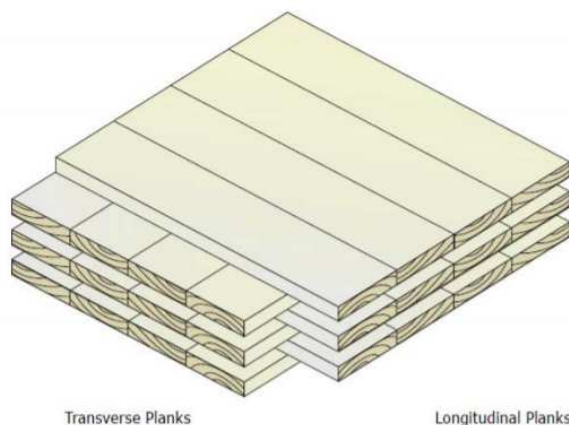


Figure 27 - 5-layered Cross-Laminated timber element (Karacabeyli and Douglas 2013)

In general, the timber which is used for the production of CLT elements is spruce wood of strength class C24, but a restricted percentage may have a lower strength class. Wood species like fir, pine, larch and douglas fir are used and species like hardwood and birch are being tested but not yet covered by the current approvals. The dimensions of CLT panels can be up to approximately 3m wide and 16m in length. Often, the limiting factor governing the size of the panels is the ability to transport the panels. The boards are 40 to 300mm wide and 6 to 45mm thick. Additionally, manufacturers can provide the outer surface of the panels with improved surface qualities, fitting groves at the narrow side or preparations in terms of cut-outs for windows or ducts.

4.3 Chances for multi-storey buildings from cross-laminated timber

Cross laminated timber has been popular in Europe for more than 20 years. The production and use of CLT is increasing dramatically as can be seen in Figure 28 that shows the CLT production growth over the last 20 years. Also in North America, CLT is gaining momentum. Extensive research helps the development of international acceptance and regulation in the building codes. In the meantime, several innovative designers are designing CLT buildings with increasing heights. The increase in use of CLT in construction are directly related to the many benefits of CLT compared to conventional (timber) building materials shown below.

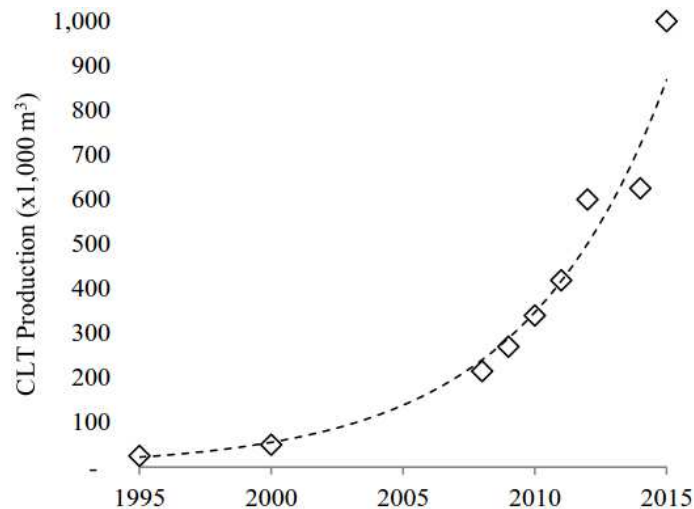


Figure 28 - Global production of CLT (Espinoza, et al. 2016)

4.3.1 Benefits of CLT

- High dimensional stability in case of climate changes (swelling and shrinkage)
- Increased connections strength due to increased splitting resistance with cross-wise gluing
- Positive effect of higher deadweight and robustness
- High axial load capacity for bearing walls because of large bearing surface area
- High thermal, acoustic and fire performance
- Very low carbon footprint
- High tolerances +/- 5 mm compared to 10 mm for concrete
- Very high erection speed
- Lighter crane for erection
- Dry connection
- Easy installation of building services (ducts & pipes), no need for drilling, just screwing
- Quieter building activities using lightweight power tools, no heavy equipment like concrete drills
- Higher heat capacity compared to timber framing
- Higher contact temperature than conventional building materials
- Higher heat resistance and easy to seal seems between the elements to achieve high airtightness
- Good seismic performance due to high ductility
- High level of prefabrication during manufacturing
- High quality of surface finishing

4.3.2 Drawbacks

- Requires external cladding to provide weatherproof envelope
- Has to be protected against moisture during erection
- Low level of experience in practice
- CLT specific calculation procedures have not yet been incorporated in current standards
- Government is cautious concerning fire safety issues for CLT high-rise

4.3.3 Global production of CLT

Currently the production and origin of the material is mainly from Austria, Germany and Scandinavia. But because of the rapidly increasing development and usage of CLT, new factories are being established, for example in the UK, USA and Japan (Watts and Helm 2015). Below, Table 8 shows the main suppliers and maximum possible production sizes of CLT panels.

Supplier/Producer	Width (mm)	Length (mm)	Thickness (mm)	Species used	Country of origin	Product
Eurban	3400	13 500	60–500	Spruce, Larch, Douglas fir	Austria	Crosslam panels
Binderholz	1250	24 000	66–34	Spruce, Larch, Pine, Douglas fir	Austria	BBS
Metsa Wood (Finnforest Merk)	4800	14 800	51–300	Spruce	Germany	Leno
KLH	2950	16 500	57–500	Spruce, Pine, Fir	Austria	KLH solid timber panels
Stora Enso	2950	2950	57–296	Spruce, Larch, Pine	Austria	CLT
Kaufmann	3000	16500	78–278	Spruce	Austria	BSP Crossplan

Table 8 - Main European suppliers of cross-laminated timber (Porteous and Kermani 2013)

4.4 Regulations and guidelines

Currently, cross-laminated timber has not been included in European standards yet. Requiring use under building law of CLT is regulated through national or European Technical Approvals (ETA's), which are stated by each individual CLT producer. These technical approvals provide the framework (in relation to the product) in conjunction to the Eurocode 5 for the engaged engineer. The approvals include minimum requirements to the product, its initial materials and its manufacture, details for verification procedures and, in case of the ETA regulations, for CE marking. In this thesis the CLT of Merk, called "Leno" is used, with ETA-10/0241 as its related technical approval.

Recently, the first European product standard for CLT, EN 16351, passed the formal vote. This document regulates the requirements that hold for the manufacture and test-methods for CLT. Currently a large group of scientists are working on the inclusion of CLT into Eurocode 5. Researchers that are studying the structural characteristics and behaviour of CLT, present their results at conferences on a regular basis, for instance in the European framework programme COST FP1402. Technical papers provide the results of research and form useful information concerning CLT.

Additional design guidance and information can be found in guidelines like e.g. the CLT Handbook (Karacabeyli and Douglas 2013), and the CLT design guide provided by the Austrian timber industry group Proholz (Wallner-Novak, Koppelhuber and Pock 2014).

4.5 Material properties

At the moment there are no strength classes available for CLT like there are for solid timber and glued laminated timber (GLT). There are two different approaches to determine the characteristic values for calculation and design, strength and stiffness properties. The first approach is based on the mechanical properties of the basic material and related bearing mechanisms, models and functions. The second one is by testing the CLT elements.

Below, the basic material properties for the layers of CLT are given. The strength and stiffness values are based on the mechanical properties of the base material, according to EN338 (strength classes for structural timber). Mainly Norway spruce is used for the production of CLT and the strength values of C24 can be assigned to the product. In certain cases the characteristic strength and stiffness values for CLT are partly connected with bearing models for GLT, which means that values for GL24h from EN14080 (requirements for GLT) can be used, as proposed for Eurocode inclusion by (Brandner, Flatscher, et al. 2016).

For certain properties the bearing model for GLT differs to that of CLT due to the cross-wise layering of the boards. These values depend on the cross-sectional build-up and are determined through extensive testing. In paragraph 4.7 and 4.8 the values are shown and explained in relation to the corresponding bearing mechanisms.

Property	Symbol	Value	Approval/Standard
Characteristic density (layer)	ρ_k	350 kg/m ³	EN 338
Characteristic density (CLT)	ρ_k	385 kg/m ³	EN 14080
Mean density	ρ_{mean}	420 kg/m ³	EN 338

Table 9 - Density material properties of CLT

Property	Symbol	Value	Approval/Standard
Flexural strength	$f_{m,k}$	24 N/mm ²	EN 338
Tensile strength //	$f_{t,0,k}$	14 N/mm ²	EN 338
Compressive strength //	$f_{c,0,k}$	24 N/mm ²	EN 14080
Compressive strength \perp	$f_{c,90,k}$	2,5 N/mm ²	EN 338
Shear strength	$f_{v,k}$	3,5 N/mm ²	EN 14080
Rolling shear strength	$f_{v,R,k}$	1,2 N/mm ²	EN 14080
Torsional strength (interface)	$f_{T,k}$	2,5 N/mm ²	ETA-10/0241

Table 10 - Strength properties for CLT

Property	Symbol	Value	Approval/Standard
Mean modulus of elasticity //	$E_{0,mean}$	11000 N/mm ²	EN 14080
5% modulus of elasticity //	$E_{0,0.05}$	9600 N/mm ²	EN 14080
Mean modulus of elasticity \perp	$E_{90,mean}$	300 N/mm ²	EN 14080
Mean shear modulus (layer)	G_{mean}	650 N/mm ²	EN 14080
5% shear modulus (layer)	$G_{0,0.05}$	575 N/mm ²	EN 338
Mean rolling shear modulus	$G_{R,mean}$	65 N/mm ²	EN 14080

Table 11 - Stiffness properties for CLT

4.6 Cross-sectional values

As a basis for the limit state verifications the calculation of the cross-sectional values have to be mentioned. In case there is a dominating direction of loading, usually CLT is treated as panel strips (of 1m wide). Verifications in the ultimate limit state may be analysed with net cross-sectional values without considering shear flexibility, while for the serviceability limit states, shear flexibility must be considered via several possible methods to calculate the effective cross-sectional values. In general ultimate limit state calculation procedures, the modulus of elasticity of the boards transverse to the fibre corresponding to the load direction is assumed with $E_{90} = 0$. In this chapter it is assumed that the cross-sections of the CLT are symmetrical and the same material is used for all layers, which means that there are no differences in moduli of elasticity between the layers.

4.6.1 Net cross-sectional values

For the determination of the relevant normal and shear stresses in CLT panels, the net cross-sectional values can be used. Because of the orthogonal layup, net cross-sectional values have to be determined for the main span direction, equal to the grain direction of the outer layers and denoted by the subscript 0. Analogously, the values can be determined for the ancillary direction. The method based on the net cross-section only takes into account the contribution of the layers which are parallel to the main direction of loading.

The contribution of the transverse layers can be neglected, because only a limited or even no transfer of normal stresses can take place in these layers. This is because of unavoidable cracks and gaps in longitudinal direction within the layers. Additionally, the modulus of elasticity of the timber in longitudinal direction is about 30 times the modulus of elasticity of timber loaded perpendicular to the grain.

The methods to calculate the net cross-sectional values are shown below for the main direction of load bearing ($\alpha = 0$). In Figure 29 shows the used designations and corresponding out-of-plane stresses.

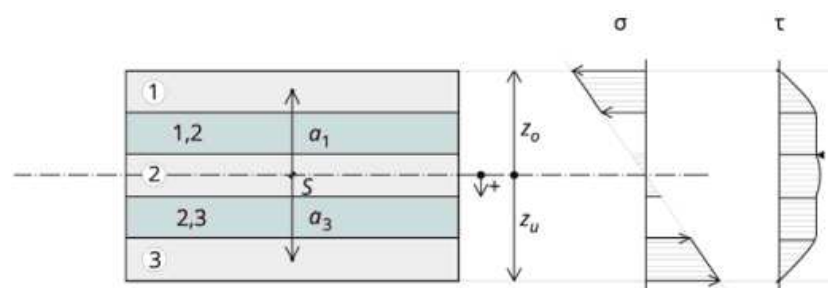


Figure 29 - CLT cross-section with designations and out-of-plane stresses (Wallner-Novak, Koppelhuber and Pock 2014)

$$\begin{aligned}
\text{Area:} \quad A_{0,net} &= \sum_{i=1}^n b \cdot h_i \\
\text{Moment of inertia:} \quad I_{0,net} &= \sum_{i=1}^n (I_i + I_{i,Steiner}) = \sum_{i=1}^n \left(\frac{b \cdot h_i^3}{12} + b \cdot h_i \cdot a_i^2 \right) \\
\text{Section modulus:} \quad W_{0,net} &= \frac{I_{0,net}}{z} \\
\text{Static moment:} \quad S_{0,net} &= \sum_{i=1}^{m_L} b \cdot h_i \cdot a_i \\
\text{(rolling shear)}
\end{aligned}$$

With: b Width of the CLT panel (usually 1 meter)
 h_i Thickness of the boards in the layer parallel to the loading direction
 a_i Distance from centre of gravity to the middle of the considered layer
 z Distance from centre of gravity to the edge of the cross section
 n Number of layers in longitudinal direction
 m_L Index of the longitudinal layer closest to the position of the centre of gravity as seen from the top edge

4.6.2 Effective cross-sectional values

Contrary to calculations related to stresses, the contribution of the transverse layers to deformations cannot be neglected. As can be seen in paragraph 4.7 and 4.8, the effective moment of inertia has been used to perform calculations related to the deformations out-of-plane, which includes buckling of a CLT panel. The deformation of a CLT panel out-of-plane consists of a pure bending and a shear portion as a consequence of the rolling deformation in the transverse layers. The portion of shear deformation depends on the cross-sectional build-up, and the element's slenderness. The following methods are available to include this effect.

- γ -method
- Shear analogy method
- Timoshenko beam theory

The γ -method is a commonly used method, which is anchored in Eurocode 5 and provided by the most CLT related technical approvals, to calculate the effective cross-sectional value. The shear analogy method according to Kreuzinger and the Timoshenko beam theory (Wallner-Novak, Koppelhuber and Pock 2014) are based on the calculation of a shear reduction factor and result in a calculation of the bending and shear deformation separately. Comparisons (Bogensperger, Silly and Schickhofer 2012) between the available methods show that all three methods are suitable for CLT and have neglectable differences, with a length to thickness ratio of the CLT of ≥ 15 , which is usual for engineering practice.

In this thesis the γ -method will be addressed and used because this method allows the calculation of deformations through pure bending in which shear flexibility is already included. The idea behind the gamma-method is that the CLT cross section can be considered as a mechanically jointed beam

according to the Möhler theory. The transverse layers of the CLT panels are modelled as equivalent joints between the layers in longitudinal direction. In order to determine the effective moment of inertia, the Steiner portion of the longitudinal layers is reduced by a factor γ , which accounts for the rolling shear flexibility in the transverse layers. The disadvantage is that the γ -factor is dependent on the length of the element.

The formulas according to the gamma method are stated below for 3 and 5-layered CLT elements, for cross sections with more layers the modified gamma method according to Schelling has to be applied.

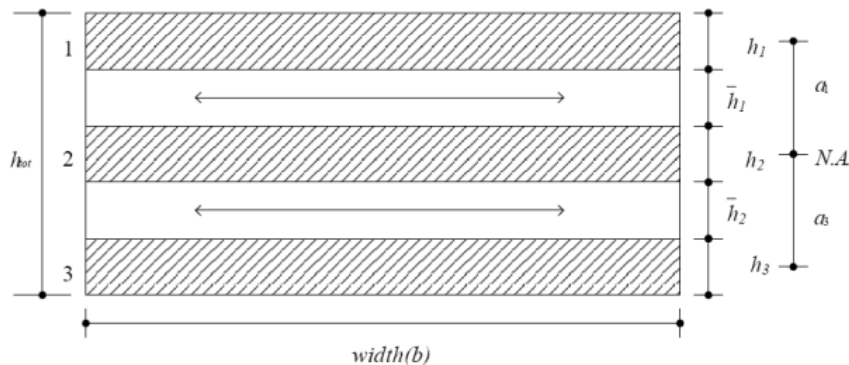


Figure 30 - Cross section of CLT element with designations (KLH Massivholz GmbH 2012)

$$\gamma_i = \frac{1}{1 + \frac{\pi^2 \cdot E_i \cdot A_i}{l_i^2} \cdot \frac{\bar{h}_i}{G_r \cdot b}}$$

$$I_{0,eff} = \sum_{i=1}^n (I_i + \gamma_i \cdot I_{i,Steiner}) = \sum_{i=1}^n \left(\frac{b \cdot h_i^3}{12} + \gamma_i \cdot b \cdot h_i \cdot a_i^2 \right)$$

With:	b	Width of the element (usually calculated for a 1m strip)
	h_i	Height of longitudinal layer
	l_i	Reference length of considered element
	\bar{h}	Thickness of intermediate layer (for a 3-layered element, $h/2$)
	G_R	Rolling shear modulus of the intermediate layers
	a_i	Distance from neutral axis of element to the middle of longitudinal layer
	n	Number of layers in longitudinal direction

4.7 Ultimate limit state verifications

In order to design a safe structure, the resistance of the CLT structure has to be verified against the actions in the ultimate limit state combinations. The occurring stresses in ULS must be smaller than the design strength values of the material. Next to the verifications at cross-sectional level, the connections and stability, e.g. buckling, has to be checked for in ULS.

For CLT and for timber in general, the design value of the resistance can be obtained by multiplying the characteristic strength value with the modification factor and dividing by the partial safety factor as follows.

$$R_d = k_{mod} \cdot \frac{R_k}{\gamma_M}$$

The modification factor k_{mod} , takes into account the effect of the load duration and the moisture content. Recommended values for CLT are shown in Table 12 for different load duration classes defined in Table 13 and are similar to the modification factors of solid timber and glued laminated timber but use is restricted to service class 1 and 2.

Load duration	Permanent	Long	Medium	Short	Very short
k_{mod}	0,60	0,70	0,80	0,90	1,10

Table 12 - Modification factor for CLT

Load duration	Definition	Examples of use
Permanent	More than 10 years	Self-weight
Long-term	6 months to 10 years	Storage loading
Medium-term	1 week to 6 months	Imposed floor loading
Short-term	Less than 1 week	Snow, wind
Instantaneous	Instantaneous	Accidental loading

Table 13 - Definition of load duration classes

Important to note is that when a load combination consists of actions belonging to multiple load duration classes, the value of the modification factor k_{mod} , should correspond to the action with the shortest duration, according to Eurocode 5 art. 3.1.3.

Currently, the partial safety factor γ_M for CLT is not yet in either the Eurocode or in the Dutch national annex to account for the material related uncertainties. In literature, a partial safety factor of 1,25 is proposed, with the recommendation that CLT should be regulated in the same way as GLT. The reason for this recommendation, are the significant lower variabilities in strength and elastic properties of CLT in comparison to the base material. This is due to the homogenization of properties caused by the mutual interaction of more than one element (Brandner, Flatscher, et al. 2016). For CLT connections, a partial safety factor γ_M of 1,30 should be used.

Another factor that, according to Eurocode 5, may be used for calculations in the ULS, is the system coefficient k_{sys} . The system coefficient accounts for the beneficial effect of parallel interacting boards in longitudinal direction. For the parallel interacting boards, it holds that the load distribution takes place via several structural elements simultaneously. This means that the chance that a defect in a

board (e.g. a knot) has catastrophic consequences is much smaller and thus, the strength of the element may be increased by k_{sys} .

The system effect may be applied when the boards are loaded in tension parallel to the fibre. These include the load situations of tension in plane and bending out of plane as can be seen in paragraph 4.7.1 and 4.7.2. In general practice, according to A. Thiel 2010 and several technical approvals, the system coefficient as shown in Figure 31 may be used, in which it is clear that the resistance of the CLT may be increased with increasing number of interacting boards (Unterwieser and Schickhofer 2013).

$$k_{sys} = \min \begin{cases} 1 + 0,025 \cdot n \\ 1,1 \end{cases}$$

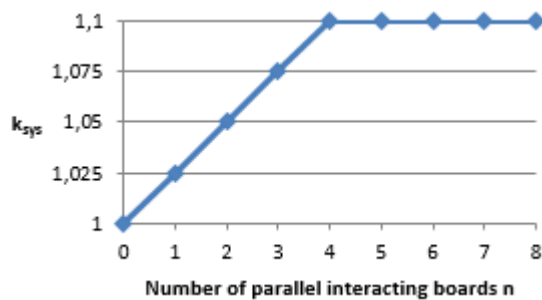


Figure 31 - Relation between number of boards parallel and system coefficient

4.7.1 Loading in plane

Tension, compression and bending

The verification of normal stresses in-plane only takes into account the net cross-sectional area, i.e. the layers in the direction of the stresses, meaning that the minor share of stresses transferred via the transverse layers is neglected. As can be seen below, the verifications of tension, compression and bending are very standard and are based on the net cross-sectional area of the corresponding layers in the strong parallel (0°) or weak in-plane transverse (90°) direction. The only points of attention are that as mentioned before, the resistance of tension in plane of CLT may be multiplied by the system factor k_{sys} . Next to that, the verification of compression in plane has to be complemented by a check against buckling for slender CLT elements, as demonstrated in 4.7.3.

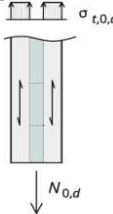
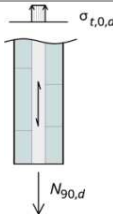
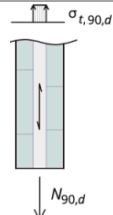
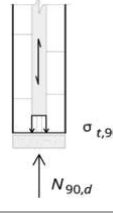
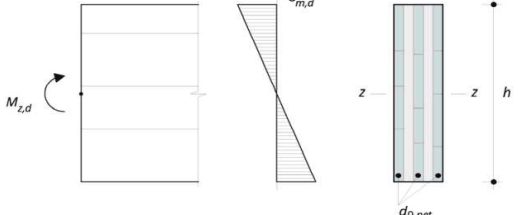
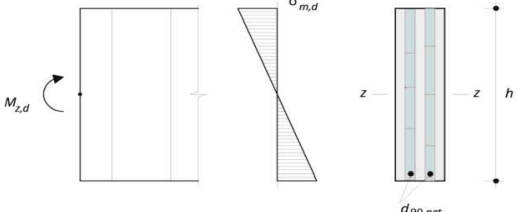
Tension parallel	$\sigma_{t,0,d} \leq f_{t,0,d}$ $\frac{N_{0,d}}{A_{0,net}} \leq k_{mod} \cdot k_{sys} \cdot \frac{f_{t,0,k}}{\gamma_M}$	
Tension transverse	$\sigma_{t,90,d} \leq f_{t,90,d}$ $\frac{N_{90,d}}{A_{90,net}} \leq k_{mod} \cdot k_{sys} \cdot \frac{f_{t,90,k}}{\gamma_M}$	
Compression parallel	$\sigma_{c,0,d} \leq f_{c,0,d}$ $\frac{N_{0,d}}{A_{0,net}} \leq k_{mod} \cdot \frac{f_{c,0,k}}{\gamma_M}$	
Compression transverse	$\sigma_{c,90,d} \leq f_{c,90,d}$ $\frac{N_{90,d}}{A_{90,net}} \leq k_{mod} \cdot \frac{f_{c,90,k}}{\gamma_M}$	
Bending parallel	$\sigma_{m,d} \leq f_{m,d}$ $\frac{M_d}{W_{0,net}} \leq k_{mod} \cdot \frac{f_{m,k}}{\gamma_M}$	
Bending transverse	$\sigma_{m,d} \leq f_{m,d}$ $\frac{M_d}{W_{90,net}} \leq k_{mod} \cdot \frac{f_{m,k}}{\gamma_M}$	

Table 14 - CLT in-plane strength verifications figures from (Wallner-Novak 2014)

Shear

Typical structural applications of CLT elements are panels used as wall and floor diaphragms making shear in-plane an important design verification. Presently, the in-plane shear capacity is still under discussion, resulting in conservative regulations. The current technical approvals for CLT products contain differing regulations on this behaviour. More detailed knowledge is necessary to fully profit from the high capacities of CLT concerning shear in-plane.

This paragraph gives more insight in the mechanisms that influence this capacity. The verification that is provided by the technical approvals up to now is based on the test results of single nodes. The procedure consists of checking the following three failure modes, as shown in Figure 32 and the accompanying verification formula:

- Gross-shear(I): Shear failure in all layers simultaneously
- Net-shear(II): Shear failure in the transverse layers in weak direction of the CLT
- Torsional shear(III): Torsional shear failure in the glued interface between the layers

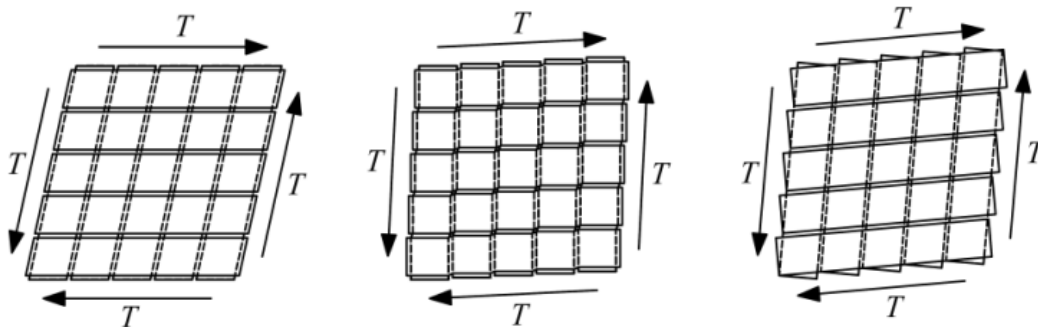


Figure 32 - Failure modes I, II and III for CLT loaded in in-plane shear (Flaig and Blaß 2013)

$$f_{v,k} = \min \left\{ \begin{array}{l} 3,5 \text{ (I)} \\ 8 \cdot \frac{h_{\text{net}}}{h_{\text{tot}}} \text{ (II)} \\ 2,5 \cdot \frac{1}{6 \cdot h_{\text{tot}}} \cdot \sum_{i=1}^{n-1} \frac{b_i^2 + b_{i+1}^2}{b_{\text{max}}} \text{ (III)} \end{array} \right.$$

With h_{net} as the smallest net cross-sectional thickness of both CLT directions and b as the layer width. Generally, the board width is not always known, which means that necessary assumptions might result in low shear strength values.

More realistic values may be based on full-scale tested CLT panels as shown in Figure 33, because lower variabilities can be expected than for single node tests. Tests that have been performed with full-scale CLT panels (Brandner, Dietsch, et al. 2015), varied in parameters like gap execution, board width, board (layer) thickness, number of layers, stress relief and layup parameter. Results show that the two parameters that do have a significant influence on the shear strength are the board thickness and the gap execution. With increasing layer thickness, a distinct decrease in net-shear strength can be identified and the specimens without gaps, but with bonded board edges, showed increased shear strengths.

Edge bonded specimen all failed in gross-shear (see Figure 33 right), but due to uncertainties in the unavoidable cracks (due to climate changes) of the timber, further research has to be conducted. So at the moment, the gross shear strength known for glulam $f_{v,gross,k} = 3,5 \text{ N/mm}^2$ is proposed.

It can also be concluded from the test results that torsional failure is only governing in case the ratio between the board thickness and the board width (t/b), exceeds 0,25. However, for commonly manufactured CLT this is hardly ever the case, also because all specimens without edge bonded boards failed in net-shear (see Figure 33 left). Consequently, a design concept based on the net-shear strength of the layers in the weak direction of $f_{v,net,k,ref} = 5,5 \text{ N/mm}^2$ is proposed (Brandner, Dietsch, et al. 2015). However, for layers in the weak direction with thicknesses between $20 \text{ mm} \leq t_{l,fail} \leq 40 \text{ mm}$ and without gaps higher shear strength values may be expected as shown below.

$$f_{v,net,k} = f_{v,net,k,ref} \cdot \min \left\{ \left(\frac{40}{t_{l,fail}} \right)^{0,3}, 1,20 \right\}$$



Figure 33 - Specimen failed net-shear (left) and gross-shear (right) (Brandner, Dietsch, et al. 2015)

In case of CLT elements with a layup parameter $\geq 0,80$, which means the thickness in the weak direction is almost the same as the thickness in the strong direction, the outer and middle layers (strong direction) are prone to fail. The potential failure of the weaker top layers can be explained by the missing “locking effect” for the outer layers. As a result it is expected that this leads to a decreasing shear strength in the magnitude of about one thickness class.

In the rare case that the torsional failure is the governing mechanism reference is made to the technical approvals again. The torsional shear strength highly depends on the annual ring orientation of the boards, however a value of $2,5 \text{ N/mm}^2$ is a safe and universally accepted value for the torsional shear strength of the single node interface between two perpendicularly crossing boards.

4.7.2 Loading out of plane

The in-plane load situation is the most beneficial load situation for CLT elements, because all fibres of the timber panel are oriented in that plane. However, a common application of CLT elements is the use of CLT as floor or roof elements. The ULS verifications in terms of compression, bending and shear of CLT loaded out of plane are presented in this paragraph. Tension out of plane is not dealt with here, because due to the low properties in this situation, generally it has to be prevented.

Compression

Common examples of this load situation are point supported floor panels and floor panels applied in platform type timber construction as can be seen in Figure 34 which will lead to compression perpendicular to the grain.



Figure 34 - Point supported CLT panels (left) and line supported CLT panels (right) (Brandner and Schickhofer 2014)

Several investigations have been conducted (Brandner and Schickhofer 2014), (Bogensperger, Augustin and Schickhofer 2011) in order to investigate the compression strength of CLT out of plane for point loads as well as line loads on different positions of load introduction. The investigations consist of finite element models which are validated through full scale tests. The models for GLT have been used to form a basis and comparison for CLT tests.

The parameters that are of importance for determining the ULS resistance against compression loads out of plane are the perpendicular to the grain compressive cube strength and the factor for the 'hang-in effect'. The latter can be explained by the positive supporting effect of the influence area next to the contact area. In comparison to GLT, CLT has the important benefit, that the cross layers cause a 'locking effect' and therefore a reduction of deformation. In testing timber/GLT cubes for compression strength, the failure mechanism is tension perpendicular to the grain, comparable by concrete cube tests. However for CLT cubes, the deformation perpendicular to the grain is significantly reduced and concentrated on each single layer.

In (Bogensperger, Augustin and Schickhofer 2011) the characteristic compressive strength perpendicular to the grain that followed from extensive testing and modelling is proposed to be 2,85 N/mm². Additionally, the coefficient $k_{c,90,CLT}$, which adjusts the basic properties in compression perpendicular to the grain to real design situations with point- and line-loads. When the values of $k_{c,90,CLT}$ which are proposed by the research are not used, A_{eff} may be increased by 30mm on both sides of the real contact area, in the direction of the fibre of the top layers, as can be seen below.

$\sigma_{c,90,d} \leq f_{c,90,d}$ $\frac{N_{90,d}}{k_{c,90} \cdot A_{ef}} \leq k_{mod} \cdot \frac{f_{c,90,k}}{\gamma_M}$ $k_{c,90,CLT} = \begin{cases} 1,90 & \text{central load (} a \geq 2 \cdot d \text{)} \\ 1,40 & \text{edge or corner load} \end{cases}$	
--	--

Table 15 - CLT out-of-plane compression verification figure from (Wallner-Novak 2014)

Even more detailed values for the $k_{c,90,CLT}$ coefficient take the layup of the CLT in consideration (Brandner and Schickhofer 2014). Optionally, the capacity of CLT in this load situation can be increased by reinforcing local areas with screws for example but additional research has to be carried out.

Bending and shear

The bending and shear verifications are more straight forward and based on the net-cross sectional values again. As mentioned in the introduction of this paragraph, the bending verification may be increased by the system factor for simultaneously interacting parallel boards. The effect side of the shear verification out-of-plane is based on the net-cross sectional area to build up, however on the resistance side, the rolling shear strength of the transverse layers closest to the neutral axis are generally decisive. In case the cross-section of the CLT has a special build-up, the shear strength $f_{v,d}$ of the layers in longitudinal direction, has to be checked as well.

Bending parallel	$\sigma_{m,d} \leq f_{m,d}$ $\frac{M_{0,d}}{W_{0,net}} \leq k_{mod} \cdot k_{sys} \cdot \frac{f_{m,k}}{\gamma_M}$	
Bending transverse	$\sigma_{m,d} \leq f_{m,d}$ $\frac{M_{90,d}}{W_{90,net}} \leq k_{mod} \cdot k_{sys} \cdot \frac{f_{m,k}}{\gamma_M}$	
Shear parallel	$\tau_{V,R,d} \leq f_{V,R,d}$ $\frac{V_{0,d} \cdot S_{0,R,net}}{I_{0,net} \cdot b} \leq k_{mod} \cdot \frac{f_{V,R,k}}{\gamma_M}$	
Shear transverse	$\tau_{V,R,d} \leq f_{V,R,d}$ $\frac{V_{90,d} \cdot S_{90,R,net}}{I_{90,net} \cdot b} \leq k_{mod} \cdot \frac{f_{V,R,k}}{\gamma_M}$	

Table 16 - CLT out-of-plane bending and shear verifications figures from (Wallner-Novak 2014)

4.7.3 Buckling

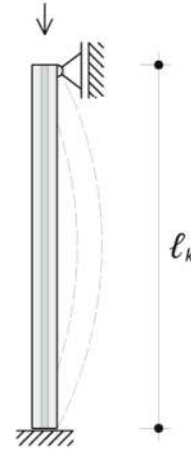
For slender members loaded by in-plane compression, the stability in terms of susceptibility to buckling has to be verified. To verify the stability of a CLT element in terms of buckling, the procedure according to Eurocode 5, clause 6.3.2, can be performed. However, in case of buckling, the shear flexibility of the transverse layers must be considered. Since their influence, however, normally is below 2%, here it is neglected (Wallner-Novak, Koppelhuber and Pock 2014).

Verification:

$$\frac{\sigma_{c,0,d}}{k_{c,y} \cdot f_{c,0,d}} + \frac{\sigma_{m,d}}{f_{m,d}} \leq 1$$

$$\frac{\frac{N_d}{A_{net}}}{k_{c,y} \cdot f_{c,0,d}} + \frac{\frac{M_d}{W_{net}}}{f_{m,d}} \leq 1$$

$$\lambda_y = \frac{l_{k,i}}{i_{y,0,ef}} = \frac{l_{k,i}}{\sqrt{\frac{I_{y,0,ef}}{A_{0,net}}}}$$



With: k_c Instability factor

$$k_{c,y} = \frac{1}{k_y + \sqrt{k_y^2 - \lambda_{rel,y}^2}}$$

k_y Buckling coefficient

$$k_y = 0,5 \cdot (1 + \beta_c \cdot (\lambda_{rel,y} - 0,3)) + \lambda_{rel,y}^2$$

β_c Coefficient of imperfection (assumed equal to 0,1 for glued laminated timber)

$\lambda_{rel,y}$ Relative slenderness¹

$$\lambda_{rel} = \frac{\lambda_y}{\pi} \cdot \sqrt{\frac{f_{c,0,k}}{E_{0,05}}}$$

$l_{k,i}$ Buckling length of the element

¹ For buckling calculations the values of $f_{c,0,k}$ and $E_{0,05}$ for glued laminated timber has to be taken into account.

4.8 Serviceability limit state

4.8.1 Stiffness and deformation

4.8.1.1 Shear in-plane

To determine the shear stiffness properties for a CLT element in-plane, a lot of research has been carried out. Investigations are based on two separate mechanisms, which can be superposed regarding flexibility. Mechanism I is a pure shear mechanism with full shear transmission between the narrow faces of the boards. In fact, the shear transmission between the narrow faces of the boards is recommended not to be considered because of cracks that will develop due to climate changes. This means that there is no difference in calculation method between CLT-elements with glued or unglued narrow faces of the boards, neither with CLT-elements with lateral gaps between the boards. Mechanism II is represented by a local torsional moment acting on both sides of the glued interfaces. Mechanism II actually contains all changes which have to be made to vanish all shear stresses at the narrow faces of the boards.

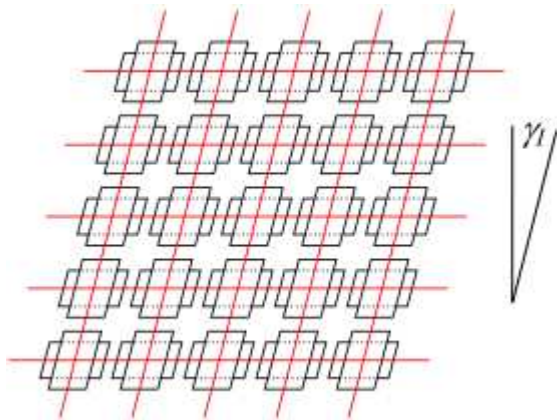


Figure 35 - Mechanism I: Shearing deformation (Bogensperger, Moosbrugger and Silly 2010)

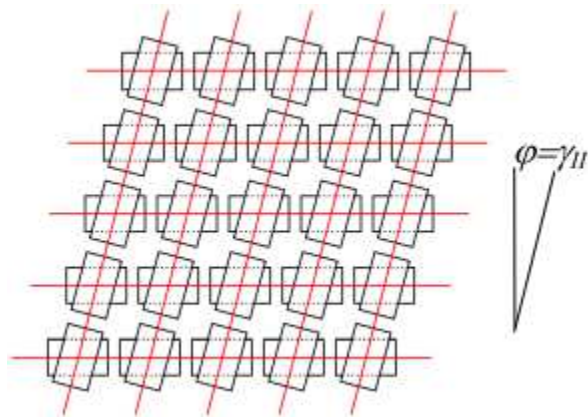


Figure 36 - Mechanism II: Torsional deformation (Bogensperger, Moosbrugger and Silly 2010)

The research that has been carried out is based, next to tests, on a representative volume element (RVE) of a CLT-element (Bogensperger, Moosbrugger and Silly 2010). This RVE can be simplified even more to the representative volume sub element of two layers including interface (RVSE).

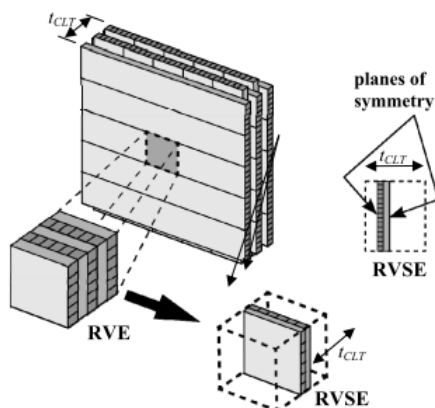


Figure 37 - RVE and RVSE elements for CLT elements (Bogensperger, Moosbrugger and Silly 2010)

Based on this simplification a finite element study was carried out to find the shear stiffness of CLT which is a reduced value compared to a homogeneous material. The following equations are the result of fitting the results of several finite element models with an increasing t/a (thickness over width of the boards) parameter.

$$G_{CLT} = G_{0,mean} \cdot \frac{1}{1 + 6 \cdot \alpha_{FE} \cdot \left(\frac{t}{a}\right)^2} \approx 0,75 \cdot G_{0,mean}$$

$$\alpha_{FE} = \begin{cases} 0,5345 \cdot \left(\frac{t}{a}\right)^{-0,7947} & (3 - layered CLT element) \\ 0,4253 \cdot \left(\frac{t}{a}\right)^{-0,7941} & (5 - layered CLT element) \end{cases}$$

4.8.2 Time dependent deformation

Finally when the deformation has to be calculated, the deformation coefficient k_{def} for the material CLT will be necessary. To calculate the deformation due to creep the instantaneous deformation has to be multiplied with the deformation coefficient, which depends on the utilisation class. The values are based on analyses of TU Graz (Jöbstl and Schickhofer 2007).

$$w_{creep} = k_{def} \cdot w_{inst,qp}$$

Deformation factor		
Utilisation class	1	2
k_{def}	0,80	1,00

Table 17 - Deformation coefficients for CLT

For the verification of deformations, long-term effects due to creep are taken into account by the product and service class specific deformation factor k_{def} . Due to the orthogonal layering of CLT, this factor also depends on the layup of CLT and requires additional attention if used for CLT composites. Because of the structure of CLT and the influence of rolling shear, it is proposed to assign CLT to plywood.

4.9 Fire Safety

This paragraph handles the fire safety aspects that are specifically of influence for CLT.

4.9.1 Charring

When sufficient heat is applied to wood, a process of thermal degradation (pyrolysis) takes place, which produces gasses, accompanied by a loss in mass. The cross-sectional dimension of the CLT element is reduced, when a charred layer is formed on the fire-exposed surface. In order to calculate the properties of the remaining cross-section, the reduced cross-section method can be used according to Eurocode 5. The part of the cross-section which will be affected by the fire consists of a charring depth and a layer thickness of $k_0 d_0$ that is affected by the elevated temperature and will no longer be able to transfer forces (SP 2010). The expression for the effective charring depth and the charring rate is shown below. When a residual laminate thickness of less than 3 mm remains, it should not be incorporated in the strength calculations.

$$d_{ef} = d_{char,n} + k_0 d_0$$

$$d_{char,n} = \beta_n \cdot t$$

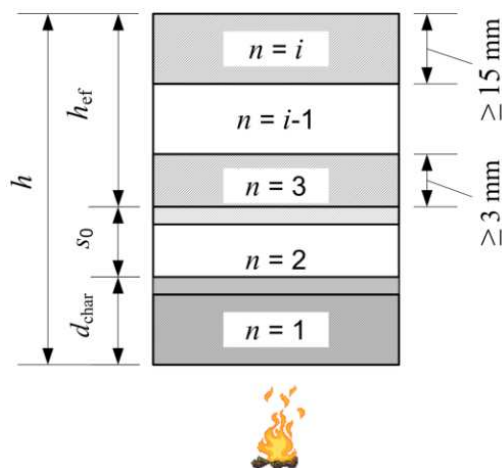


Figure 38 - Residual cross section, char layer and zero-strength layer (SP 2010)

In practice often a value of 7 mm for $k_0 d_0$ and a charring rate β_n of 0,65 millimetre per minute is adopted.

4.9.2 Delamination

The disadvantage of CLT compared to homogeneous solid timber panels is the possibility of delamination of the glued interfaces. Some types of adhesives are not able to withstand higher temperatures when charring occurs at the glued interface. The result is falling-off of charred layers. After falling-off, the charring rate is increased significantly because the timber is no longer protected by the former, protective layer. Also the positioning of the CLT elements, like walls or ceilings, significantly influences the charring rate because of the susceptibility for delamination (Frangi, Fontana, et al. 2008). At this moment there is no universally valid structural design method. In practical structural design the effect of delamination is often not incorporated. More detailed elaboration can be found in a recent research about self-extinguishment of CLT (Crielaard 2015).

4.9.3 Verification

In case of a fire situation the verifications may be based on values without considering the safety factors and with higher strengths (20% fractile).

At stress level the verification is as follows:

$$\sigma_{fi,d} \leq f_{fi,d}$$

$$\sigma_{fi,d} \leq k_{mod,fi} \cdot \frac{f_{20}}{\gamma_{M,fi}}$$

$$\sigma_{fi,d} \leq k_{fi} \cdot k_{mod,fi} \cdot \frac{f_k}{\gamma_{M,fi}} = 1,15 \cdot f_k$$

With: $k_{mod,fi}$ = 1,00 Modification factor in the event of fire
 f_{20} 20% fractile of strength at normal temperature
 k_{fi} = 1,15 Conversion coefficient for CLT from 5% to 20% fractiles
 $\gamma_{M,fi}$ = 1,00 Partial safety factor for timber in the event of fire

4.10 Connections

Due to the high stiffness and bearing resistance of CLT, the performance of solid timber structures e.g. CLT highly depends on the connections applied. This section reviews two connection types for an application in CLT elements. A lot of ways to connect timber elements are available and are being used, however in the scope of this thesis, glued-in rods and screws will be examined for an application in CLT in more detail. Screws are simple and low cost connectors. Glued-in rods are very strong and rigid. These two connection methods are concealed connections, which makes them aesthetically attractive and fire protected. This chapter describes the most important characteristics of these connections and the required design parameters for strength and stiffness.

To give a qualitative indication about the deformation behaviour of different connection types, a comparison is given in the load-slip curve of Figure 39, which is based on composite timber-concrete floors. This comparison is merely indicative and cannot be quantified exactly for each one, since they are highly dependent on different kind of aspects involved, as for example the test configuration (Dias 2005).

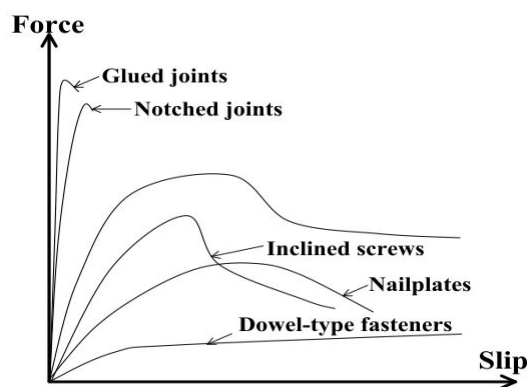


Figure 39 - Load slip curves for connections in timber-concrete composite floors (Dias 2005)

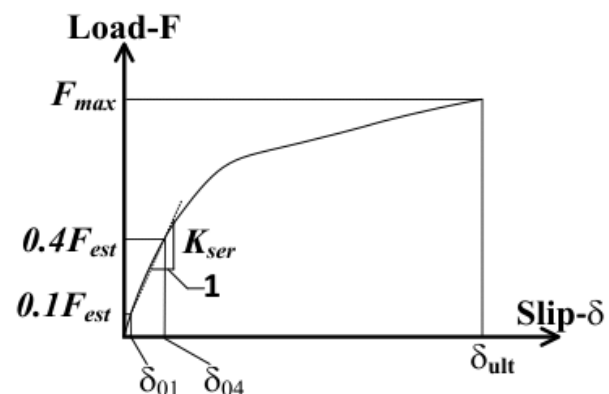


Figure 40 - Determination of K_{ser} (EN 26891)

Consequently, the calculation methods for the fire resistance is indicated. The rules given in the Eurocode 1995-1-2 are applicable to connections between members under standard fire exposure and for fire resistances not exceeding 60 minutes. In order to achieve higher fire resistances, a portion of the CLT thickness is considered in the same way as if it would be a wood-based panel that provides a passive fire protection.

4.10.1 Glued-in rods

A glued-in rod connection consists of a threaded steel rod that is glued in timber with an adhesive resin. For heavy timber construction, glued-in rods are becoming increasingly popular. This is mainly driven by the recent developments in CNC machining technology and the desire for a high level of prefabrication to reduce assembly time and cost (Karacabeyli and Douglas 2013).

Glued-in rods can be considered like a combination of a glued- and dowel-type connection. As indicated in Figure 39, a glued connection has a very high strength but a low ductility. On the other hand, the dowel type connection has a lower strength and is very ductile. When designed properly, a glued-in rod connection combines the qualities of both, to achieve high strength and good ductility.

The behaviour of a glued-in rod connection is a very complex problem, due to the interaction of three materials (wood, adhesive and steel). A lot of investigations have been carried out, primarily in order to predict the pull-out strength of glued-in rods. Despite many successful applications in practice, there is still a lack of consensus amongst researchers. Currently, there are no generally accepted design rules, because there are too many different theoretical approaches for the mechanisms and parameters governing the performance and strength of glued-in rods (Stepinac, et al. 2013). To arrive at safe strength values and realistic stiffness values, the design rules according to the German code DIN1052 are used and stiffness results from tests with CLT (Koets 2012) are used.

4.10.1.1 Execution

Several ways of gluing the rods into timber are possible. Generally, a hole of 1 to 4mm larger than the thickness of the rod is drilled into the timber. Preferably the difference between the thickness of the hole and the rod is minimized because many adhesives perform better with thin glue-lines and the necessary quantity of expensive adhesive is reduced. The adhesives that are most commonly used to make glued-in rod connections are 2-component PUR (polyurethanes) and EPX (epoxies).

After the hole is drilled, it should be cleaned thoroughly to get rid of any sawdust and assure a good bond. If the rod is situated at the top of the element, a certain amount of adhesive can be poured in the hole and the rod can be inserted, which drives the adhesive to the top as shown in Figure 41. The quality control is an important aspect of the execution of glued-in rods. Unfortunately this method of gluing has the disadvantage that there is no adequate control of the glue line quality, because it can not be assured that the glue line fills all cavities and no voids are present in the hole (Steiger, et al. 2015).

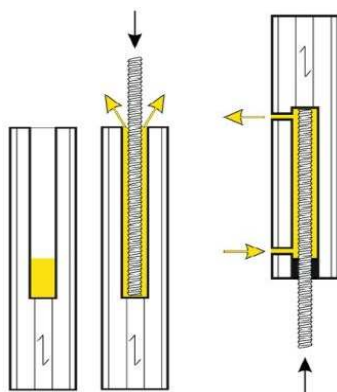


Figure 41 - Gluing the rods (Steiger, et al. 2015)

A better gluing technique is to drill additional holes perpendicular to the rod hole and to inject adhesive under pressure. When the rod hole is sealed at the end, the adhesive should be injected from the bottom, until it can be observed that the surplus of adhesive pours out at the top hole. Additionally, during the execution of a glued-in rod connection, unwanted inclinations of the drilled hole or the rod, eccentric position of the rod and incomplete insertion of the rod should be avoided to achieve a reliable connection.

4.10.1.2 Influence parameters

The three main components (wood, adhesive and rod) and the overall connection have their own parameters that interact with each other and are of influence to the performance of the glued-in rod connection as shown in Figure 42. The high number of material and/or geometrical parameters that determine the connection strength and stiffness are one of the main reasons for glued-in rods not being permanently included in the Eurocode.

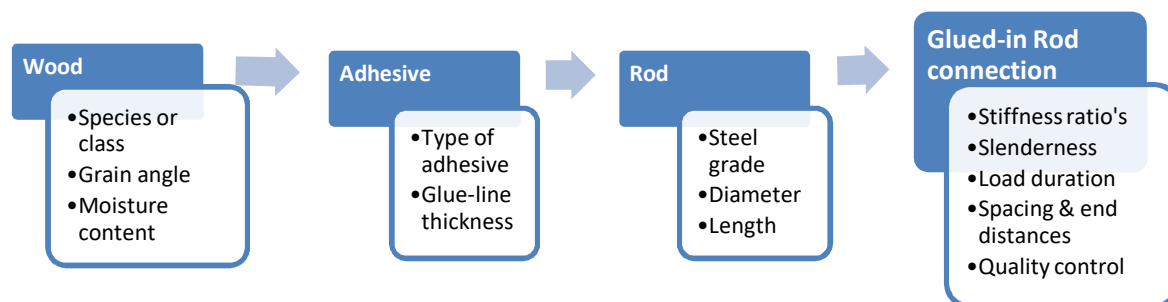


Figure 42 - Parameters influencing a Glued-in rod connection

4.10.1.3 Failure mechanisms

The majority of studies concerning glued-in rods are focused on the axial pull-out strength. To determine the axial pull-out strength, like every connection, the failure mechanisms need to be investigated. In Figure 43 the failure mechanisms are shown which will be explained.

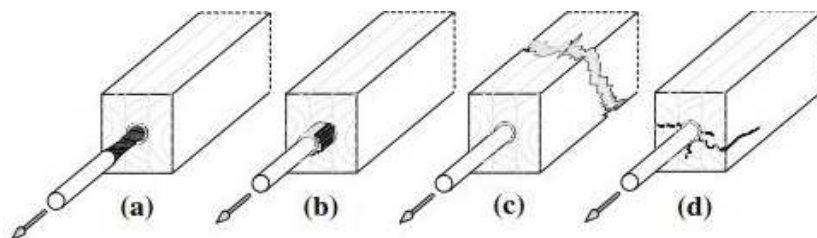


Figure 43 - Failure mechanisms for a single glued-in rod (Steiger, et al. 2015)

- Yield failure of the rod (a)
- Shear failure along the rod (b)
- Tensile failure of timber cross section (c)
- Splitting failure of timber (d)

If the rod's effective cross section of steel is the weakest link, yield failure of the effective cross section of the rod will occur. For metric threaded rods the effective diameter of a rod corresponds to about 90% of the outer diameter. The next failure mechanism is shear failure along the rod. This will happen in case the interface between the timber and adhesive fails in shear. In practice, a type of

adhesive is chosen with a higher strength than the shear strength of the timber. So when the strength of the adhesive is not critical, this will generally result in the extraction of a wood plug from the timber for shear failure along the rod. The susceptibility for this mechanism can be improved by countersinking the drill hole, or to shift the anchorage zone away from the surface by applying no adhesive at the face end (see Figure 41), in order to overcome peaks in the shear stress distribution (Tlustochowicz, Serrano and Steiger 2011).

The tensile failure of the timber cross section can also be a critical failure mode. This may happen at the end of the glued-in rod and characterizes rods glued-in perpendicular to the grain direction. At last splitting failure of timber starting at the end face can be the governing failure mode. This is usually caused by tension stresses perpendicular to the grain, as a result of imperfect axial loading or mixed load mode (axial and lateral). Minimum end distances are established in relation to this mechanism. CLT is much less prone to this mechanism because of the crossed layers which provide reinforcement for wood fibres from splitting in the longitudinal direction.

In a proper structural design, a ductile failure is recommended in order to provide sufficient robustness to the connection. The design strategy should assign the weakest link to an element of the glued-in rod system which provides sufficient ductility. Since the failure modes concerning the timber are all brittle (b, c and d), yield failure of the rod (a) is the preferred mechanism and can be assured by either choosing the right diameter of rods or by selecting a relatively low steel grade. Additionally, the glued-in rod should have a sufficient unbonded length to allow for elongation without damaging the glue bond.

4.10.1.4 Performance

As noted above, the performance of connections with glued-in rods is governed by very complex mechanisms and is dependent on a large number of geometrical, material and configuration parameters and their combinations. For this thesis, the strength will be considered according to a conservative design formula from DIN 1052. The stiffness values will be deducted from performed tests (Koets 2012).

Strength

The following formula describes the axial strength capacity according to the German code DIN 1052, which is the minimum value of the tensile capacity of the steel rod and the shear capacity of the bond line.

$$R_{ax,k} = \min \left\{ \begin{array}{l} f_{y,k} \cdot A_{ef} \\ \pi \cdot d \cdot l_a \cdot f_{k,1,k} \end{array} \right.$$

$f_{y,k}$	Characteristic yield strength of the rod
A_{ef}	Effective cross-sectional area of the rod
d	Nominal diameter of a rod
l_a	Anchorage length

And $f_{k,1,k}$ as being the characteristic bond line strength. This strength value can be calculated as follows to incorporate the nonlinear influence of the anchorage length.

$$f_{k,1,k} = \begin{cases} 4 & l_a \leq 250 \text{ mm} \\ 5,25 - 0,005 \cdot l_a & \text{for } 250 \leq l_a \leq 500 \text{ mm} \\ 3,5 - 0,0015 \cdot l_a & 500 \leq l_a \leq 1000 \text{ mm} \end{cases}$$

While this design formula is on the conservative side, it forms a reliable basis to verify the relatively complex connection. This is shown In Table 20, which allows the capacity for glued-in rods (M16 & M20) according to DIN 1052 to be compared with the values derived from tests with CLT with different rod to grain angles.

For the lateral capacity of glued-in rods, the rules for laterally loaded dowels according to Eurocode 5 section 8 apply. According to DIN 1052, for laterally loaded glued-in rods inserted parallel to the grain, the embedding strength should be taken as 10% of the embedding strength perpendicular to the grain (Tomasi 2012). This is a much bigger embedding strength reduction then by only using the factor k_{90} which is defined in Eurocode 5 for laterally loaded bolts.

When using the calculation method according to DIN 1052 the minimum spacing, end and edge distances have to comply with the following requirements shown below.

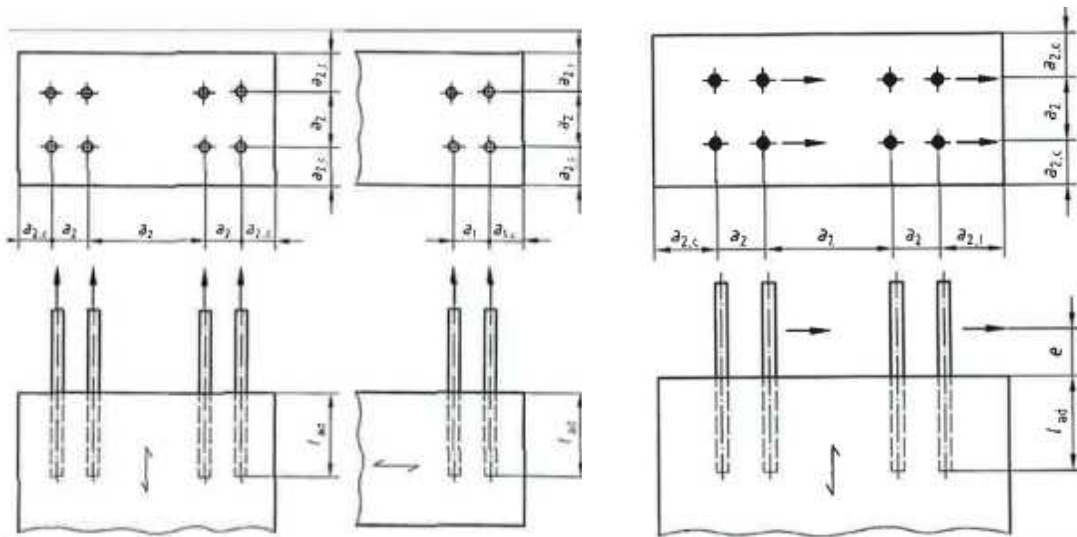


Table 18 - Designations of minimum spacing, end and edge distances for glued-in rods (DIN 1052)

GIR direction	parallel to fibre		perpendicular to fibre			
Minimum distance	a_2	$a_{2,c}$	a_1	$a_{1,c}$	a_2	$a_{2,c}$
	$5 \cdot d$	$2,5 \cdot d$	$4 \cdot d$	$2,5 \cdot d$	$4 \cdot d$	$2,5 \cdot d$

Table 19 - Minimum spacing, end and edge distances for glued-in rods

Stiffness

The stiffness forms an assumption for the finite element modelling of this connection. In literature there are big differences in the range of stiffness that should be adopted. In addition, there is the influence of the material CLT on the stiffness behaviour of the joint. In order to arrive at realistic stiffness values, the results of experiments (Koets 2012) have been used.

As mentioned before, the ductility of the connection is strictly related to its stiffness. If the pull-out failure is decisive in the design of the connection with glued-in steel rods, the connection has very high stiffness with negligible deformation up to sudden failure. If, on the contrary, steel rods failure is

decisive, the connection will have lower stiffness than in the previous case, but the connection will fail in a ductile manner, exhibiting visible warning displacements (Tlustochowicz 2011).

The axial stiffness of glued-in rods which is measured by (Koets 2012), shown in Table 20, is divided into two components. The first stiffness component K_I is the stiffness of the real glued-in part of the joint. The second component K_{II} represents the unglued part of the steel rod, which is EA/l . These two components are linked in series and can be modelled as two springs arranged in series to result in a combined axial stiffness K_{III} which is measured by the linear variable differential transformer (LVDT) in the experiments.

$$\frac{1}{K_I} + \frac{1}{K_{II}} = \frac{1}{K_{III}}$$

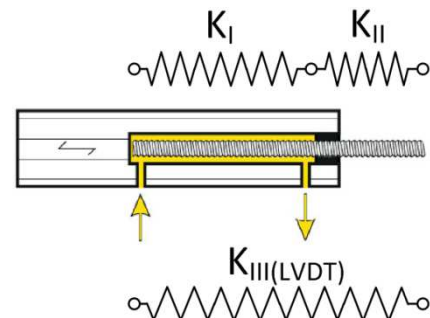


Figure 44 - Springs representing the Glued-in rod connection

Size	Grain angle α [°]	Anch. L. l_{ad} [mm]	$F_{ax,u}$ test [kN]	$F_{ax,k}$ DIN 1052 [kN]	K_I [kN/mm]	K_{II} [kN/mm]	K_{III} (LVDT) [kN/mm]
M16	0	240	76	48	388	198	131
	90	240	100	48	388	116	89
M24	0	360	152	94	436	312	182
	90	360	211	94	436	229	150

Table 20 - Performance parameters for glued-in rod connections in CLT (Koets 2012)

The value of K_{III} is determined by considering the 10% and 40% values of the maximum load as shown Figure 40 according to EN26891. From there the stiffness value of the glued-in part can be deduced.

For rods inserted parallel to the grain, the slip modulus K_{ser} (lateral stiffness) should be taken as follows as proposed by (Larsen and Munch-Andersen 2011).

$$K_{ser,lateral} = 0,08 \cdot d \cdot \rho_{mean}^{1,5}$$

The benefit for the glued-in rod of having such a high stiffness is due to there being no movement in hole clearance, because all voids in the glue-line are filled. Another phenomenon that can be seen from the results in Table 20 is the higher strength, but lower stiffness if the grain angle is changed from 0° to 90°. With GIR inserted parallel to the fibre, the wood plug pull out failure mechanism is governing, which leads to less capacity and more brittle failure.

4.10.2 Screws in CLT

A screwed connection is the most common way of connecting CLT elements, since roughly 60% of joints for the average CLT building are screwed (Flatscher, Bratulic and Schickhofer 2014). This paragraph presents the results on tests and the models to calculate the withdrawal- and shearing-off resistance of fully threaded self-tapping woodscrews. These screws, which are suitable for structural applications are in the range of 8 - 12 mm in diameter and normally up to 600 mm in length. In the past, tests have been done to determine empirical formulas for the resistance of screws in CLT (Uibel and Blaß 2007). Difference is made between screws in the surface and in the narrow face of a CLT element and additionally, the angle between the screw axis and the direction to the fibre.

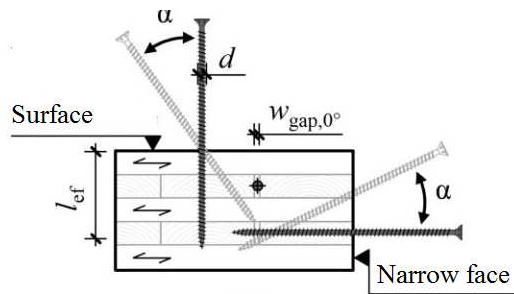


Figure 45 - designation for screw positions (Ringhofer, Brandner and Flatscher, et al. 2015)

4.10.2.1 Axial withdrawal capacity

The load bearing capacity of a fully threaded, self-tapping screw in the direction of its axis is determined by the minimum value of the resistance against withdrawal and the tensile load-bearing capacity of the screw's core cross-section. The characteristic value of the resistance against withdrawal can be calculated by the formula below, which is determined through extensive testing (Uibel and Blaß 2007).

$$R_{ax,s,k} = \frac{0,35 \cdot d^{0,8} \cdot l_{ef}^{0,9} \cdot \rho_k^{0,75}}{1,5 \cdot \cos^2 \varepsilon + \sin^2 \varepsilon}$$

With: d nominal screw diameter
 l_{eff} effective penetration depth
 ρ_k characteristic density
 $\rho_k = 400 \text{ kg/m}^3$ for screws on the surface
 $\rho_k = 350 \text{ kg/m}^3$ for screws on the narrow face i.e. edge joints
 ε angle between the screw axis and CLT layer direction
 $\varepsilon = 90^\circ$ for screws on the surface
 $\varepsilon = 0^\circ$ for screws on the narrow face

For tensile connections in the front face of cross-laminated timber, normally it cannot be ensured that the screw gets to rest in the centre of a side member. Therefore, it is conservatively assumed that the screw axis lies in the direction of the fibre ($\varepsilon = 0$).

The tensile load-bearing capacity of the screw can be calculated as follows with $f_{u,k} = 800 \text{ N/mm}^2$:

$$R_{ax,k} = f_{u,k} \cdot \frac{(0,6 \cdot d)^2 \cdot \pi}{4} = 800 \cdot \frac{(0,6 \cdot d)^2 \cdot \pi}{4} = 14,48 \text{ kN (with } d = 8 \text{ mm)}$$

4.10.2.2 Lateral shearing-off capacity

The shearing-off capacity of a single screw is dependent on the embedment strength. Uibel and Blaß (2007) tested to establish empirical formulas for the embedment strength of screws on the surface of CLT elements and the narrow faces. Because the embedding strength of screws in the surface of the CLT concerns the whole cross section while the embedding strength in the narrow face is about the relevant layers, different characteristic densities must be accounted for (Uibel and Blaß 2007). The embedment strength of screws, subject to shearing-off in the surface of a CLT element is as follows:

$$f_{h,k} = 0,112 \cdot d^{-0,5} \cdot \rho_k^{1,05} \quad \text{with } \rho_k = 400 \text{ kg/m}^3$$

The embedding strength of screws subject to shearing-off in the narrow face of the element independent of the angle between screw axis and grain direction:

$$f_{h,k} = 0,862 \cdot d^{-0,5} \cdot \rho_k^{0,56} \quad \text{with } \rho_k = 350 \text{ kg/m}^3$$

4.10.2.3 Performance of screwed joint assembly

In order to enable verifications and modelling of screwed joint assemblies, the capacities in terms of strength and stiffness have to be elaborated. Recently at the University of Graz, experiments have been done to investigate the behaviour of axially and laterally loaded self-tapping screw joint assemblies with different screw angles, seen in Figure 46.

The test results show high stiffness and load carrying capacity of an axially loaded self-tapping screw joint compared to laterally loaded joints for screws inserted at an angle of 90°. The relatively poor properties for only lateral loaded screws can be prevented by providing the screws with an inclination, as can be seen in the values in Table 21 for combined laterally and axially loaded screws.

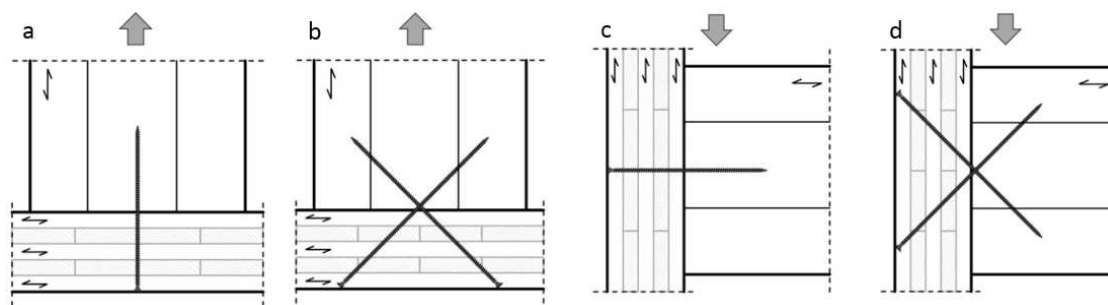


Figure 46 - Tested screwed connection configurations with axial- and lateral load (Flatscher, Bratulic and Schickhofer 2014)

Test setup	Screw angle [°]	F _{max} [kN]	K _{ser} [kN/mm]
Axial a	90	20,8	17,6
b	45 (per pair)	33,6	16,6
Lateral c	90	10,3	0,5
d	45 (per pair)	30,0	19,9

Table 21 - Test results of screwed connections (Flatscher, Bratulic and Schickhofer 2014)

Note: in the execution of screwed joints it should be ensured that the joined elements are clamped together to prevent the risk of the screw driving the components apart.

Different calculation models for the strength capacity can be found in published studies. The strength capacity for screwed joints can be calculated according to the above mentioned formulas according to Uibel and Blaß (2007). If the screw has a load(-component) in the axial direction, the withdrawal capacity will determine the strength capacity, as the withdrawal stiffness is many times higher than the embedding stiffness. If there is no axial component, the strength can be calculated by using the Johansen's formulas from Eurocode 5 including the 'rope'-effect. The validations between this calculation method and the test results found acceptable correlations for the axial load situation, however, comparatively higher deviations appear for inclined (45°) screws. This is mainly due to the withdrawal capacity according to Uibel and Blaß 2007 which is only applicable to grain to screw axis angle $\varepsilon = 0^\circ$ or 90° .

Recently, a more accurate and universal (in terms of applicability) approach to determine the strength of screwed CLT connections has been published (Ringhofer, Brandner and Flatscher, et al. 2015). This method is focused on the withdrawal failure mode and based on numerous investigations done in the past. Using multiplicative k-factors and k-functions, CLT related parameters are captured. This calculation method incorporates the effects of the joint angle, gaps in CLT and the system effect of screws penetrating multiple layers of the CLT. By using the following formulas the characteristic axial strength ($f_{ax,k}$) and capacity per screw ($F_{ax,k}$) can be calculated. Per pair of inclined screws the capacity has to be multiplied by $2 \times \cos(\alpha)$ for the axial and $2 \times \sin(\alpha)$ for the lateral load condition.

$$R_{ax,k} = f_{ax,k} \cdot d \cdot \pi \cdot l_{eff}$$

$$f_{ax,k} = k_{ax,k} \cdot k_{sys,k} \cdot f_{ax,ref,k} \cdot \left(\frac{\rho_k}{\rho_{ref,k}} \right)^{k_\rho}$$

$$f_{ax,ref,k} = 0,013 \cdot \rho_{ref,k}^{1,11} \cdot d^{-0,33}$$

The corresponding k-factors and k-functions are shown below which incorporates the characteristic effects of joint angle ($k_{ax,k}$), gaps (k_{gap}), density influence due to screw angle (k_ρ) and penetrating multiple layers ($k_{sys,k}$) with α as the angle between the grain and the screw axis.

$$k_{ax,k} = \begin{cases} 1,00 & \text{if } 45^\circ \leq \alpha \leq 90^\circ \\ 0,64 \cdot k_{gap} + \frac{1 - 0,64 \cdot k_{gap}}{45} \cdot \alpha & \text{if } 0^\circ \leq \alpha \leq 45^\circ \end{cases}$$

$$k_{gap} = \begin{cases} 0,90 & \text{CLT narrow edge} \\ 1,00 & \text{Other} \end{cases}$$

$$k_{sys,k} = \begin{cases} 1,00 & \text{Sawn timber (CLT narrow face)} \\ 1,10 & \text{CLT (N} \geq 3 \text{ surface, see Tablee22)} \end{cases}$$

$$k_\rho = \begin{cases} 1,10 & \text{if } 0^\circ \leq \alpha \leq 90^\circ \\ 1,25 - 0,05 \cdot d & \text{if } \alpha = 0^\circ \end{cases}$$

Eventually the minimum value of the capacities of the screw in the two elements will govern.

N	1	2	3	4	5	6	7	8
$k_{sys,k}$	1,00	1,06	1,10	1,12	1,13	1,14	1,15	1,16

Table 22 - $k_{sys,k}$ values in dependence of N (Ringhofer, Brandner and Schickhofer 2013)

4.10.2.4 Minimum spacing, end and edge distances for screws in CLT

The above mentioned capacities of screws in CLT are only valid when the following requirements concerning minimum spacing, end and edge distances are met. These requirements rule out the possibility of failure due to splitting and ensure that the full bearing capacity of the fastener is achieved. Splitting is a very brittle failure mechanism, so it has to be prevented at all times.

In Table 23, the values of the minimum spacing and end distances for screws in CLT are given. Figure 47 shows the distance designations for screws in the narrow face and surface of CLT with different load directions.

As can be seen in Table 23, spacing and end distances are less critical for fasteners inserted perpendicular to the plane (in surface) of the CLT due to cross laminations which tend to reinforce the cross-section. The subscript "t" refers to the stressed edge and the subscript "c" refers to the non-stressed end distance.

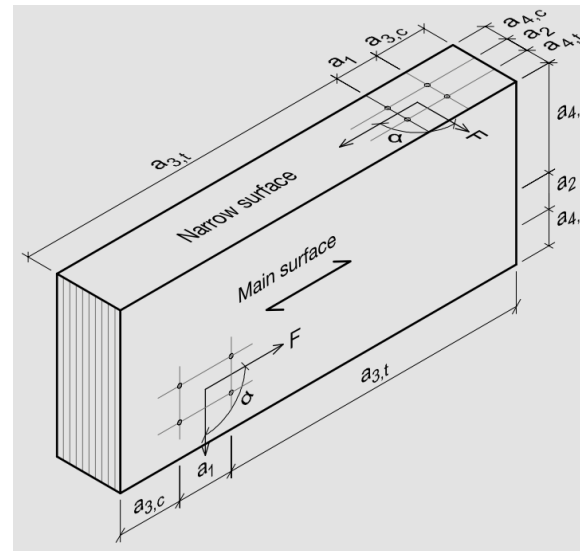


Figure 47 - Minimum spacing, end and edge distances (MERK Timber GmbH 2013)

Screw inserted	a_1	$a_{3,t}$	$a_{3,c}$	a_2	$a_{4,t}$	$a_{4,c}$
In narrow face	$10 \cdot d$	$12 \cdot d$	$7 \cdot d$	$3 \cdot d$	$6 \cdot d$	$3 \cdot d$
In surface	$4 \cdot d$	$6 \cdot d$	$6 \cdot d$	$2,5 \cdot d$	$6 \cdot d$	$2,5 \cdot d$

Table 23 - Minimum spacing, end and edge distances of screws in CLT (Uibel and Blaß 2007)

4.10.2.5 Effective number of fasteners

According to the Eurocode, the resistance of a connection with a group of screws should be determined using the statically effective number of screws. For the withdrawal resistance of a group of screws, the effective number of screws is $n_{eff} = n^{0,9}$. When the screws are subject to shearing-off, the effective number of screws depends on the spacing between the screws when they are inserted into the narrow face. For screws inserted in the surface of the CLT element, the reduction of the statically effective number of fasteners is not necessary. This is because of the transverse tensile reinforcement that can be assumed due to the element build-up, which prevents brittle failure by splitting.

n_{eff}	In narrow face	In surface
Withdrawal	$n^{0,9}$	$n^{0,9}$
Shearing-off	$n^{0,85} (a_1 \geq 10 \cdot d)$ $n^{0,9} (a_1 \geq 14 \cdot d)$	n

Table 24 - Effective number of screws for different configurations

4.10.2.6 Fire resistance

The fire resistance of screwed connections in CLT can be based on the fire resistance calculation method of timber-concrete composite slabs with screwed connections (Frangi, Knobloch and Fontana 2010).

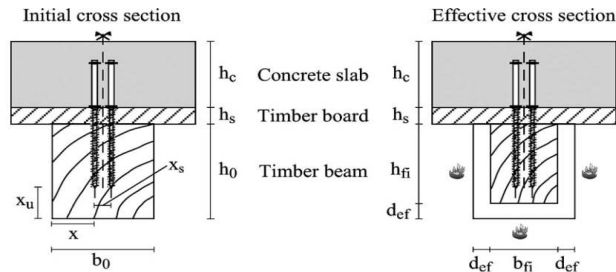


Figure 48 - Determination of the effective cross section in fire for timber-concrete composites (Frangi, Knobloch and Fontana 2010)

To reduce the connection strength in case of fire the following modification (reduction) factors for screwed connections can be used, depending on the side cover denoted by distance x .

Distance x	$k_{mod,fi}$
$x \leq 0,6t$	0
$0,6t \leq x \leq 0,8t + 5$	$\frac{0,44x - 0,264t}{0,2t + 5}$
$0,8t + 5 \leq x \leq t + 28$	$\frac{0,56x - 0,36t + 7,32}{0,2t + 23}$
$x \geq t + 28$	1

Table 25 - Modification factor for screwed connection strength in fire

The reduction factors of screwed connections in fire correspond to the following graph, which shows the reduction for different fire resistances.

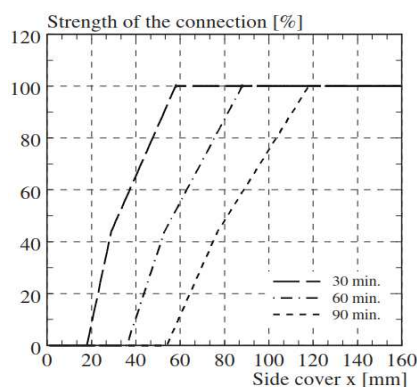


Figure 49 - Strength reduction of screws in case of fire (Frangi, Knobloch and Fontana 2010)

Due to the duration of this thesis project, verifications concerning resistances of connection in case of fire have not been performed. Nevertheless, as can be seen in Figure 49, the a significant drop of connection strength can be observed in case of a fire resistance of 90 minutes. Therefore, this can be a critical design limit. Solutions are a more eccentric position of screws and/or glued-in rods or extra fixation at the outside of the module.

5 Structural design

5.1 Introduction

This section deals with the structural design of the modular cross-laminated timber building that is investigated in this thesis. As previously noted, the building that forms a basis for the structural design being investigated is Hotel Jakarta in Amsterdam. First, the general design assumptions that are relevant for structural analysis are stated and explained. Then, the structural design and detailing of the module is shown and at last, the total building structure with inter-modular connections will be shown and explained.

5.2 General assumptions

An important practical assumption for the structural design is that the inside of the modules is only accessible during fabrication. This is due to the high level of prefabrication of the hotel rooms and the risk of damaging the finishing of the module interior with equipment during stacking and securing of the modules.

The design and calculations are based on the following general design assumptions:

- Design working life category: 3 (50 years)
- Consequence class: CC2 (residential/hotel/office ≤ 70 m)
- Reliability class: RC2
- Concrete strength class: C45/55 (common for prefab)
- CLT Merk Leno
- Location: Amsterdam

Apart from compliance with the requirements set by the governing legislation to build in Amsterdam, a requirement set to ensure comfort of the building is that there is no tension allowed between the modules in vertical direction for serviceability limit state verifications. This assumption is used to ensure that the modules will rest upon each other in the serviceability limit state. It has to be prevented that a change of sign (both tension and compression) in the vertical force due to wind, between two stacked modules will result in discomfort e.g. rattling sound.

The modules are assumed to be inherently robust in their construction. This means that the modules itself as well as the total assembly of modules is assumed to be 'self-supporting' against the acting load combinations.

The CLT that's being used, is produced by Merk and is CLT without lateral glued interfaces at the narrow faces of the boards, but without gaps (because of the preferred smooth esthetical finishing and air-tightness).

5.3 Module

In this thesis a module with a concrete floor will be investigated in more detail. As a qualitative indication, the possible design of a module with a CLT floor is given here as well. For both, the walls and the ceiling of the modules are constructed from CLT.

The key of the two variants is that in both cases, high compression stresses perpendicular to the grain of the timber are prevented. For the module with a concrete floor, the platform construction method is applied, because the floor is part of the wall. When the floor is made from CLT, the balloon construction type is applied, because the walls are continuous and the floors are attached to them.

The walls, ceilings and/or floors are cut from one piece of CLT, so there will be no longitudinal (lap) joints that have to be considered.

5.3.1 Dimensions

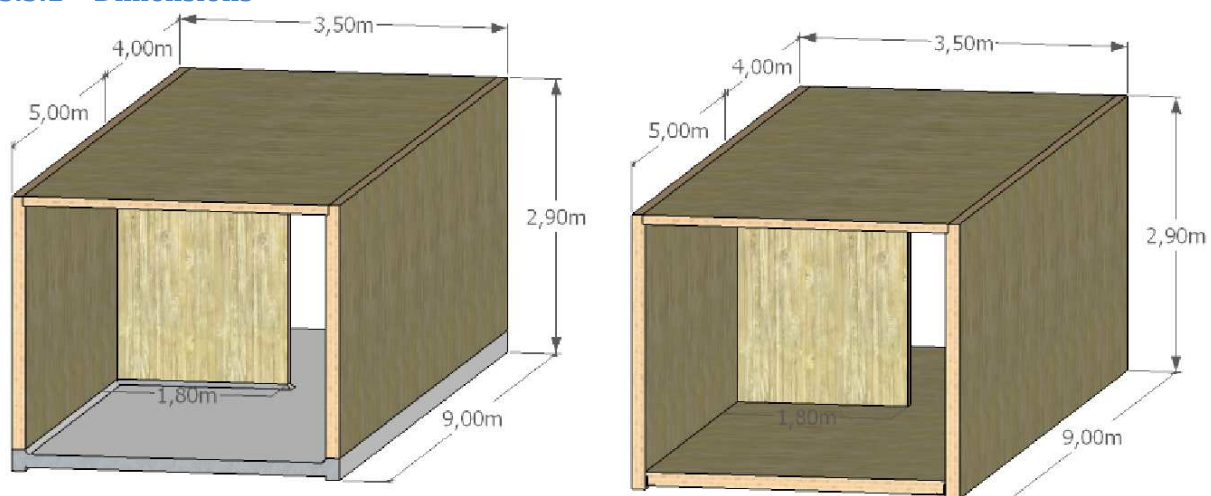


Figure 50 - Representation and dimensions of module with concrete (left) and CLT (right) floor

5.3.2 Detailing

The detailing of the modules itself consists of three different connection methods namely, screws, glued-in rods and screwed angle profile. The connection method of CLT elements to each other consists of screws, except for the CLT floor to wall connection, screwed steel angle profile is used. Screws are used because the simplicity and predictability of this connection method is beneficial. The modules are produced inside the factory, so accessibility is not an issue. Normally the lack of accessibility to screw two CLT parts together, is the reason that (angle) brackets are used. Additionally, the behaviour of screwed connections can be modelled more easily, because unlike (angle) brackets, no eccentricities are of influence for load application to CLT elements. The screws are positioned as inclined screw pairs under an angle of 45° . It is an inclination in one direction, due to the protection from fire and since dominating force direction is desired to be in-plane as much as possible.

The concrete floor is connected to the CLT elements by means of glued-in rods as can be seen in Figure 52 (left). Glued-in rods are used because of the high capacity and rigidity that can be achieved. Next to that, the rods are aesthetically beneficial, because they are hidden inside the CLT, which also protects the rods in a fire situation. The bolt anchors need to be accurately positioned inside the precasting mold before pouring the concrete. After hardening, rods can be screwed onto the bolt anchors and after that the CLT panels can be placed over the rods and then glue can be injected as shown in previous chapter.

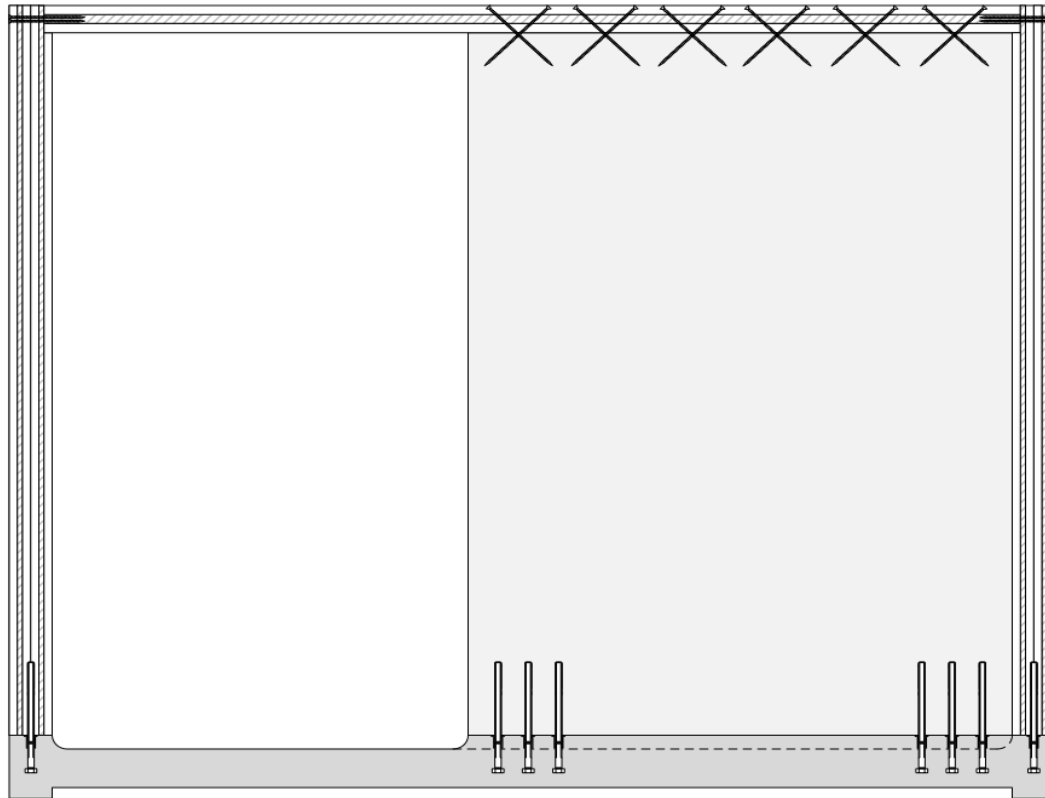


Figure 51 - Transverse cross-section of module (concrete floor)

The CLT floor can be placed upon steel angle profiles to be connected to the side walls as can be seen in Figure 52 (right). The steel angle profiles are screwed onto the side wall and the floor. If only screws were used, then the lateral load direction would be dominating. Since the capacity of screws is not sufficient, a steel angle profile is used to form a strong and stable support for the CLT floors. In positioning the connections in the element the minimum spacing and end distances have been taken into account.

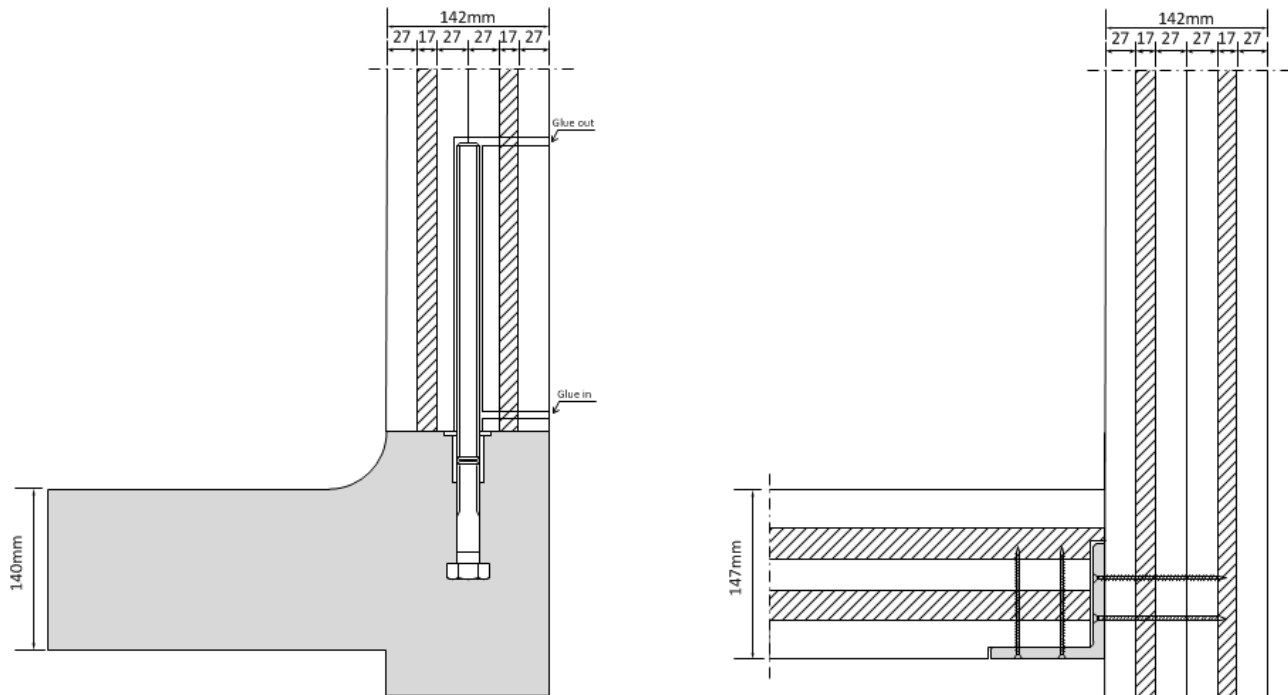


Figure 52 - Cross section wall-floor concrete (left) and CLT (right)

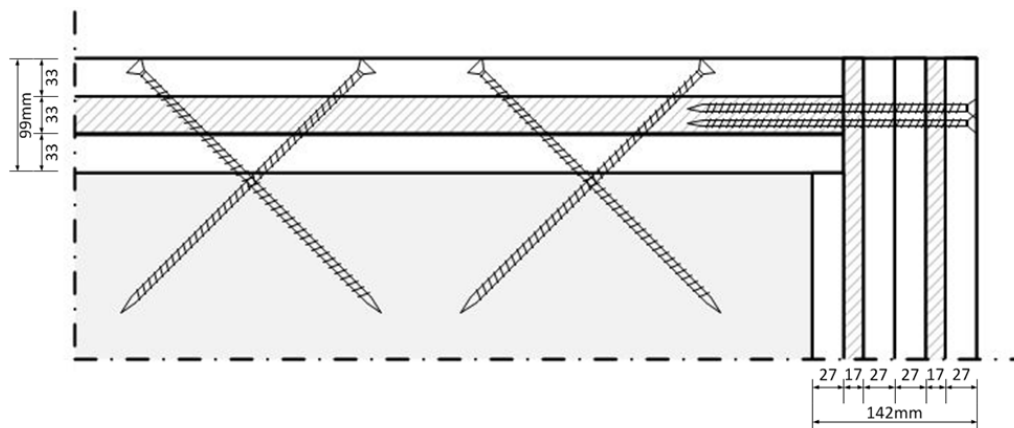


Figure 53 - Cross section wall-ceiling-stabilization wall

5.4 Modular building structure

The modular building structure simply consists of stacked modules onto a concrete podium structure. The modules are connected to each other by means of inter-modular connections.

5.4.1 Modular assembly

Below in Figure 54, the assembly of modules together with the podium structure is shown. The same figure contains the designations for the number of modules on top of each other (n) and for the number of modules next to each other (m). In this thesis the focus is put on a modular configuration $m \times n$ of 8×8 .

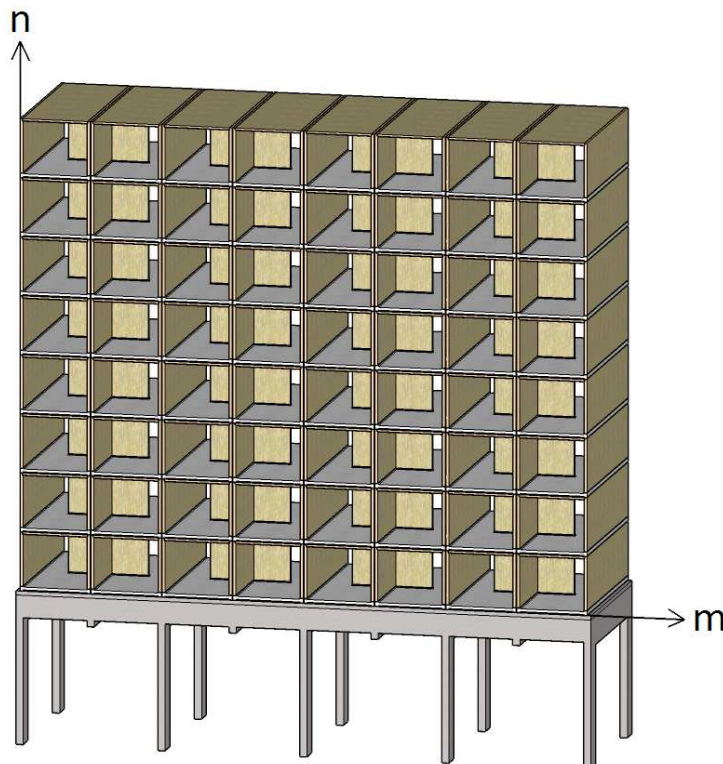


Figure 54 - Modular building structure (8 x 8)

By taking a closer look to the podium structure in Figure 55, it can be seen that all the side walls are supported by a concrete beam. These horizontal beams are assumed to be 1,40 m in height and 0,35 m thick. The same thickness holds for the columns that have a width of 1 m. The very heavy side beams support the podium beams that are not supported by a column. In this thesis no distinction is made in the stiffness of the different podium beams.

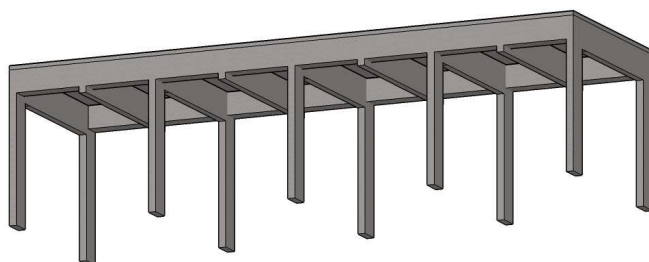


Figure 55 - Concrete podium structure

5.4.2 Inter-modular detailing

Below the inter-modular detailing is shown. The inter-modular connections designed consist of a steel T-shaped angle plate with pins. The steel pins fit accurately into the steel cones that should be casted into the pre-fabricated floor slab. The reasoning behind the connection consists of the following steps. After two horizontal modules are placed next to each other, the T-shaped angle plate can be screwed on top of two neighbouring side walls. During screwing, the three T-shaped angle plates in a row should be held accurately into position by using a mold over the 6 pins that corresponds mold used for precasting the steel cones in the concrete floor. The next step is to place the third module over the angle plate (as seen in the right bottom figure) and to secure the angle plate onto the concrete slab by using (drilled or glued) anchors. After that, the fourth module can be placed with the accurately pre-casted cones over the steel pins.

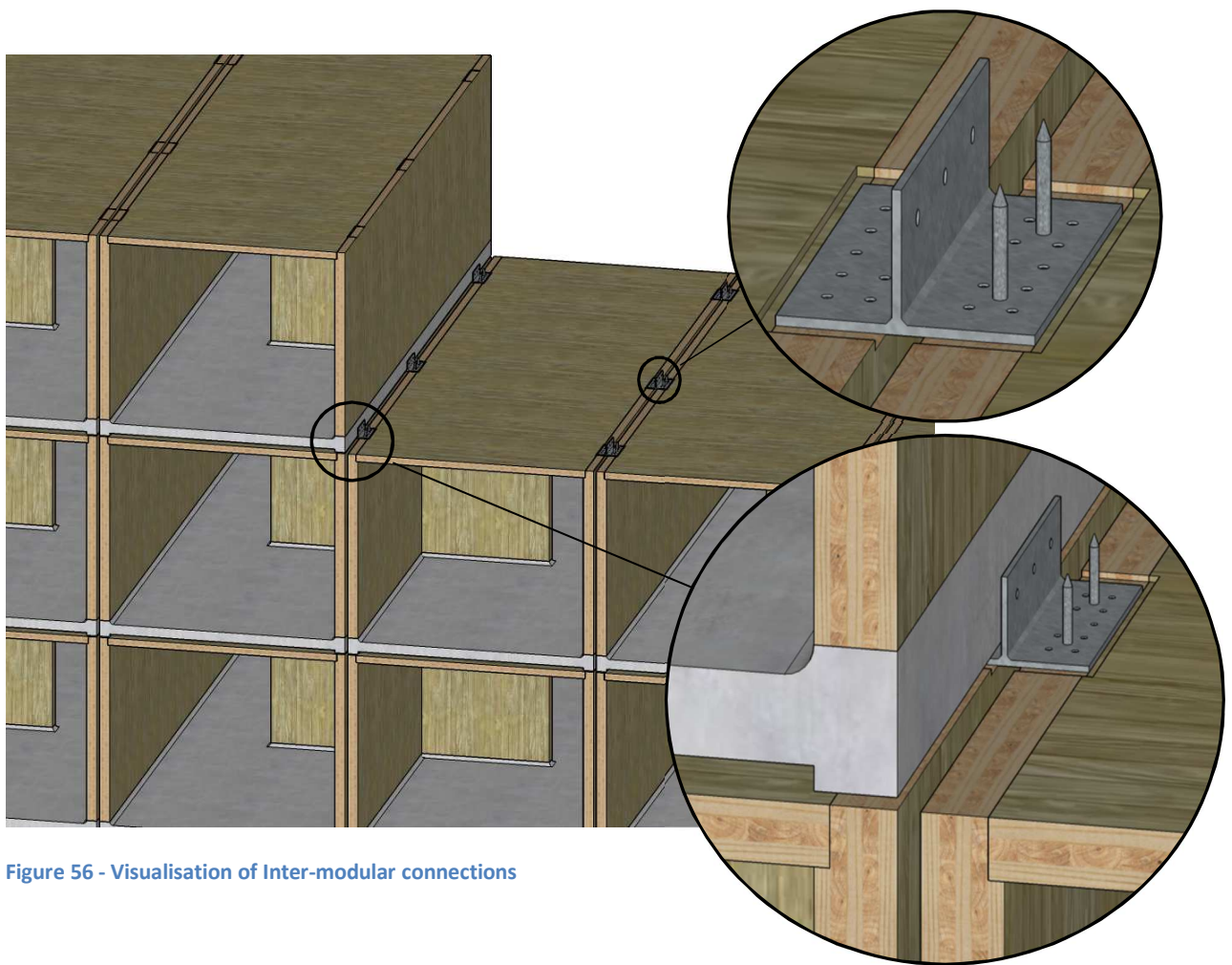


Figure 56 - Visualisation of Inter-modular connections

Bearing strips

According to a modular case study (Getzner 2015), it appears that 90% of sound transmission takes place through the walls of the modules. In order to significantly reduce sound and vibration transmission through the modular walls, Sylomer elastic bearing strips can be used, to equally transfer the loads from one module to another without causing sound- and vibration bridges. The strips can be seen in **Figure 57**, in which it is shown that the strips can be applied both between the walls as well as in between the inter-modular connections.



Figure 57 - Sylomer elastomeric bearing strips

6 Loads

In order to investigate the structural behaviour of a module and the behaviour of the modular building, the different load cases and load combinations must be made clear. In addition to quantifying the loads according to EC 1991, the values will be converted to a one meter strip width value which acts on the side edge of the floor elements. First the different load cases that act on the building are set and then the load combinations which have to be resisted in ultimate limit state and serviceability limit state.

6.1 Load cases

The modules and the structural system of the stacked modules are loaded by the following load cases. Load case 3, includes the notional horizontal loads that should be combined with wind load as described in paragraph 3.3.1.

- Permanent loads
- Variable loads
- Wind load (+notional horizontal loads)

6.1.1 Permanent loads

The permanent loads shown below are a result of the self-weight of the structural and non-structural components of the building and are converted from floor loads to line loads along the side walls.

Floor loads:

Module		Concrete floor	CLT floor
• Floor concrete/CLT h = 140/142 mm	=	3,50 kN/m ²	0,66 kN/m ²
• CLT ceiling h = 99 mm	=	0,45 kN/m ²	0,45 kN/m ²
• Permanent partition walls/finishing	=	0,30 kN/m ²	0,30 kN/m ²
• Installations	=	0,20 kN/m ² +	0,20 kN/m ² +
• Total		4,45 kN/m²	1,61 kN/m²

Roof		
• Extra CLT ceiling height h = 43 mm	=	0,20 kN/m ²
• PV (solar) cells	=	0,70 kN/m ²
• Insulation/bitumen	=	0,20 kN/m ² +
• Total	=	1,09 kN/m²

Line loads (onto side wall):

Module			
• CLT wall t = 142 mm, h = 2,75 m	=	1,69 kN/m	1,69 kN/m
• Floor loads x 1,75 m	=	8,10 kN/m +	2,81 kN/m +
• Total q _G	=	9,79 kN/m	4,51 kN/m

Roof		
• Roof load q _{G,roof} x 1,75 m	=	1,91 kN/m

6.1.2 Imposed loads

The variable loads on the building originate from people and furniture and are shown below. These floor loads are determined for a probability of exceeding of 5% in 50 years, according to the Eurocode.

Module (Category A)		Floor load	x 1,75 m	Line load
• Sleeping room in hotel	=	1,75	kN/m ²	3,06 kN/m
• Stairs	=	2,00	kN/m ²	
• Balconies	=	2,50	kN/m ²	

Roof (Category H)

• Roofs	=	1,50	kN/m ²	2,63 kN/m
---------	---	------	-------------------	-----------

Because these loads are extreme values, the probability that they will ever occur for every floor at the same moment is very small. That is why, according to art. 6.3.1.2 (11) of the Dutch national annex of EN 1991-1-1, the extreme values of the imposed floor load only has to be applied on the two floors for which the result of the load has the largest effect on the structure. The imposed floor loads on the other floors may be reduced by a factor ψ_0 . If the imposed floor load is not the main variable load, then every imposed floor load has to be multiplied by ψ_0 . These reduction factors for simultaneously acting variable loads on the structure are shown in the paragraph about load combinations (0). Note: Roofs are generally not considered as floors concerning this approach.

6.1.3 Wind load

The most significant horizontal load that acts on the modular building is the wind load. In this chapter the wind loads are examined according to the European standard EN 1991-1-4. The wind load will vary for different building configurations in terms of total building height, width and depth. In order to obtain an accurate value of the wind for different building configurations, the calculation method is shown below and is worked out in a parametric calculation sheet.

Assumptions wind load

Building dimension		⊥ on modules	// on modules
Height	h	n x 2,90 m + 7,33 m	n x 2,90 m + 7,33 m
Width	b	m x 3,5 m	9 m
Depth	d	9 m	m x 3,5 m

Table 26 - Input of building dimensions for wind load calculations

Wind area II (Amsterdam)
 Terrain category II (rural)

The general formula to calculate the force acting on the structure or structural component is as follows:

$$F_w = c_s c_d \cdot \sum c_f \cdot q_p(z_e) \cdot A_{ref}$$

In which:

$c_s c_d$ Structural factor
 c_f Force coefficient for location of structural element
 $q_p(z_e)$ Peak velocity pressure at reference height z_e
 A_{ref} Reference area on structure or structural element

Peak velocity pressure

The peak velocity pressure $q_p(z)$ at height z depends on the air density ρ , the turbulence intensity, the terrain factors and the mean wind velocity that belongs to the associated terrain category and wind area respectively. In Table 27, the method to determine the peak velocity pressure according to the Eurocode is described.

Parameter	Formula	Constants	EC 1991-1-4
Peak velocity pressure	$q_p = (1 + 7 \cdot I_v(z)) \cdot \frac{1}{2} \cdot \rho \cdot v_m^2$	$\rho = 1,25 \text{ kg/m}^3$	Form 4.8
Turbulence intensity	$I_v(z) = \frac{k_1}{c_0(z) \cdot \ln\left(\frac{z}{z_0}\right)}$	$k_1 = 1$ $z(0) = 0,2 \text{ m}$	Form 4.7
Mean wind velocity	$v_m(z) = c_r(z) \cdot c_0 \cdot v_{b,0}$	$v_b = 27 \text{ m/s}; c_0 = 1$	Form 4.3
Roughness factor	$c_r(z) = k_r \cdot \ln\left(\frac{z}{z_0}\right)$		Form 4.4
Terrain factor	$k_r = 0,19 \cdot \left(\frac{z_0}{z_{0,II}}\right)^{0,07}$	$z_{0,II} = 0,05 \text{ m}$	Form 4.5

Table 27 - Method to calculate the peak velocity pressure

Once the peak velocity pressures are elaborated, the velocity pressure distribution on the building depends on the height of the building in relation to the width of the building. If the height is smaller than the width of the building, a uniform distribution is allowed. If the building is higher than the width, but smaller than two times the width of the building, the distribution comprises of two parts. For buildings higher than two times the width, multiple parts have to be considered as shown in Figure 58.

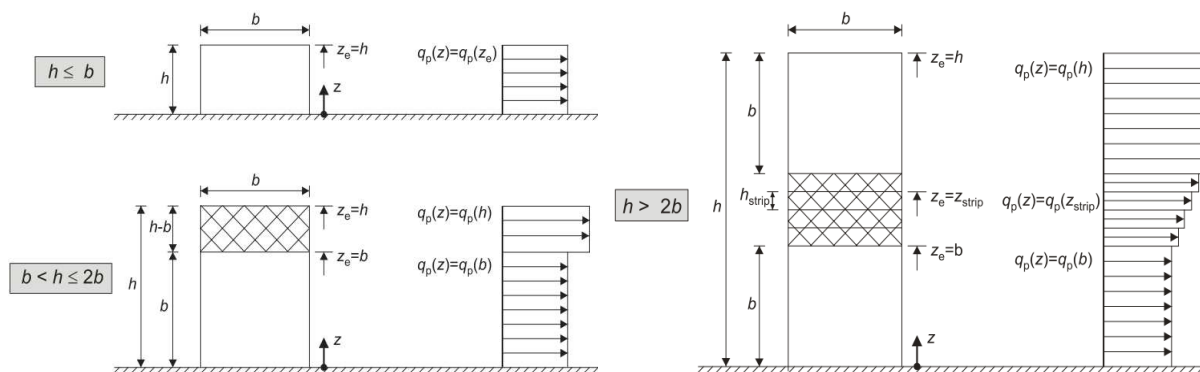


Figure 58 - Peak velocity pressure profiles over building height (EN 1991-1-4)

Structural factor

The structural factor $c_s c_d$ should take into account the probabilistic aspects of peak wind pressures on the surfaces subject to wind forces, in relation to the structure's vibrations as a result of turbulence. In Table 28, the method to determine the structural factor, according to the Eurocode, is described.

Parameter	Formula	Constants	EC 1991-1-4
Structural factor	$c_s c_d = \frac{1 + 2 \cdot k_p \cdot I_v(z_s) \cdot \sqrt{B^2 \cdot R^2}}{1 + 7 \cdot I_v(z_s)}$	$z_s = 0,6 h$	Form 6.1
Background factor	$B^2 = \frac{1}{1 + \frac{3}{2} \cdot \sqrt{\left(\frac{b}{L(z_s)}\right)^2 + \left(\frac{h}{L(z_s)}\right)^2 + \left(\frac{b}{L(z_s)} \cdot \frac{h}{L(z_s)}\right)^2}}$ $L(z_s) = L_t \cdot \left(\frac{z_s}{z_t}\right)^\alpha ; \alpha = 0,67 + 0,05 \cdot \ln z_0$	$L_t = 300 \text{ m}$ $z_t = 200 \text{ m}$	Form C.1 Form B.1
Resonance-response factor	$R^2 = \frac{\pi^2}{2 \cdot \delta} \cdot S_L(z_s, n_{1,x}) \cdot K_s(n_{1,x})$ $S_L = \frac{6,8 \cdot f_L(z_s, n_{1,x})}{1 + 10,2 \cdot f_L(z_s, n_{1,x})}$ $f_L = \frac{n_{1,x} \cdot L(z_s)}{v_m(z_s)}$ $K_s = \frac{1}{1 + \sqrt{(G_y \cdot \phi_y)^2 + (G_z \cdot \phi_z)^2 + \left(\frac{2}{\pi} \cdot G_y \cdot \phi_y \cdot G_z \cdot \phi_z\right)^2}}$ $\phi_y = \frac{c_y \cdot b \cdot n_{1,x}}{v_m(z_s)} ; \phi_z = \frac{c_z \cdot b \cdot n_{1,x}}{v_m(z_s)}$	$\delta = 0,06^2$ $n_{1,x} = 46/h$ $G_y = 1/2$ $G_z = 3/8$ $c_y = 11,5$ $c_z = 11,5$	Form C.2 Form B.2 Form C.3
Peak factor	$k_p = \sqrt{2 \cdot \ln(v \cdot T)} + \frac{0,6}{\sqrt{\ln(v \cdot T)}}$ $v = n_{1,x} \cdot \sqrt{\frac{R^2}{B^2 + R^2}} ; v \geq 0,08 \text{ Hz}$	$T = 600 \text{ m}$	Form B.4 Form B.5

Table 28 - Method to calculate the structural factor

Force coefficients

To determine the resulting wind load on the structure in horizontal direction, the force coefficients c_f of the structures for external pressure have to be taken into account. This is done for pressure on the windward side (D) and suction on the leeward side (E). Table 14 shows the external pressure coefficients, according to the Eurocode, which have to be linearly interpolated for ratio of h/d bigger than 1.

h/d	$c_{f,A}$	$c_{f,B}$	$c_{f,C}$	$c_{f,D}$	$c_{f,E}$
5	-1,2	-0,8	-0,5	0,8	-0,7
≤ 1	-1,2	-0,8	-0,5	0,8	-0,5

Table 29 - External pressure coefficients for facades (EN 1991-1-4 Table NB.6 - 7.1)

The lack of correlation between the windward side and the leeward side may be incorporated by a reduction factor of 0,85 on the resulting windforce, according to the Dutch national annex. This will result in the formula below for the windforce due to pressure and suction on the facades.

$$F_{w, \text{pressure+suction}} = c_s c_d \cdot (c_{f,D} + c_{f,E}) \cdot 0,85 \cdot q_p(z_e) \cdot A_{ref}$$

² Logarithmic decrement of structural damping for timber structures is chosen to be in between the value of a steel (0,05) and a concrete (0,10) structure.

In addition to external pressure, the effects of friction on the surfaces parallel to the direction of the wind may contribute to the resulting horizontal force. In most cases, the effects of wind friction on the surface can be disregarded when the total area of all surfaces parallel with the wind is equal to or less than 4 times the total area of all external surfaces perpendicular to the wind (windward and leeward) according to the Eurocode 1991-1-4 (art. 5.3 (4)). In addition, the reference area A_{ref} , on which the friction forces should be applied, is the part of the external surfaces parallel to the wind, located beyond a distance from the windward side, equal to the smallest value of $2 \times b$ or $4 \times h$ (art. 7.5 (3)).

$$F_{w,friction} = c_s c_d \cdot c_{fr} \cdot q_p(z_e) \cdot A_{ref}$$

Below, the resulting wind forces in perpendicular and parallel direction (indicated in Figure 59) are demonstrated for a building of 8 modules high and 8 modules in a row ($n \times m = 8 \times 8$).

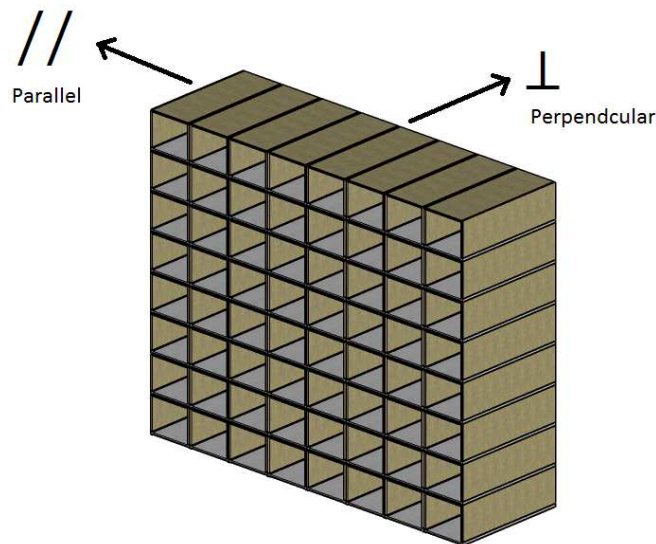


Figure 59 - Wind directions applied to modules

The values that are most interesting for the resulting forces on the governing module are the horizontal shear force on the first module and the moment on podium level.

Top of module	Height h [m]	Σh [m]	Pressure $q(z)$ [kN/m ²]	Wind load $F_{pr+suct}$ [kN]	ΣF_{total} [kN]	Moment ΣM [kNm]
8	2,90	30,53	1,21	55,12	55	
7	2,90	27,63	1,18	107,56	163	160
6	2,90	24,73	1,18	107,56	270	632
5	2,90	21,83	1,18	107,56	378	1415
4	2,90	18,93	1,18	107,56	485	2511
3	2,90	16,03	1,18	107,56	593	3918
2	2,90	13,13	1,18	107,56	700	5638
1	2,90	10,23	1,18	107,56	808	7669
Podium	7,33	7,33	1,18	189,71	998	10012
				135,93	1134	17326

Table 30 - Horizontal wind forces perpendicular on the building ($n \times m = 8 \times 8$)

In the other wind direction the following stepped wind profile can be observed.

Top of module	Height		Pressure $q(z)$ [kN/m ²]	Wind load		Moment ΣM [kNm]
	h [m]	Σh [m]		$F_{pr+suct}$ [kN]	ΣF_{total} [kN]	
8	2,90	30,53	1,21	19,63	20	
7	2,90	27,63	1,21	39,26	59	57
6	2,90	24,73	1,21	39,26	98	228
5	2,90	21,83	1,21	39,26	137	512
4	2,90	18,93	1,05	34,12	172	911
3	2,90	16,03	1,00	32,40	204	1408
2	2,90	13,13	0,93	30,38	234	2000
1	2,90	10,23	0,86	27,93	262	2679
Podium	7,33	7,33	0,82	47,10	309	3440
				33,75	343	5707

Table 31 - Horizontal wind forces parallel on the building ($n \times m = 8 \times 8$)

Notional horizontal load

As described in paragraph 3.3.1, notional horizontal loads as a result of inaccuracies and imperfections should be applied in combination with the wind loads. The notional horizontal force per module has to be determined as a percentage of the factored vertical loads. The vertical load per module is as follows.

Concrete floor module: $G + Q = (q_G + q_Q) \cdot 2d = 176,26 + 31,50 = 207,76 \text{ kN}$

CLT floor module: $G + Q = (q_G + q_Q) \cdot 2d = 81,10 + 31,50 = 112,60 \text{ kN}$

Secondly, the factored vertical load per module is shown.

Concrete floor module: $1,2 \cdot G + 1,5 \cdot Q = 211,52 + 82,69 = 294,21 \text{ kN}$

CLT floor module: $1,2 \cdot G + 1,5 \cdot Q = 97,32 + 82,69 = 180,01 \text{ kN}$

Finally the notional horizontal force per module can be calculated, which is as follows for a building height of 8 modules.

Concrete floor module: $F_{notional} = F_{v,factored} \cdot 0,2 \cdot n^{0,5} \% = 294,21 \cdot \frac{0,2 \cdot n^{0,5}}{100} = 1,66 \text{ kN}$

CLT floor module: $F_{notional} = F_{v,factored} \cdot 0,2 \cdot n^{0,5} \% = 180,01 \cdot \frac{0,2 \cdot n^{0,5}}{100} = 1,02 \text{ kN}$

6.2 Load combinations

To investigate the effects of loads on the structural behaviour it is required that structures and members are designed for all possible combinations of actions that can occur simultaneously. The load combinations are based on the Dutch national annex of EN 1990 for buildings with consequence class 2. The load combinations for the ultimate limit state as well as for the serviceability limit state and the combination factors for variable loads are investigated.

6.2.1 Ultimate limit state

For the fundamental combinations in the ultimate limit state (ULS), partial factors have to be applied to perform strength verifications as shown below.

Combination	Permanent actions		Leading variable action	Accompanying variable actions	
	Unfavourable	Favourable		Main (if any)	Others
Eq. 6.10a	1,35 $G_{k,sup}$	0,9 $G_{k,inf}$		1,5 $\psi_0 Q_{k,1}$	1,5 $\psi_0 Q_{k,i}$
Eq. 6.10b	1,2 $G_{k,sup}$	0,9 $G_{k,inf}$	1,5 $Q_{k,1}$		1,5 $\psi_0 Q_{k,i}$

Table 32 - Load combinations for ultimate limit state

In addition to the fundamental combinations, there is the accidental limit case for verifications in case of fire, blasts or collisions. In case of an accidental situation the partial factors will all be 1 and the combination factor will be ψ_2 , except for wind loads in case of a fire situation, then ψ_1 must be accounted for.

$$E_d = G_k + \psi_1 Q_{k,1} \text{ (wind with fire)} + \sum \psi_2 Q_{k,i} \text{ (other variable loads)}$$

The reasoning behind this, is that the chance of occurrence of a fire in combination with an extreme load situation is very small.

6.2.2 Serviceability limit state

In serviceability limit state (SLS) the following load combinations must be accounted for.

Combination	Permanent actions		Variable actions	
	Unfavourable	Favourable	Leading	Others
Characteristic	$G_{k,sup}$	$G_{k,inf}$	$Q_{k,1}$	$\psi_0 Q_{k,1}$
Frequent	$G_{k,sup}$	$G_{k,inf}$	$\psi_1 Q_{k,1}$	$\psi_2 Q_{k,i}$
Quasi-permanent	$G_{k,sup}$	$G_{k,inf}$	$\psi_2 Q_{k,1}$	$\psi_2 Q_{k,i}$

Table 33 - Load combinations for serviceability limit state

6.2.3 Combination factors

Load	ψ_0	ψ_1	ψ_2
Category A: Domestic, residential areas	0,4	0,5	0,3
Category H: Roofs	0	0	0
Snow loads on buildings	0	0,2	0
Wind loads on buildings	0	0,2	0
Temperature on buildings (non fire)	0	0,5	0

Table 34 - Corresponding ψ factors for buildings

Combining the load combinations with the combination factors in ULS results in Table 35 for ultimate limit state verifications and Table 36 for serviceability limit state verifications.

	Equation ULS	Combination	Selfweight Permanent	Floor Variable	Wind Variable
1	6.10 a	$1,35 \cdot \text{Permanent} + 1,50 \cdot \psi_0 \cdot \text{Floor}$	1,35	0,6	0
2	6.10 b	$1,20 \cdot \text{Permanent} + (0,4 + 1,2/n) \cdot 1,50 \cdot \text{Floor}$	1,20	0,825	0
3		$1,20 \cdot \text{Permanent} + 1,50 \cdot \text{Wind}$	1,20	0	1,5
4		$1,20 \cdot \text{Permanent} + 1,50 \cdot (\psi_0 \cdot \text{Floor} + \text{Wind})$	1,20	0,6	1,5
5		$0,90 \cdot \text{Permanent} + 1,50 \cdot \text{Wind}$	0,9	0	1,5
6		$0,90 \cdot \text{Permanent} + 1,50 \cdot (\psi_0 \cdot \text{Floor} + \text{Wind})$	0,9	0,6	1,5
7		$0,90 \cdot \text{Permanent} - 1,50 \cdot \text{Wind}$	0,9	0	-1,5
8		$0,90 \cdot \text{Permanent} + 1,50 \cdot (\psi_0 \cdot \text{Floor} - \text{Wind})$	0,9	0,6	-1,5
9		$1,20 \cdot \text{Permanent} + 1,50 \cdot (\psi_0 \cdot \text{Floor} - \text{Wind})$	1,20	0,6	-1,5

Table 35 - Load combinations for the ultimate limit state

	Type SLS	Combination	Selfweight Permanent	Floor Variable	Wind Variable
1	Characteristic	$\text{Permanent} + (0,4 + 1,2/n) \cdot \text{Floor}$	1	0,48	0
2		$\text{Permanent} + \psi_0 \cdot \text{Floor} + \text{Wind}$	1	0,4	1
3		$\text{Permanent} + \psi_0 \cdot \text{Floor} - \text{Wind}$	1	0,4	-1
4		$\text{Permanent} + \text{Wind}$	1	0	1
5		$\text{Permanent} - \text{Wind}$	1	0	-1
6		Permanent	1	0	0
7	Frequent	$\text{Permanent} + \psi_2 \cdot \text{Floor} + \psi_1 \cdot \text{Wind}$	1	0,3	0,2
8		$\text{Permanent} + \psi_2 \cdot \text{Floor} - \psi_1 \cdot \text{Wind}$	1	0,3	-0,2
9		$\text{Permanent} + \psi_1 \cdot \text{Wind}$	1	0	0,2
10		$\text{Permanent} - \psi_1 \cdot \text{Wind}$	1	0	-0,2
11		$\text{Permanent} + \psi_1 \cdot \text{Floor}$	1	0,5	0
12		Permanent	1	0	0
13	Quasi permanent	$\text{Permanent} + \psi_2 \cdot \text{Floor}$	1	0,3	0
14		Permanent	1	0	0

Table 36 - Load combinations for the serviceability limit state

As mentioned in previous paragraph, only two floor levels should be loaded by the maximum imposed floor load. This means that the load combination is dependent on the parameter of number of modules in top of each other (n). Therefore, in the second ULS combination and first SLS combination a factor of $\frac{2+(n-2)\psi_0}{n} = 0,4 + \frac{1,2}{n}$ is used. It must be noted that the two floors that are loaded by the maximum imposed floor load, should be at the most unfavourable position.

	Equation Fire	Combination	Selfweight Permanent	Floor Variable	Wind Variable
1	Fire	$\text{Permanent} + \psi_2 \cdot \text{Floor} + \psi_1 \cdot \text{Wind}$	1	0,3	0,2

Table 37 - Load combination for the accidental fire limit state

7 Verifications

This chapter deals with verifications to check whether the modular building complies with all the requirements stated by the regulations. First, the deformation verifications in serviceability limit state are performed and after that, the strength verifications ultimate limit state are performed.

7.1 SLS – FEM modelling

7.1.1 Introduction

In this chapter the structural elements of the modules are modelled in a finite element program in order to verify the maximum displacements of a single module, as well as the modular building configuration as a system. First the element discretization is given and the finite element design choices are explained. Subsequently, the boundary conditions and the loading are demonstrated. Then the deformation and force analysis is performed and checked against the requirements given by the Dutch national annex of EN 1990. Finally, the contributions of the individual components to the overall displacement are compared. This is done to obtain the relative importance concerning the deformation and to indicate the possibilities for optimization and expansion.

7.1.2 Element discretization

The discretization of finite elements can be divided into 2D shell elements (panels), 1D beam elements (table structure) and all 2D interface elements representing the connections between the other elements. Below, the elements are described, design choices explained and stiffness properties quantified. This paragraph describes the build-up of the total model. The development of the model and the accompanying choices described in this paragraph, are the result of an iterative process. This process consisted of verifying whether the elements and model are correctly implemented with respect to the real building and validating to check by tests whether the accuracy of the elements and model is sufficient to the objective of the model, which is the determination of the maximum horizontal displacement of the building.

7.1.2.1 2D elements

As is previously clarified, the cellular character of the building and the modules predominantly results in diaphragm action. Additionally, when the stabilization wall becomes active, out-of-plane stresses will develop in the horizontal diaphragm elements, i.e. floor and ceiling. The 2D elements are all modelled as quadrilateral shell elements. Shell elements are a combination of plane stress elements and plate elements. Plane stress elements (i.e. only in-plane stresses allowed) are meant to model 2D elements with only in-plane loading i.e. diaphragm action. Plate elements are meant to model 2D elements with only out-of-plane loading i.e. membrane forces. Shell elements are used because both in-plane and (sometimes small) out-of-plane stresses do occur due to the unsymmetrical modules. Below the graphical representation of the mentioned elements to model the 2D panels is given.

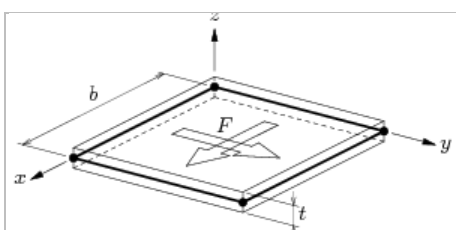


Figure 60 - Plane stress element

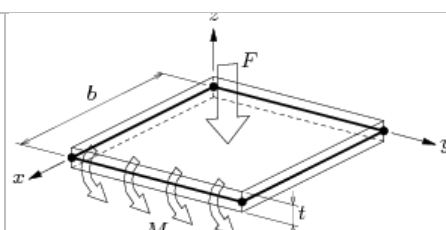


Figure 61 - Plate element

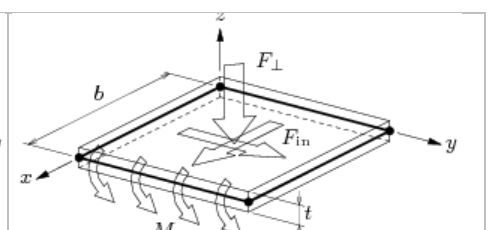


Figure 62 - Shell element

Special care is put into the assigning of stiffness properties of the elements. The finite element program that is being used is AxisVM. This program and other common finite element software in practice are built for analysis of structures with materials that have inhomogeneous properties in a maximum of two directions. This is evident from the fact that the only stiffness's that can be manually assigned, are the Young's moduli (E_x and E_y) of the two in-plane directions (local x- and y axis). CLT elements however, have different stiffness properties in three directions, which implies some simplifications in the modelling. First of all, as can be seen in Table 38, the in-plane stiffness does not equal the out-of-plane stiffness of CLT and secondly, the program's build-in relationship for the shear stiffness (G) does not hold for CLT. Therefore, it is necessary to identify for every type of element which mechanism of force transfer is dominating for the horizontal displacements.

Before the separate 2D elements will be elaborated, Table 38 is shown to give an overview of the different stiffness properties of the CLT panel thicknesses that is used for the modules. As is addressed in chapter 4, the out-of-plane (bending) Young's modulus depends on the effective second moment of inertia. The effective second moment of inertia is determined according to the gamma method as explained in paragraph 4.6.2 and as demonstrated at the buckling calculation for a 142 mm panel in paragraph 0. Next to that, the corresponding lengths of the panels for the calculation of the effective second moments of inertia are incorporated. The in-plane Young's modulus depends on the thickness of the layers in the considered direction. This is shown below with $E_{0,layer} = 11000 \text{ N/mm}^2$ as the layers Young's modulus in the direction parallel to the fibre.

$$\text{Out-of-plane: } E_{eff} = \frac{I_{eff}}{I_{total}} \cdot E_{0,layer}$$

$$\text{In-plane: } E_{netto} = \frac{t_{net}}{t_{total}} \cdot E_{0,layer}$$

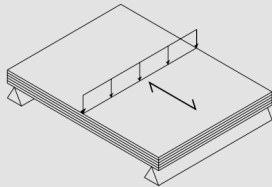
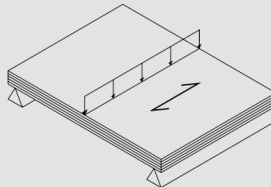
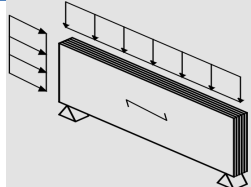
CLT	Out-of-plane			In-plane		
t	E_y	E_x	$G_{(R)}$	E_y	E_x	G_{xy}
99 mm	9610	410	60	7330	3670	430
142 mm	7960	1768	60	8370	2630	510
						

Table 38 - Real mean stiffness properties of used CLT panels in N/mm²

Stabilization wall

The main load bearing mechanisms for the stabilization wall is in-plane shear and in-plane bending in the strong direction of the CLT. This means that the stiffness's that can be assigned are the in-plane stiffness's. The shear stiffness (G_{xy}) however, is automatically calculated by the program using the following method which is based on the Poisson coefficient and the two Young's moduli as follows (demonstrated for a 142 mm thick CLT panel).

$$\nu_{xy} = \begin{cases} \nu & \text{if } E_x \geq E_y \\ \nu \cdot \frac{E_x}{E_y} & \text{if } E_x \leq E_y \end{cases} = \begin{cases} 0,2 & \text{if } 2634 \geq 8366 \\ 0,2 \cdot \frac{2634}{8366} = 0,06 & \text{if } 2634 \leq 8366 \end{cases} = 0,06$$

$$G_{xy} = \frac{E_x \cdot E_y}{E_x + E_y + 2 \cdot \nu_{xy} \cdot E_y} = \frac{2634 \cdot 8366}{2634 + 8366 + 2 \cdot 0,06 \cdot 8366} = 1828 \text{ N/mm}^2$$

According to paragraph 4.8.1.1, the actual in-plane shear stiffness of a 142mm thick CLT panel with a conservative layer width of 150 mm results in the following value.

$$\alpha_{FE} = 0,4253 \cdot \left(\frac{t_{mean}}{a} \right)^{-0,7941} = 0,4253 \cdot \left(\frac{23,67}{150} \right)^{-0,7941} = 1,84 \text{ for a 5 layered CLT element}$$

$$G_{xy,CLT} = G_{0,mean} \cdot \frac{1}{1 + 6 \cdot \alpha_{FE} \cdot \left(\frac{t_{mean}}{a} \right)^2} = 650 \cdot \frac{1}{1 + 6 \cdot 1,84 \cdot \left(\frac{23,67}{150} \right)^2} = 510 \text{ N/mm}^2$$

The actual in-plane shear stiffness of the CLT is significantly lower than the automatically calculated value by the finite element program. Since the shear deformation is an essential aspect in the considerations of the horizontal displacement parallel to the stabilization wall and to prevent the overestimation of the stiffness, the shear modulus has to be reduced. The actual in-plane shear stiffness that results from the specific cross-sectional build-up of CLT elements will be obtained by using a fictitious Young's modulus E_x^* in the weak (x-) direction. This fictitious Young's modulus is derived by inverting the standard calculation method of the program and inserting the actual shear stiffness $G_{xy,CLT}$.

$$E_x^* = \frac{E_y}{\left(\frac{E_y}{G_{xy,CLT}} - 1 - 2 \cdot \nu \right)} = \frac{8366}{\left(\frac{8366}{510} - 1 - 2 \cdot 0,2 \right)} = 558 \text{ N/mm}^2$$

One may argue whether this drastic stiffness reduction of the weak in-plane direction of the CLT is of influence for the overall deformation. However, when considering the force distribution in the stabilization wall, there are practically no stresses in the weak in-plane (σ_{xx}) direction. Moreover, the little influence there is, is on the conservative side. This is because the in-plane moments in the stabilization wall as a result of the horizontal wind forces, will be carried by the strong local y-direction of the CLT panel.

Side wall

The dominant mechanism of force transfer in the side walls are the vertical forces in the strong direction of the CLT panels. At first sight, it appears straight forward that it should suffice to use the actual Young's moduli in x- and y-direction but problems arise when the forces will be distributed towards the columns of the table structure. The table (podium) structure consists of heavy columns and heavy concrete beams. Under every two side walls that are placed next to each other, there is a concrete beam of 1,40m x 0,35m, to partially support the side walls of the modules. Partially, because the CLT side walls can be considered as stocky or non-slender beams that are able to provide an arch effect. The CLT side wall, that spans from column to column, has a considerable height which means that the shear component to the deflection is no longer neglectable as it is for a slender Euler-Bernoulli beam. The theory of Timoshenko combines the deformation from bending and shear, which provides us with the following deflections due to bending and shear at midspan as a result of a distributed load q as shown in Figure 63.

$$u_{bending} = \frac{5}{384} \cdot \frac{qL^4}{E_x I} = \frac{5}{384} \cdot \frac{5 \cdot 8^4}{2634000 \cdot \frac{1}{12} \cdot 0,142 \cdot 2,65^3} \cdot 10^3 = 0,46 \text{ mm}$$

$$u_{shear} = \frac{1}{8} \cdot \frac{qL^2}{GA_s} = \frac{1}{8} \cdot \frac{5 \cdot 8^2}{510000 \cdot 0,142 \cdot 2,65} \cdot 10^3 = 0,21 \text{ mm}$$

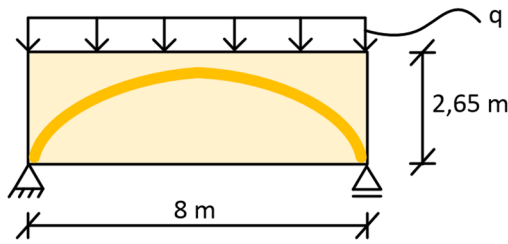


Figure 63 - CLT side wall with arch effect

From these formulas an expression can be deduced to obtain the relative importance of the shear contribution to the deflection at midspan as follows.

$$\frac{u_{shear}}{u_{bending} + u_{shear}} = \frac{1}{1 + \frac{5}{48} \cdot \frac{G_{xy} A L^2}{E_x I}} = \frac{1}{1 + \frac{5}{48} \cdot \frac{510000 \cdot 0,142 \cdot 2,65^2 \cdot 8^2}{2634000 \cdot \frac{1}{12} \cdot 0,142 \cdot 2,65^3}} = 0,31$$

From the deflections and the relative importance, it can be seen that the shear portion is almost half as much as the bending portion of the deflection. This means that the shear contribution cannot be neglected in the model. Once again, a fictitious Young's modulus in the weak (x-) direction has to be applied, but this time, unlike the stabilization wall, this Young's modulus is of importance for the deflection as well. Therefore, the fictitious Young's modulus E_x^* and hence the shear modulus G^* as well, are chosen in a way that the resulting deflection at midspan equals the deflection that corresponds with the 'real' stiffness moduli as follows.

$$u_{total} = u_{total}^* = \frac{5}{384} \cdot \frac{qL^4}{E_x I} + \frac{1}{8} \cdot \frac{qL^2}{G A_s} = \frac{5}{384} \cdot \frac{qL^4}{E_x^* I} + \frac{1}{8} \cdot \frac{qL^2}{G_{xy}^* A_s}$$

The program's automatic calculation for the shear modulus can be simplified as follows with $\nu = 0,2$.

$$G_{xy}^* = \frac{E_x^* \cdot E_y}{1,4 \cdot E_x^* + E_y}$$

This can be substituted in the relation for the total deflection together with the 'real' stiffness's ($E_x = 2634 \text{ N/mm}^2$, $G_{xy} = 510 \text{ N/mm}^2$ and $E_y = 8366 \text{ N/mm}^2$). Subsequently, the relation can be solved to obtain a slightly reduced Young's modulus in weak direction $E_x^* = 2026 \text{ N/mm}^2$ and an increased shear modulus $G = 1513 \text{ N/mm}^2$, which together result in exactly the same deflection at midspan as was the case for the deflection with the actual stiffness's. So despite changing the relative importance of the shear and bending contributions to the deflection at midspan, the resulting deflection in the model remains the same. This is important because a deflection at midspan of the side walls, contributes to the horizontal displacement of the total building when loaded by horizontal wind forces parallel to the building.

Lastly, it has to be noted that changing the shear modulus has an effect on the shear deformation due to the wind loads perpendicular to the building. However, this effect is extremely small and not relevant because the cross-section loaded by shear consists of the total width of the side wall. This means that for 20 modules on top of each other, the horizontal displacement as a result of the wind load perpendicular to the building is less than 0,01 mm and can be neglected.

Ceiling

As mentioned before, it is necessary to identify, for every type of element, which mechanism of force transfer is dominating for the horizontal displacement. Once identified, the stiffness properties of that particular mechanism may be adopted in the modelling. For the ceiling element it holds that out-of-plane bending is the dominating mechanism. The wind load directed parallel to the building results in vertical forces in the stabilisation wall of every module and have to be resisted by the ceiling and floor elements. This is the rocking mechanism, which is explained further on in this section.

Here, the out-of-plane stiffness properties of 99 mm thick CLT will be used in the model. The shear deflection only needs to be calculated and incorporated if the ratio of element length and element thickness is less than 30 ($L/T < 30$) according to (MERK Timber GmbH 2013). For the ceiling element it holds that $L/T = 3244/99 = 33$, which means that the ceiling is slender enough to neglect the out-of-plane shear deformation contribution.

The automatically calculated in-plane shear modulus that results from the out-of-plane Young's moduli is 383 N/mm^2 . Fortunately, this is very close and on the conservative side to the 'real' in-plane shear modulus of the panel of 428 N/mm^2 . Additionally, it has to be noted that by using the out-of-plane properties, the in-plane normal stiffness will be slightly overestimated in the strong direction and underestimated in the weak direction. However, this effect will be diminished by the concrete floor, which is placed and connected on top of the ceiling and assists the ceiling element in distributing the loads from wind parallel to the building.

Floor

In assigning the stiffness value of the concrete shell floor elements, special attention should be given to the possible presence of cracks in the concrete. This can be estimated by checking the cracking moment of the concrete strip under the stabilisation wall against the governing maximum bending moment as a result of the characteristic load situation. As a result of wind directed parallel to the building, the stabilization wall causes a point load, approximately at midspan of the concrete floor element. An effective concrete width of about 6 times the width of the stabilization wall ($6 \times 150 = 900\text{mm}$), which is a common approximation in practice, can be used to calculate the concrete cracking moment as follows.

$$M_{cr} = W \cdot f_{ctm} = \frac{1}{6} \cdot b_{eff} \cdot h^2 \cdot f_{ctm} = \frac{1}{6} \cdot 900 \cdot 140^2 \cdot 3,8 = 11,17 \text{ kNm}$$

Subsequently, the characteristic loads of the selfweight, imposed loads and the point load from wind parallel to the building by the stabilization wall (as shown in Figure 64) result in the following bending moments.

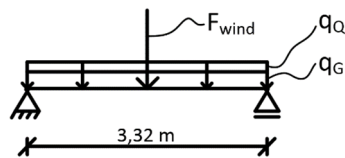


Figure 64 - Loads on concrete floor strip

$$M_{G+Q} = \frac{1}{8} \cdot b_{eff} \cdot (q_G + q_Q) \cdot l^2 = \frac{1}{8} \cdot 0,9 \cdot 6,20 \cdot 3,32^2 = 7,69 \text{ kNm}$$

$$M_{wind} = \frac{1}{4} \cdot F_{wind} \cdot l = \frac{1}{4} \cdot F_{wind} \cdot 3,32 = 0,83 \cdot F_{wind}$$

When comparing the bending moments due to the loads against the cracking moment of the concrete floor strip, the result is that from a wind load of about 4 kN the concrete starts to crack. A point load of 4 kN on the concrete strip corresponds to a horizontal wind load of about 2 kN per module, which according to paragraph 6.1.3 already will be exceeded for one module. From this it can be concluded that the horizontal deformations, as a result of wind directed parallel to the building, depend on the stiffness of cracked concrete. Next to that, Eurocode 2 art. 7.4.3 states that deformations due to loading may be assessed by using the effective modulus of elasticity of the concrete. The most accurate modulus of elasticity of cracked concrete can be calculated using the $M-\kappa$ diagram. However, the wind load that acts on the concrete floor is not the same for every module, but decreases with the height of the building. Therefore, a value of $\frac{1}{2} \cdot E_{mean}$ is chosen. To summarize, Table 39 gives an overview of the assigned properties for the used 2D elements.

Element	Material	Thickness [mm]	$E_x^{(*)}$ [N/mm ²]	E_y [N/mm ²]	G_{xy} [N/mm ²]	Dominating def. mechanism
Side wall	CLT	142	2026	8366	1513	In-plane N, V and M
Stabilization wall	CLT	142	558	8366	510	In-plane V and M
Ceiling	CLT	99	407	9184	383	Out-of-plane M
Floor	Concrete	140	16000	16000	6667	Out-of-plane M

Table 39 - Modelling input shell elements

7.1.2.2 1D elements

In determining the deformation of a number of modules on top of each other, it is necessary to do this without considering the interaction with the supporting system. As already mentioned in the stiffness considerations of the side walls, every two side walls next to each other, are supported by a concrete beam of 1,40m x 0,35m as part of the table structure. These beams are modelled as simply supported 1D beam elements. As is addressed in previous paragraph, depending on the relative stiffness's, the deflection of the beams in the table structure, together with the diaphragm action in the side walls, determines the force distribution in the modules and so the deflection of the modular building. Just as it holds for the concrete floors, the cracking moment of the beams in the table structure are as follows

$$M_{cr} = W \cdot f_{ctm} = \frac{1}{6} \cdot b \cdot h^2 \cdot f_{ctm} = \frac{1}{6} \cdot 350 \cdot 1400^2 \cdot 3,8 = 434,47 \text{ kNm}$$

This cracking moment in the beam corresponds with the following distributed load on a beam.

$$q = \frac{8 \cdot M}{l^2} = \frac{8 \cdot 434,47}{8^2} = 54,31 \text{ kN/m}$$

This distributed load is already exceeded by two modules on top of each other. Therefore it can be concluded that, despite the redistribution of stresses by the diaphragm action in the side walls, the use of the effective stiffness of $\frac{1}{3} \cdot E_{mean}$ is justified for the concrete beams. Note: In reality, every beam in the table structure carries two side walls, but the model contains a beam element under every side wall to avoid eccentricities. Because of that, the stiffness that is used in the model is halved and becomes $\frac{1}{6} \cdot E_{mean}$, which is 6000 N/mm² for a strength class of C45/55.

7.1.2.3 Connection elements

The most critical aspect for deformation analysis and at the same time the most difficult to model accurately, are the connection elements in timber structures. In reality the screw and GIR connections are discrete joints. However, the behaviour of (multiple) connections in timber is relatively unknown, especially for application in CLT panels. For reasons of simplicity and to avoid irrelevant complex behaviour close to the CLT panels' edge, it is chosen to model the connections in a continuous manner by using line-to-line interface elements. Line-to-line interface elements are often used to model the interface between wall and floor elements. The used line-to-line link elements, as shown in Figure 65, can be placed between the edges of shell elements and assigned stiffness's in three translational (and three rotational) degrees of freedom (Inter-CAD Kft. 2015).

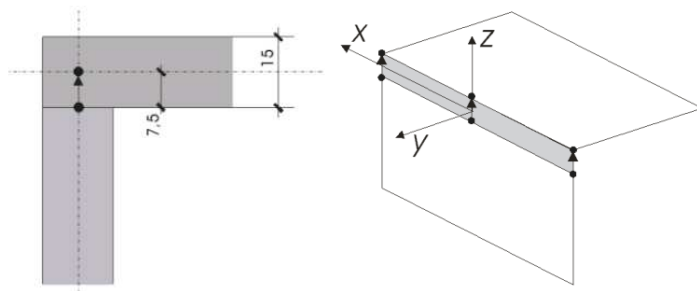


Figure 65 - Graphical representation of a line-to-line interface element

The model contains 6 different types of connections as can be seen in Figure 66. The 2D elements edges/centre-lines are represented by the thick lines and the line-to-line connections are represented by the arrows. The arrow starts at the location of the interface and ends at the centre-line of the 2D element. The cross-section with the junction of four modules contains all the relevant modelled connection.

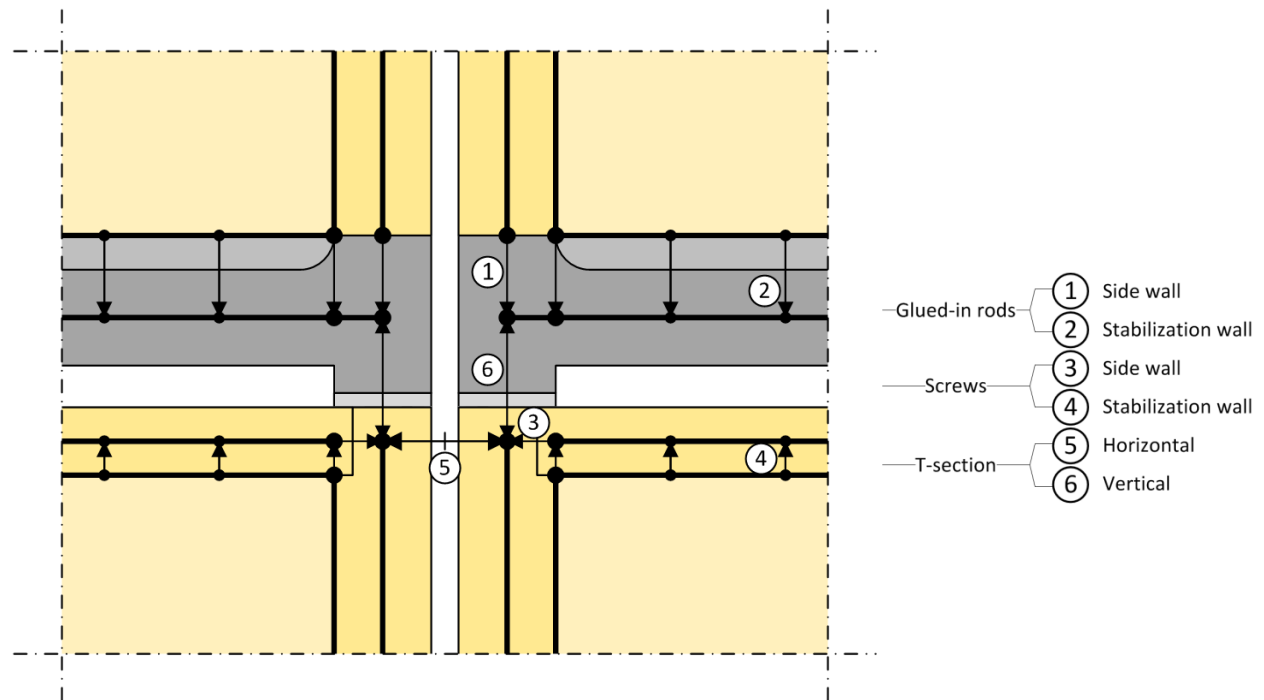


Figure 66 - Representation of modelled connections

As can be seen in local system of coordinates in Figure 65, K_x represents the in-plane shear stiffness, K_y the out-of-plane shear stiffness and K_z the axial stiffness of the connection. In assigning the stiffness's of the (inter-modular) connections, reference is made to the stiffness values given in paragraph 4.10. These stiffness values of the single connectors are then linearly extrapolated, depending on the number of connectors per meter, to obtain the stiffness's per meter of line-to-line interface. Table 40 shows an overview of the assigned stiffness's for the line-to-line connections.

Type	Nr.	Position	Single [kN/m]			# /m	Line-to-line [kN/m/m]		
			K_x	K_y	K_z		K_x	K_y	K_z
GIR	1	Side wall	13772	13772	1E+10	1	13772	13772	1E+10
	2	Stab. wall	13772	13772	156500	3,33	45907	45907	521667
Screws (pair)	3	Side wall	19900	1000	16600	3	59700	3000	49800
	4	Stab. wall	19900	1000	16600	3,33	66333	3333	55333
T-sect.	5	Horizontal	-	-	-	-	1E+6	0	1E+6
	6	Vertical	-	-	-	-	1E+4	1E+4	1E+10

Table 40 - Modelling input line-to-line link elements

It must be noted that the connections that transfer the vertical loads in the side walls, indicated by number 1 and 6 are predominantly loaded in compression due to the selfweight of the structure. The only situation in which tension could occur would be when the stresses due to the moment from wind loads perpendicular to the building would exceed the stresses from selfweight. The exact

behaviour of these connections would imply a non-linear, e.g. bi-linear force displacement diagram in z-direction. In compression, the CLT side walls are subject to direct force transmission with the concrete contact area, which means a theoretically infinitely stiff interface. In tension however, the 'real' connection will be activated and thus, the axial stiffness of the connections should be accounted for.

An accuracy appropriate to the objectives of this thesis is chosen to be a linear behaviour of the connections and materials. Initially, all the vertical connections of the side walls (K_z) are modelled infinitely stiff ($1E+10$ kN/m/m). It is only after running the analysis, that the parts of the meshed line-to-line connection which are in tension, will be assigned with the actual corresponding (pull-out) connection stiffness.

A similar behaviour holds for the other connections, when subjected to axial loading, however it is chosen as a conservative approach to model the other line-to-line connections with a linear behaviour. The axial stiffness for the glued-in rods (with 20 mm diameter) is obtained by linearly interpolating the stiffness values from Table 20 and the lateral stiffness is calculated as follows.

$$K_{ser} = 0,08 \cdot d \cdot \rho_{mean}^{1,5} = 0,08 \cdot 20 \cdot 420^{1,5} = 13772 \text{ kN/m}$$

The stiffness's per pair of self-tapping screws are obtained from Table 21 and by considering the test setup b for K_z , c (two times) for K_y and d for K_x from Figure 46. Since the stiffness of screws is only dependent on the diameter and density of the element, the same stiffness's are used, since the same diameter is used. The stiffness of the T-section is relatively unknown and depends on a lot of factors. The stiffness of the T-sections in vertical direction are estimated to be less than the GIR's, but again infinitely stiff in vertical direction. The T-sections in horizontal direction are modelled locally, which implies 3 line-to-line interfaces of 40cm length, one centred at the position of the side wall and the other two are both positioned one meter from the edge of the side wall.

7.1.3 Loads and boundary conditions

Once the elements are defined, the loads and boundary conditions need to be applied to introduce the forces and displacements. As explained in the introduction of this thesis, the objective of the finite element model is to estimate the overall displacement of the total modular building in order to verify this against the requirements. With this in mind and the aim to represent the true behaviour of the structure under relevant actions to an accuracy appropriate to the objectives of the calculations as stated by Eurocode 2 art. 7.4.3(2), all modelling choices are made.

That implies that the loads are applied in the following manner as shown in Figure 67. The vertical loads from the dead load (DL) and live load (LL) are represented by a constant distributed load applied at the edge of the concrete element. That position is chosen due to the fact that the concrete floor covers 2/3th of the total selfweight and the live load is the variable floor load.

The wind load perpendicular to the building (Wind \perp) is represented by directly placed point loads at the four top corners of the side walls. Corresponding to paragraph 6.1.3 and Eurocode 1991-1-4, $\frac{0,8}{(0,8+0,7)}$ of the wind load is placed on the windward side and $\frac{0,7}{(0,8+0,7)}$ on the leeward side of the building. The wind load parallel to the building (Wind $//$) is represented by distributed loads at the top of the side walls. Again the same portions are placed on the windward and the leeward side of

the building. The loads are placed directly on the relevant edges because it is assumed that the façade elements distribute the loads to the elements edges. These elements are not part of the main load bearing structure, and therefore not included in the model.

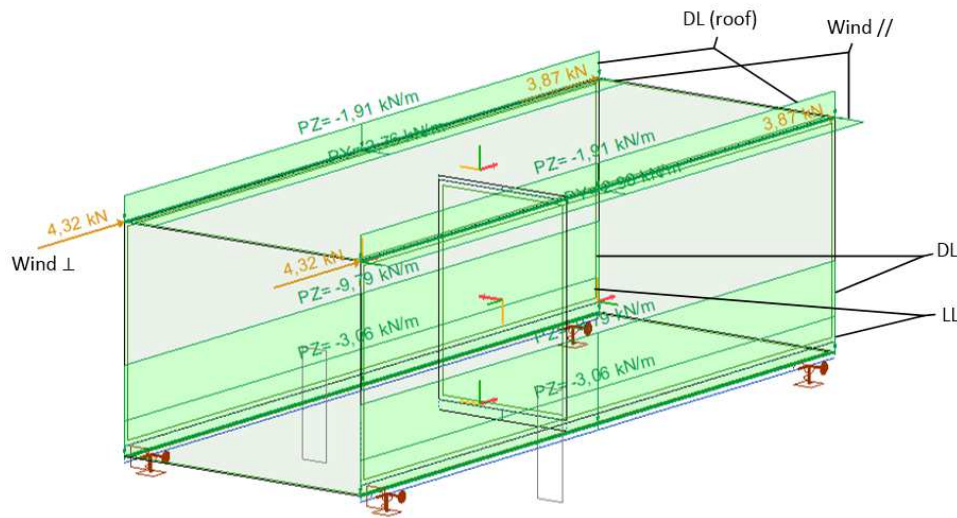


Figure 67 - Graphical representation of load and boundary conditions application

As described in the element discretization, the beams of the table-structure are included in the model. The boundary conditions in the model consist of simply supporting the beams in the model. This means that the model is resisted against horizontal displacements at the top level of the table structure. The horizontal deformation of the table structure is dependent on a lot of factors, i.e. the stiffness of the foundation, the position and dimensions of the stabilization walls or elements. This can be a whole model on its own and is not included in the scope of this thesis. Instead, the horizontal deformation of the table structure is assumed to be the maximum allowed horizontal deformation.

7.1.4 Finite element analysis results

Once the elements with the right properties are in place, the boundary conditions defined, the loads applied and the elements meshed, the program is ready to run. In postprocessing, the results special interest is put into the verification against maximum horizontal deformation in the direction perpendicular and parallel to the building to comply with the requirements in serviceability limit state. Additionally, essential mechanisms that determine the behaviour of the building in terms of deformation are elaborated. This is initially executed for a building configuration of 8 modules next to each other and 8 modules on top of each other.

7.1.4.1 Deformation verification

While ULS situations relate to the safety of people and of the structure with all its contents, the SLS situations relate to the prevention of loss of functionality and comfort of the structure. To ensure the functionality and comfort of the building an important requirement is the maximum horizontal displacement of the building.

The maximum horizontal displacement that results from the finite element modelling in the characteristic load combination is 41,83 mm in parallel direction and 9,19 mm in perpendicular direction as can be seen in Figure 68.

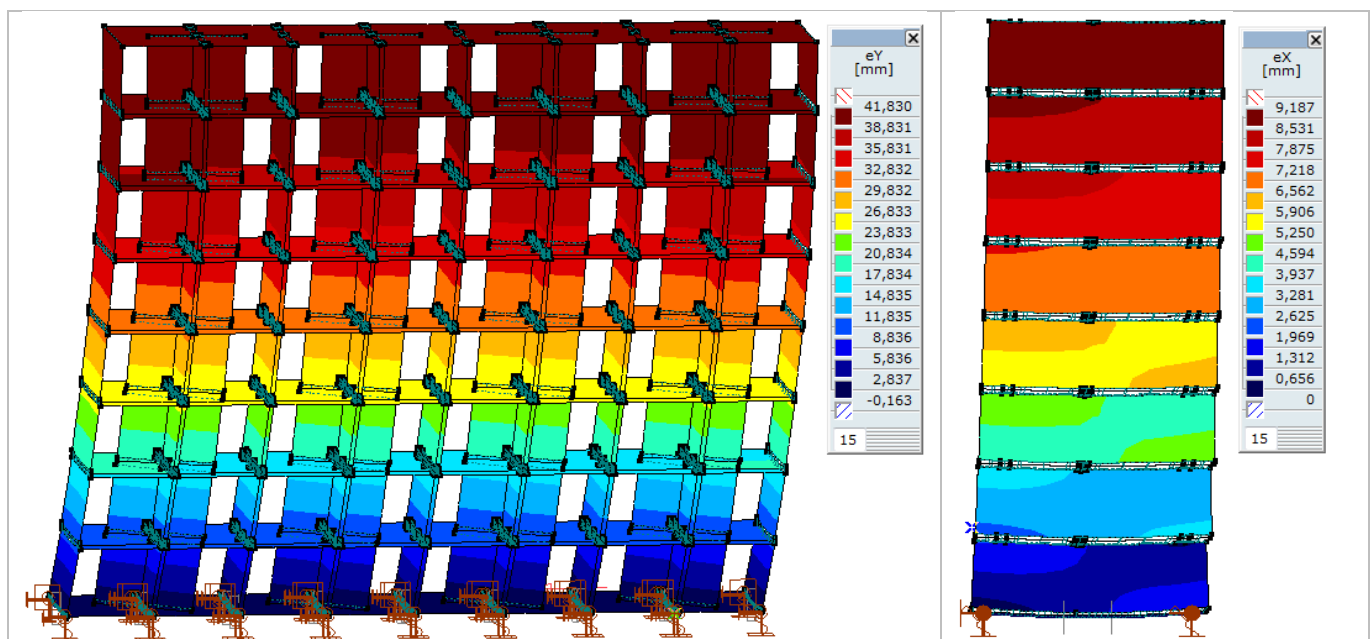


Figure 68 - Max horizontal parallel y- (left) and perpendicular x-direction (right) displacements

The governing load combination that results in the maximum horizontal displacement of the building is the vertical force from selfweight with wind load parallel to the building. This shows that despite the much lower wind-load in parallel direction (due to the smaller surface subject to wind pressure), the stiffness of the building in parallel direction is a lot lower than the stiffness in perpendicular direction. Obviously, this has everything to do with the very stiff side walls in perpendicular direction, compared to the stabilization walls in parallel direction.

The next step is to verify whether the maximum horizontal displacement from the finite element model does not exceed the requirement stated by the building regulations. The Dutch national annex

of EN 1990 states that the total horizontal displacement for buildings with more than one layer subject to the characteristic load combinations must at least be limited to:

$$u_{hor,total} \leq \frac{H}{500}$$

For a modular building of 8 modules next to each other and 8 modules on top of each other, the requirement results in the following maximum horizontal displacement.

$$u_{max,hor,total} = \frac{H_{total}}{500} = \frac{h_{podium} + H_{modules}}{500} = \frac{7330 + 2900 \cdot 8}{500} = 14,66 + 46,40 = 61,06mm$$

As previously mentioned, the horizontal displacement of the podium structure is assumed to be maximum, resulting in a maximum displacement of 46,40 mm for the modular part of the building. Thus it can be concluded that the maximum horizontal displacement from the finite element model (41,83 mm) does not exceed the requirement from the standards (46,40 mm).

Another requirement stated by the same standard, involves the maximum horizontal displacement for one building storey (module in this case).

$$u_{max,hor,storey} \leq \frac{h}{300} \left(= \frac{2900}{300} = 9,7 \text{ mm} \right)$$

The element which is responsible for this requirement is the stabilization wall. The next paragraph deals with the deformation behaviour of the stabilization wall in more detail.

7.1.4.2 Stabilization wall

As it is clear that the stabilization wall causes the governing horizontal displacement of the total building, this paragraph gives more insight to the different components that are involved in this deformation behaviour. The stabilization wall acts as a shear wall to provide horizontal stability against wind loads parallel to the building. In general, for CLT shear walls, three main deformation contributions are responsible for the total horizontal displacement of a shear wall (Flatscher, Bratulic and Schickhofer 2014) as can be seen in the overview given by Figure 69.

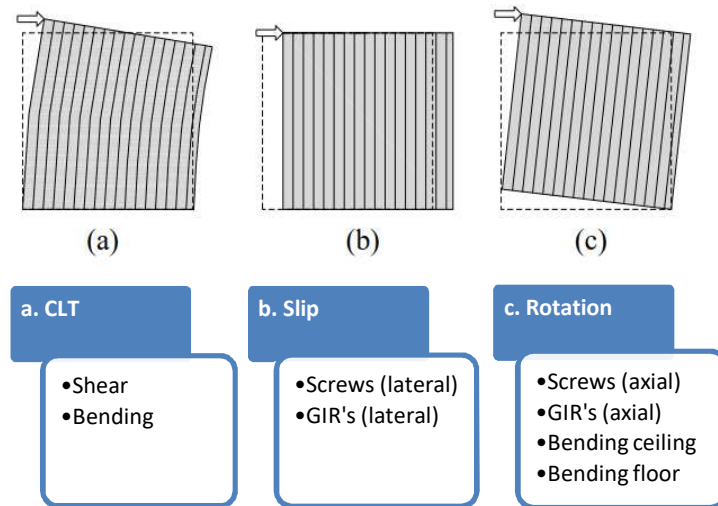


Figure 69 - Deformation contributions of stabilizing wall

The horizontal deformation of the CLT wall configuration on the top is a sum of the CLT's deformation itself (composed of bending and shear), the translation component of slip in the connections (lateral) and rocking (rotation) component in the connections (axial). Additionally, specifically for the modular configuration, bending in the ceiling and floor provides an extra contribution. The first two main contributions (a & b) can be calculated by hand as follows in which F_k is the total horizontal force on the modules divided by the number of modules next to each other (8). It has to be noted that this implies the assumption of horizontal forces from wind parallel to the building being equally distributed over multiple modules next to each other. However this assumption is justified, as Figure 68 (left) shows that the bottom row has a constant displacement and the shear stress output shows the same magnitude for every stabilization wall at the bottom row

$$\text{CLT shear} \quad w_s = \frac{F_k \cdot h}{G \cdot A_s} = \frac{44,43 \cdot 10^3 \cdot 2900}{510 \cdot 1800 \cdot 142} = 0,99 \text{ mm}$$

$$\text{CLT bending} \quad w_b = \frac{F_k \cdot h^3}{3 \cdot E \cdot I} = \frac{44,43 \cdot 10^3 \cdot 2900^3}{3 \cdot 8366 \cdot \frac{1}{12} \cdot 142 \cdot 1800^3} = 0,63 \text{ mm}$$

$$\text{Slip screws} \quad w_{\text{screws}} = \frac{F_k}{K_x \cdot b} = \frac{44,43 \cdot 10^3}{66333 \cdot 1,8} = 0,37 \text{ mm}$$

$$\text{Slip GIR's} \quad w_{\text{GIR's}} = \frac{F_k}{K_x \cdot b} = \frac{44,43 \cdot 10^3}{45907 \cdot 1,8} = 0,54 \text{ mm}$$

The sum of the first two main contributions (a & b) is 2,53mm. As can be seen from Figure 70, this is about 25% of the total horizontal displacement of the bottom row of modules. This leaves 75% of the

horizontal deformation to be appointed to the rocking component, which is clearly visible in deformed state of the bottom row of modules. The high rocking component in the total horizontal deformation of the stabilization wall corresponds to the results of full scale shear wall tests done to give a comparison of the load carrying components of full scale shear walls (Flatscher, Bratulic and Schickhofer 2014).

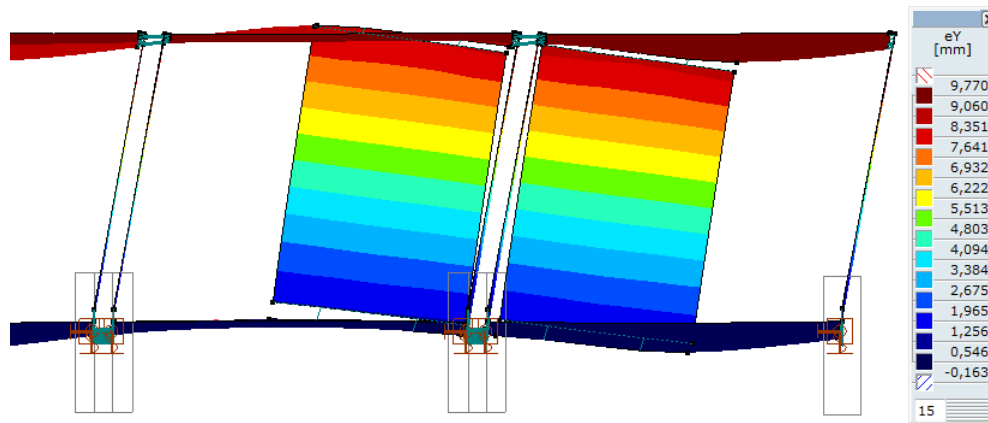


Figure 70 - Horizontal deformation of lower modules

The high rocking component can be decreased by locally increasing the thickness of the concrete floor under the stabilization wall to create a rib. This implies (apart from increasing the stiffness of the floor itself) that the downward deflection of the floors will be restrained by the table structure or the ceiling of the module below. In like manner, the upward deflection of the ceilings of mirrored modules will be restrained by the selfweight of the modules on top. Next to that, the stabilization walls will carry a portion of the selfweight of the modules on top, which then again implies an increased friction that increases the slip stiffness of the connection.

That being said and referring to the previous paragraph and Figure 70, it can be noted that the maximum horizontal displacement of a single storey from the model (9,77mm) practically meets the requirement (9,67mm) of a single storey. However, when bending deformation of the concrete floor is restrained, the result is a significant decrease of rocking behaviour and so the horizontal deformation requirement can be easily met.

7.1.4.3 Stress analysis side walls and podium structure

As previously described, for the parallel building direction, the focus is put on the structure's behaviour under horizontal loads with minor positive effects from selfweight. For the perpendicular building direction however, the relative stiff side walls provide the stability against horizontal loads and carry all the vertical loads, as a result of the modelling method presented. Considering the inter-modular connections and their (lack of) tension capacity in vertical direction, it is vital that tension stresses (as a result of the wind moment) in serviceability limit state are prevented by the vertical loads in the side walls. Another interesting phenomenon is the effect of the stiffness of the podium structure in comparison to the stiffness of the side walls for the stress distribution in the side walls. This paragraph illustrates the effect of the vertical deflection of the podium structure (beams) to the stress distribution in the side walls.

To begin with, Figure 71 below shows the vertical normal stresses (σ_{yy}) in the side walls. First, the results due to only the vertical load from selfweight and imposed floor loads and almost infinitely stiff podium beams (left) are shown. Then, the perpendicular wind load is added (middle) and at last the effective stiffness of the podium beams is added (right). Because every side wall axis is loaded by practically the same amount of horizontal and vertical load in the perpendicular load situation, the same stress distribution holds for every side wall axis.

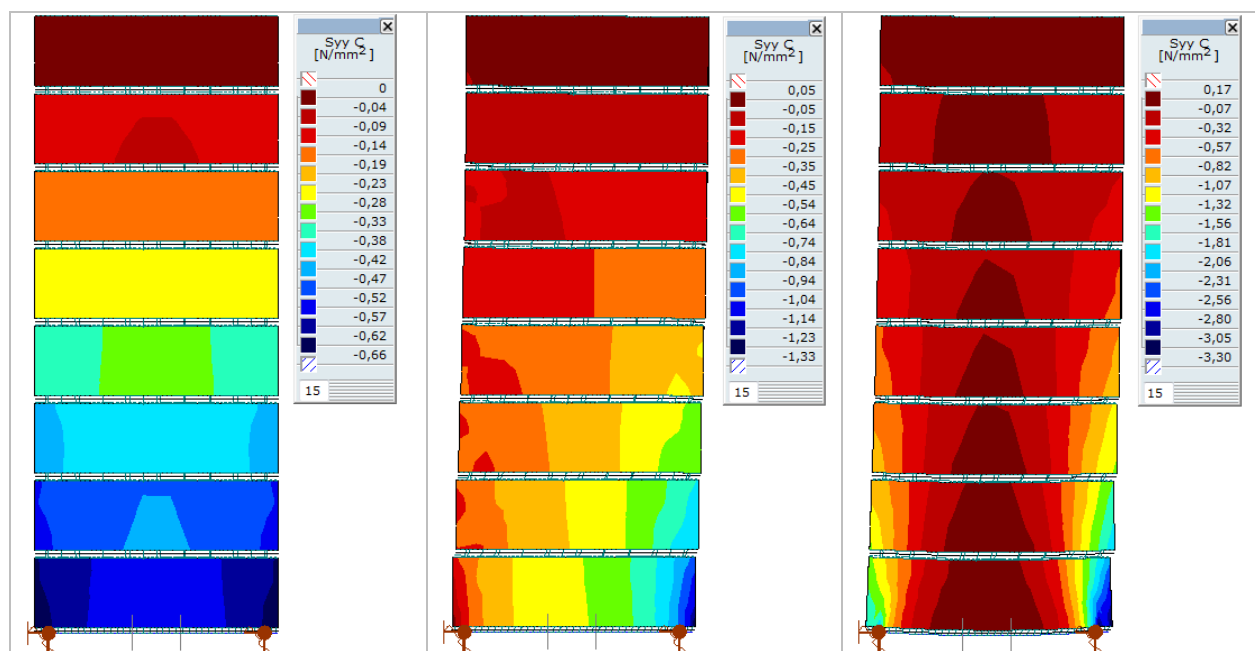


Figure 71 - Vertical normal stresses in side walls

In comparing these vertical stress distributions, it can be seen that for only vertical forces and stiff podium beams, the vertical stresses practically gradually increase with decreasing storey level. When the perpendicular wind load is added, the moment from wind load brings the compression stresses at left bottom practically down to zero and increases the compression stresses at right bottom. This implies that by further increasing the building height with more modules on top of each other, more and more tension stresses will develop at the left bottom. The interesting thing that happens when the effective stiffness of the podium beam is incorporated, is the increase of compression stresses at both edges of the side walls. Corresponding to the vertical stresses, the same force distribution can be seen in Figure 72, which shows the axial line-load carried by the line-to-line connections between

the side walls. From a practically constant line-load without the wind-load, to an increasing line-load when the wind-load is added, to a parabolic line-load towards the edges when the effective concrete beam stiffness is added as well.

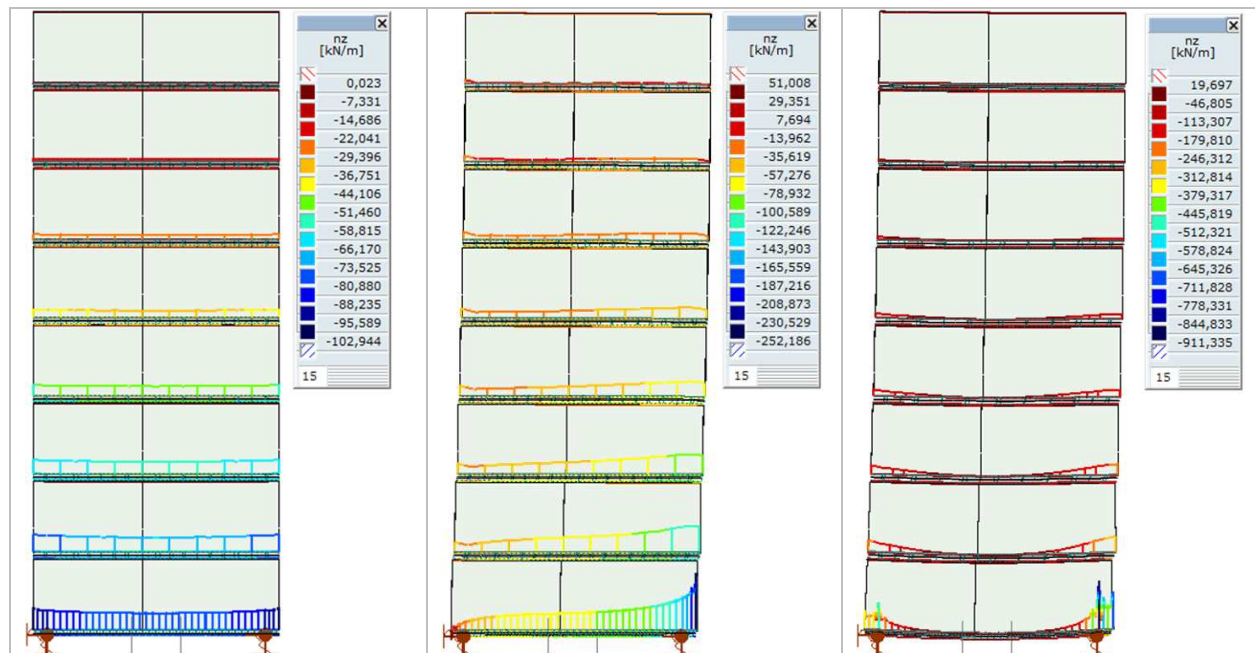


Figure 72 - Axial force in line-to-line connections

It has to be noted that there appear some peaks in the stress distribution. These peaks are a result of singularities in the finite element model. Theoretically, stresses at point loads/supports are infinitely high, which results in increasing stress peaks with finer meshes. Because the podium columns are modelled as point supports, stress peaks appear. In reality (which holds for every point support), the stress is distributed over a certain area, in this case the cross-section of the column.

The side walls themselves contribute to the vertical load distribution towards the podium columns because of the arch effect. The arch effect can be further illustrated by analysing the shear stresses and bending stresses in the side walls. As described in previous paragraph, apart from the load carrying capacity of the podium beams, with increasing deflection, shear and bending stresses are developed in the side walls. Figure 73 below, shows the difference in shear stresses (σ_{xy}) as a result of vertical loads and wind-loads, with an infinitely stiff podium beam (left) compared to the actual situation with the podium beams with effective stiffness (right). In the left, shear stresses develop as a result of the horizontal wind loads towards the bottom, but are very small because of the large width of the side walls and low shear stiffness compared to the normal stiffness in the strong direction of the CLT. In the right, increased shear stresses can be seen, as the side walls act as deep beams that assist in transferring the vertical load towards the podium columns.

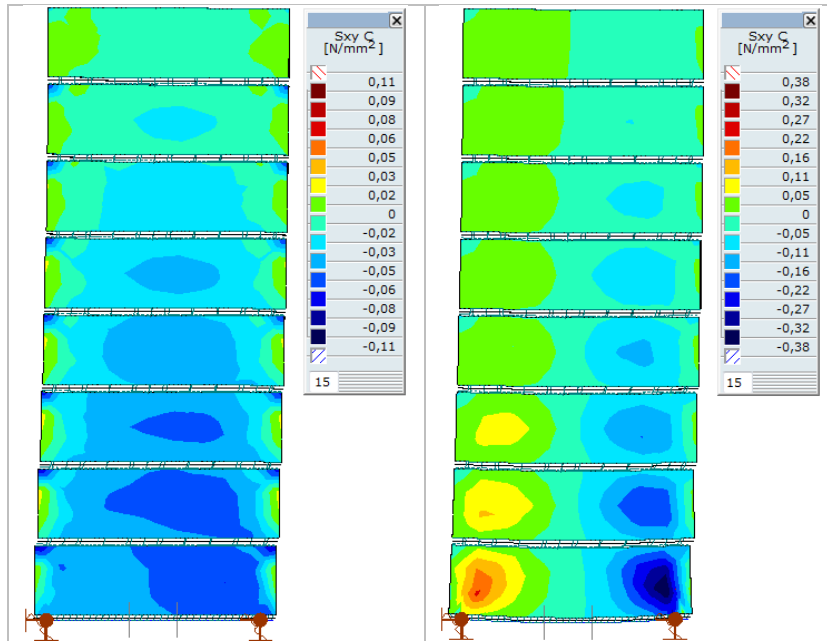


Figure 73 - Shear stresses in side walls, podium beam stiffness infinite (left) and effective (right)

A similar explanation can be given for the horizontal normal stresses (σ_{xx}) in the side walls shown in Figure 74. In the right the bending component in the beam is clearly visible.

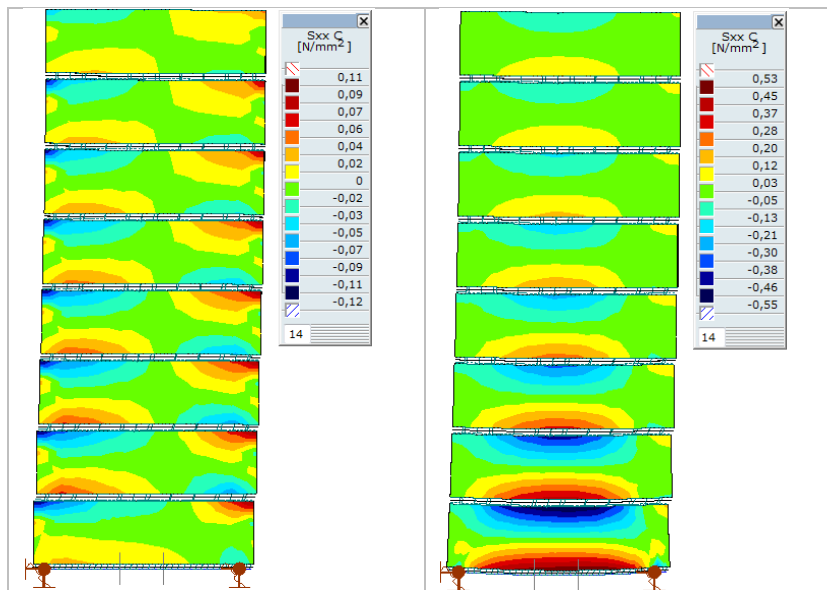


Figure 74 – Hor. Normal stresses in side walls, infinite- (left) and effective (right) podium stiffness

It must be noted that the actual horizontal normal stiffness of the side wall is a little higher and the actual shear stiffness is much lower than the fictitious stiffness's in the model. Meaning that the shear stresses are lower and horizontal normal stresses are higher in reality, but result in a realistic ratio of load distribution between the podium beam and side walls.

7.1.5 Conclusions FEM

As it holds for every model, the finite element model is created being as a simplification of reality. The finite element model of the modular structure was made to verify whether the horizontal displacements meet the requirements set by legislation under linear force distribution. Due to some limitations in the finite element program, the panel elements are discretized in a way that approximates the actual behaviour as close as possible by making use of fictitious or effective stiffness's. Through an iterative process of finding the dominant load bearing mechanism for the different panel elements these stiffness's were determined. The properties of the connection elements were estimated using available research as much as possible and by logic thinking.

After analysing the results, it can be concluded that the maximum horizontal deformation of a configuration of 8 modules next to each other and 8 modules on top of each other complies with the requirements. Despite the much higher wind-load in perpendicular direction, the governing direction for the horizontal deformation is the situation involving wind loads parallel to the building, since the amount of CLT responsible for providing stability is a lot less in this direction. In examining the deformed structure in parallel direction, a clear shear deformation profile along the height of the building can be noted. Next to that, the results confirm the assumption of horizontal wind loads in parallel direction being equally distributed over the number of horizontal modules.

Analysing the aspects that contribute to the horizontal displacement of the stabilization walls revealed the high rocking component as a result from bending of the floor and ceiling. The high rocking component mainly exists because the stabilizing walls are not subject to any influence from vertical loads and the lack of vertical continuity between stabilizing walls in the modelling method given. Subsequently, while varying the element properties to examine the influence on the horizontal displacement of the total building, it turned out that the (effective) stiffness of the concrete floors should be above 16000 N/mm² to comply with the requirements.

The perpendicular building direction is not governing concerning the horizontal displacement due to the very stiff side walls. However due to the characteristics of the inter-modular connections, tension stresses between the side walls and podium structure, as a result of the moment due to perpendicular wind loads in serviceability limit state, should be prevented. By means of analysing the stress distribution in the side walls in relation to the stiffness of the podium structure, the high relative stiffness of the side walls has proven to be very effective. Due to the shear and bending contribution of the side walls in transferring the vertical loads towards the podium columns, vertical stresses become more concentrated at the edges of the side walls. Thereby, preventing tension stresses from wind-loads.

From the analysis results it can be concluded that the CLT panels show an almost rigid in-plane behaviour, compared to the connections and out-of-plane behaviour. Unfortunately, there is also much more uncertainty in the connection stiffness and the effective concrete stiffness. This is important to keep in mind during the modelling process, as there is no benefit in trying to resolve a model to greater accuracy than the input data admits.

7.1.6 Discussion

Discussion can be held on the possibility of obtaining more accurate results. Several possibilities are given together with the necessary actions.

The high rocking behaviour can be eliminated by including a locally increased concrete thickness under the stabilization wall to create a rib. This would make the magnitude of the effective concrete stiffness irrelevant as well. In this case the downward deflection of the floors will be restrained by the table structure or the module below and the upward deflection for the neighbouring stabilisation wall will be restrained by the selfweight of the module on top. However, this improvement would imply a bi-linear behaviour, because tension stresses cannot be transmitted between two stabilization walls on top of each other.

Apart from using a rib under the stabilization walls, in order to make a more realistic model, it would be helpful to obtain the stiffness values for the glued-in rod connections and screw assemblies through testing. Next to that, the axial stiffness of the screws and glued-in rods in the stabilization wall are based on the tension stiffness. But when loaded in compression, the axial stiffness should be infinite. This would imply a bi-linear behaviour and thus a non-linear model. Other aspects that could be included when executing a non-linear model are the friction coefficient on the connection stiffness and the non-linear behaviour of (cracked) reinforced concrete. However, one may argue whether this increased accuracy may lead to more meaningful results.

7.2 Second order effects

From the deformation analysis it follows that the horizontal displacement of the modular building is only significant in the parallel wind direction. As mentioned in the conclusions for the finite element modelling, a clear shear deformation profile along the height of the building can be noted. In order to verify the susceptibility of the modular building configuration, critical buckling load can be determined to obtain the magnification factor for second order effects.

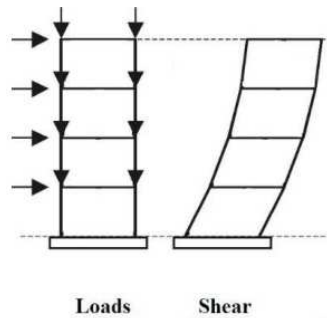


Figure 75 - Shear deformation profile

When the building would be modelled as a rigidly connected column with a certain shear stiffness K_s , the maximum deflection at the top would be the following.

$$u = \frac{q \cdot l^2}{2 \cdot K_s}$$

Since the deformation at the top of the modular building follows from the finite element results and the distributed load can be taken as the average distributed load over the height of the building, the shear stiffness can be obtained as follows.

$$K_s = \frac{q \cdot l^2}{2 \cdot u} = \frac{\frac{355,44}{(8 \cdot 2,9)} (8 \cdot 2,9^2)}{2 \cdot 0,042} = 98164 \text{ kN}$$

The critical buckling load for a shear column, as shown in paragraph 3.3.2, is as follows.

$$P_{cr} = 2 \cdot K_s = 2 \cdot 98164 = 196330 \text{ kN}$$

Subsequently the critical buckling load can be divided by the total factored vertical load for 8 modules on top of each other to obtain the ratio n .

$$n = \frac{P_{cr}}{F_{v,Ed,max}} = \frac{196330}{15980} = 11,7$$

In which the total factored vertical load, should correspond to the combination for extreme wind loads, so all the imposed floor loads should be multiplied by ψ_0 .

$$F_{v,Ed,max} = 1,2 \cdot F_G + 1,5 \cdot \psi_0 \cdot F_Q = 1,2 \cdot 11560 + 1,5 \cdot 0,4 \cdot 3530 = 15980 \text{ kN}$$

Finally, the magnification factor can be determined as follows.

$$\frac{n}{n-1} = \frac{12,3}{12,3-1} = 1,09 < 1,1 \quad \text{OK}$$

From the magnification factor it follows that the second order effects are smaller than 10%. This means that second order effects do not have to be considered for this building configuration. It can be concluded that despite the relatively low shear stiffness in parallel wind direction, due to the relatively low selfweight of the (timber) building, the factored vertical load is sufficiently small compared to the critical buckling load.

For a configuration with 2nd order effects bigger than 10%, the corresponding ratio n would be smaller than 11. By using the critical buckling load as calculated, the maximum factored vertical load, for which 2nd order effects do not have to be taken into account, results in the following.

$$F_{v,Ed,max} = \frac{P_{cr}}{n} = \frac{196330}{11} = 17850 \text{ kN}$$

For a configuration of 9 modules in height, the factored vertical load results in 17940 kN, which implies that for building higher than 8 modules, an additional load from 2nd order effects should be accounted for.

7.3 ULS verifications

As mentioned before, the verifications in ultimate limit state are performed to verify whether the resistance of the structure and its components is higher than the impact from the governing load combinations. In this paragraph a distinction is made between the parallel and perpendicular wind load situation, for which respectively the stabilization wall and side wall is treated. For the modules at the bottom of the building, the following basic situations that have to be verified in the following paragraphs

7.3.1 Parallel wind direction – stabilization wall

In the situation with wind loads directed parallel to the building, only the stabilization walls are responsible for transferring the horizontal loads as a result from only wind and notional loads. Since the vertical load from selfweight and variable floor loads is carried completely by the side walls of the module, no positive effect (e.g. friction) from vertical loads is present. Therefore, the loads on the side walls can be considered as short term loads ($k_{\text{mod}} = 0,9$). Additionally, the horizontal loads in parallel direction are assumed to be equally distributed over the number of modules next to each other (as justified further on in paragraph 7.1.4). Figure 76 shows components for which the resistances are determined in the following.

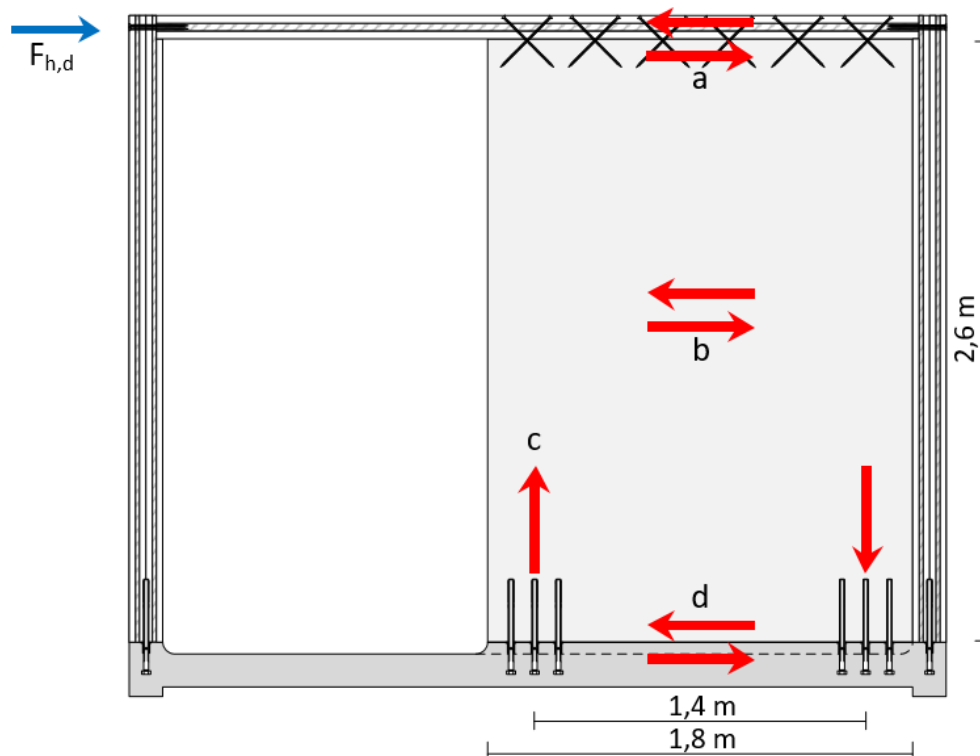


Figure 76 - ULS checks for stabilization wall

First, the shear resistance for the screwed connection of the ceiling to wall connection (a) will be determined, then the shear capacity of the CLT stabilization wall (b). Subsequently, the resistance of the glued-in rod with bolt anchor connection in tension (c) and finally the shear resistance of the glued-in rod with bolt anchor (d) for the wall to floor connection.

The horizontal design load that has to be resisted by the stabilization wall is calculated below. Which is the wind load F_w on top of the bottom module taken from Table 31 and divided by 8 modules in a row and the notional horizontal load of 7 modules on top, multiplied by the variable load factor.

$$F_{h,d} = 1,5 \cdot \left(\frac{F_w}{8} + F_{notional} \cdot 7 \right) = 1,5 \cdot \left(\frac{262}{8} + 1,66 \cdot 7 \right) = 1,5 \cdot 44 = 66 \text{ kN}$$

7.3.1.1 Screws ceiling - wall shear connection resistance (a)

To determine the shear resistance of the crossed screw pairs that connect the ceiling with the stabilization wall, the k-factor method as described in paragraph 4.10.2.3 has been used. The axial (reference) strength of an 8 mm screw under an angle of 45° in the (weakest) narrow face of the stabilization wall is as follows.

$$f_{ax,ref,k} = 0,013 \cdot \rho_{ref,k}^{1,11} \cdot d^{-0,33} = 0,013 \cdot 350^{1,11} \cdot 8^{-0,33} = 4,36 \text{ N/mm}^2$$

$$f_{ax,k} = k_{ax,k} \cdot k_{sys,k} \cdot f_{ax,ref,k} \cdot \left(\frac{\rho_k}{\rho_{ref,k}} \right)^{k_p} = 1,00 \cdot 1,00 \cdot 4,36 \cdot \left(\frac{350}{350} \right)^{1,10} = 4,36 \text{ N/mm}^2$$

Subsequently, the axial resistance of this screw for a (conservative) penetration length of the ceiling thickness into the stabilization wall can be calculated.

$$R_{ax,k} = f_{ax,k} \cdot d \cdot \pi \cdot l_{eff} = 4,36 \cdot 8 \cdot \pi \cdot 99\sqrt{2} = 15,34 \text{ kN}$$

The lateral (shear) resistance of a crossed screw pair results in the following.

$$R_{lat,pair,k} = 2 \cdot \sin \alpha \cdot R_{ax,k} = 2 \cdot \sin 45 \cdot 15,34 = 21,70 \text{ kN}$$

Multiplying this value with the effective number of crossed screw pairs results in the following characteristic and design (lateral) shear resistance of the connection.

$$R_{screws,lat,k} = n^{0,9} \cdot R_{lat,pair,k} = 6^{0,9} \cdot 21,70 = 108,84 \text{ kN}$$

$$R_{screws,lat,d} = k_{mod} \cdot \frac{R_{screws,lat,k}}{\gamma_M} = 0,9 \cdot \frac{108,84}{1,30} = 75 \text{ kN} > 66 \text{ kN} \rightarrow \text{OK}$$

7.3.1.2 CLT stabilization wall shear resistance (b)

Using the method described in paragraph 4.7.1, the shear resistance of the CLT stabilization wall has been calculated below. First the shear strength of the 142 mm thick element is calculated as the minimum of gross shear, net shear and torsional shear strength failure mechanisms.

$$f_{v,k} = \min \left\{ \begin{array}{l} 3,5 \\ 8 \cdot \frac{h_{net}}{h_{tot}} \\ 2,5 \cdot \frac{1}{6 \cdot h_{tot}} \cdot \sum_{i=1}^{n-1} \frac{b_i^2 + b_{i+1}^2}{b_{max}} \end{array} \right\} = \min \left\{ \begin{array}{l} 3,5 \\ 8 \cdot \frac{2 \cdot 17}{142} \\ 2,5 \cdot \frac{1}{6 \cdot 142} \cdot \frac{68,5^2 + 68,5^2}{68,5} \cdot 4 \end{array} \right\} = \min \left\{ \begin{array}{l} 3,5 \\ 1,92 \\ 1,61 \end{array} \right\} = 1,61 \text{ N/mm}^2$$

Then by multiplying this value with the shear surface area the characteristic and design shear resistances are obtained.

$$R_{v,k} = f_{v,k} \cdot A_s = 1,61 \cdot 142 \cdot 1800 \cdot 10^{-3} = 296 \text{ kN}$$

$$R_{v,d} = k_{\text{mod}} \cdot \frac{R_{v,k}}{\gamma_M} = 0,9 \cdot \frac{296}{1,25} = 213 \text{ kN} > 66 \text{ kN} \rightarrow \text{OK}$$

7.3.1.3 Glued-in rods wall – floor tension connection resistance (c)

Using the method described in paragraph 4.10.1.4 based on DIN 1052, the axial tension resistance of a M20 glued-in rod has been calculated below. First the bond line strength value is calculated based on an anchorage length l_a chosen as 320 mm, to ensure a relatively ductile failure of the steel rod.

$$f_{k,1,k} = \begin{cases} 4 & l_a \leq 250 \text{ mm} \\ 5,25 - 0,005 \cdot l_a & \text{for } 250 \leq l_a \leq 500 \text{ mm} \\ 3,5 - 0,0015 \cdot l_a & 500 \leq l_a \leq 1000 \text{ mm} \end{cases}, \text{ so } f_{k,1,k} = 3,65 \text{ N/mm}^2$$

The characteristic and design tension resistances are calculated below, with yielding of the steel rod as the governing failure mechanism.

$$R_{ax,k} = \min \left\{ f_{y,k} \cdot A_{ef} \right. \\ \left. \pi \cdot d \cdot l_a \cdot f_{k,1,k} \right\} = \min \left\{ 235 \cdot 245 \cdot 10^{-3} \right. \\ \left. \pi \cdot 20 \cdot 320 \cdot 3,65 \cdot 10^{-3} \right\} = \min \left\{ 57,58 \text{ kN} \right. \\ \left. 73,38 \text{ kN} \right\} = 58 \text{ kN}$$

$$R_{ax,d} = k_{\text{mod}} \cdot \frac{R_{ax,k}}{\gamma_M} = 0,9 \cdot \frac{57,58}{1,30} = 40 \text{ kN}$$

The three rods together have the following tension resistance.

$$R_{ax,GIR',d} = 3 \cdot R_{ax,d} = 3 \cdot 39,86 = 120 \text{ kN}$$

Assuming an internal lever arm of 1,5 m, results in the following maximum horizontal load on the module for the glued-in rods loaded in tension.

$$F_{ax,GIR',d} = \frac{z \cdot R_{ax,GIR',d}}{h} = \frac{1,5 \cdot 119,58}{2,6} = 69 \text{ kN} > 66 \text{ kN} \rightarrow \text{OK}$$

A M20 bolt anchor has a design tensile resistance of 90,7 kN (Halfen 2015), so the glued-in rod will be governing.

7.3.1.4 Glued-in rods wall – floor shear connection resistance (d)

To calculate the resistance of the glued-in rod laterally, the Johansen's theory has to be used. In order to do so, first the embedding strength and the yield moment of the rod is determined.

$$f_{h,0,k} = 0,082 \cdot (1 - 0,01 \cdot d) \cdot \rho_k = 0,082 \cdot (1 - 0,01 \cdot 20) \cdot 385 = 25,26 \text{ N/mm}^2$$

$$M_{y,k} = 0,3 \cdot f_u \cdot d^{2,6} = 0,3 \cdot 360 \cdot 20^{2,6} = 260676 \text{ Nmm}$$

The used Johansen's formulas are the formulas that correspond to a thick steel plate in single shear under the assumption that the concrete will behave like this compared to the relatively low embedding strength parallel to the grain. Due to the rods being glued-in parallel to the grain, a reduction factor of 0,10 has to be used for the embedding strength (Tomasi 2012). For the rope-effect, the characteristic axial resistance as calculated above is used.

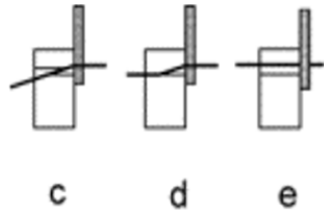


Figure 77 - Lateral failure mechanisms for glued-in rod

$$R_{v,k} = \min \left\{ \begin{array}{l} 0,1f_{h,k}t_1d \left[\sqrt{2 + \frac{4M_{y,Rk}}{f_{h,k}d t_1^2}} - 1 \right] + \frac{R_{ax,k}}{4} \\ 2,3 \sqrt{M_{y,Rk}0,1f_{h,k}d + \frac{R_{ax,k}}{4}} \\ 0,1f_{h,k}t_1d \end{array} \right. = \min \left\{ \begin{array}{ll} 21 & (c) \\ 23 & (d) \\ 16 & (e) \end{array} \right. = 16,17 \text{ kN}$$

As can be seen from Figure 77, the failure mechanism with only rod embedding is the governing failure mechanism, due to the relatively low embedding strength parallel to the fibre.

$$R_{v,d} = k_{mod} \cdot \frac{R_{v,k}}{\gamma_M} = 0,9 \cdot \frac{16}{1,30} = 11,19 \text{ kN}$$

The six rods together have the following shear resistance.

$$R_{v,GIR',d} = 6 \cdot R_{v,d} = 6 \cdot 11,19 = 67 \text{ kN} > 66 \text{ kN} \rightarrow \text{OK}$$

It can be concluded that the lateral resistance of the glued-in rod connection (d), is governing for the maximum horizontal load on the stabilization wall. This resistance can be directly linked to the wind-load on a single stabilization wall. The horizontal resistance of the stabilization wall can be compared to the horizontal loads of wind and notional load from imperfections, for different building configurations in terms of modular height and width.

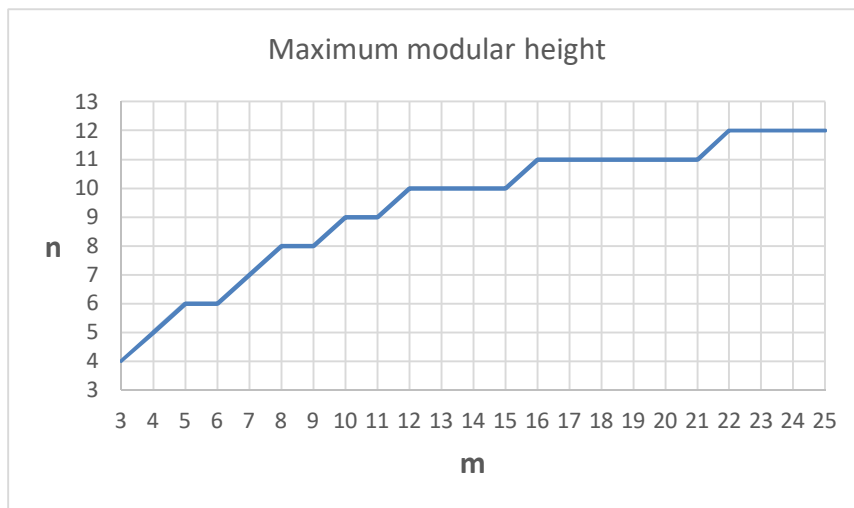


Figure 78 - Maximum number of modules in height (n) for a given modular width (m)

7.3.2 Perpendicular wind direction – side wall

In the situation with wind loads directed perpendicular to the building, the side walls are responsible for transferring both the horizontal loads as a result from wind and notional loads, as well as vertical loads from self-weight and imposed floor load. Contrary to the parallel direction, the loads per module can be divided by 2, since every module has 2 side walls. First the design loads are determined for the side walls as follows.

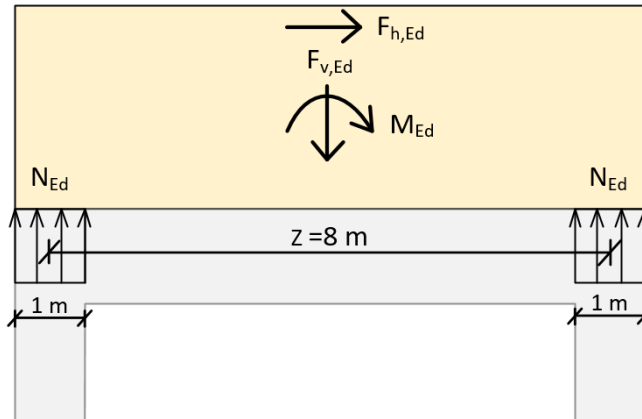


Figure 79 - Design loads for bottom module side wall

The horizontal design load is the wind load F_w on top of the bottom module taken from Table 30 and divided by 8 modules in a row and 2 side walls in a module and the notional horizontal load of 8 modules on top and multiplied with the variable design load factor.

$$F_{h,Ed} = 1,5 \cdot \left(\frac{F_w}{8 \cdot 2} + \frac{F_{notional} \cdot 8}{2} \right) = 1,5 \cdot \left(\frac{808}{8 \cdot 2} + \frac{1,66 \cdot 8}{2} \right) = 1,5 \cdot 57 = 86 \text{ kN}$$

The design bending moment at the interface of the bottom module and the podium structure, is the wind moment M_w at the top of the podium as taken from Table 30 together with the moment that results from notional horizontal forces, multiplied with the variable load factor. For the side wall the total wind moment can be divided by 8 modules and 2 side walls and the notional load for 8 modules can be divided 2 walls and multiplied by half the height of the stacked modules, to obtain the following design bending moment.

$$M_{Ed} = 1,5 \cdot \left(\frac{M_w}{8 \cdot 2} + \frac{F_{notional} \cdot 8}{2} \cdot \frac{8 \cdot 2,9}{2} \right) = 1,5 \cdot \left(\frac{10012}{8 \cdot 2} + \frac{1,66 \cdot 8}{2} \cdot \frac{8 \cdot 2,9}{2} \right) = 1,5 \cdot 703 = 1054 \text{ kNm}$$

The maximum vertical design load, to be used for the governing load combination, at the bottom module, is the sum of the factored line-load from selfweight and imposed floor load times the width of the module (9m). The factored selfweight load is the sum of 8 times the line-load for the module selfweight plus the line-load for the roof weight, times the permanent load factor. The factored variable load is 8 modules times the partial factor for office floors, times the imposed floor line-load, multiplied with the variable load factor of 1,5.

$$F_{v,Ed,max} = 9 \cdot (1,2 \cdot (8 \cdot q_G + q_{G,roof}) + 1,5 \cdot 8 \cdot \psi_0 \cdot q_Q) = 9 \cdot (1,2 \cdot (8 \cdot 9,79 + 1,91) + 1,5 \cdot 8 \cdot 0,4 \cdot 3,06) = 998 \text{ kN}$$

The minimum vertical design load is the same vertical design load from selfweight, but now with a load factor of 0,9 and without the imposed floor load.

$$F_{v,Ed,min} = 9 \cdot (0,9 \cdot (8 \cdot q_G + q_{G,roof})) = 9 \cdot (0,9 \cdot (8 \cdot 9,79 + 1,91)) = 650 \text{ kN}$$

To find out from which modular height tension forces will act between the modules in ULS, the contribution of the wind moment should exceed the contribution of the minimum vertical load from self-weight to N_{Ed} . It is only from 16 modules in height that tension forces will act between the modules as can be seen in the following formula.

$$N_{Ed,min} = -\frac{F_{v,Ed,min}}{2} + \frac{M_{Ed}}{z} = -\frac{1285}{2} + \frac{5180}{8} = -643 + 648 = 5 \text{ kN (tension)}$$

The horizontal shear resistance at the bottom wall of 8 stacked modules can be calculated by considering the static friction resistance, due to the minimum vertical load from self-weight as follows. The elastomer bearing strips have a static friction coefficient of $\mu_s = 0,7$ for both concrete and steel (thus assumed for timber as well).

$$F_{fr,h,Rd} = \mu_s \cdot F_{v,Ed,min} = 0,7 \cdot (9 \cdot 0,9 \cdot (8 \cdot q_G + q_{G,roof})) = 455 \text{ kN} < 86 \text{ kN}$$

The horizontal friction resistance is much higher than the maximum horizontal load under a bottom side wall and thus it can be stated that inter-modular horizontal shear forces are no critical criteria. This means as well, that the inter-modular connections are only necessary for position fixation and transferring horizontal forces to horizontal neighbouring modules, but not for transferring shear forces to vertically neighbouring modules.

7.3.2.1 Buckling

A critical design constraint can be the resistance against buckling of the side wall for the maximum vertical load in the modules at the bottom. For this failure mode, the side wall of the module that is unconstrained by any stabilization wall, is considered. The calculations to verify the critical wall against buckling, have been worked out in an excel spreadsheet in order to allow for parametric design concerning the height of the building. As already mentioned in the conclusion of the stress analysis in serviceability limit state, due to the arch-effect in the CLT side walls, the stresses will be highly concentrated above the columns of the podium structure. That is why the maximum vertical design load N_{Ed} is assumed to be concentrated in a one meter strip, above to column, as can be seen in Figure 79. The side wall of the bottom module is not loaded by its own module selfweight and imposed floor load, since the concrete floor is major contributor to the selfweight, which is at the bottom. That's why the vertical design load used for buckling is based on the remaining 7 modules on top as follows.

$$\begin{aligned} F_{v,Ed,max} &= 9 \cdot (1,2 \cdot (q_G + q_{G,roof}) + 1,5 \cdot 7 \cdot \psi_0 \cdot q_Q) \\ &= 9 \cdot (1,2 \cdot (7 \cdot 9,79 + 1,91) + 1,5 \cdot 7 \cdot 0,4 \cdot 3,06) = 877 \text{ kN} \end{aligned}$$

The maximum vertical design load N_{Ed} can be calculated as follows for 8 modules on top of each other, loaded by the vertical forces and perpendicular wind load.

$$N_{Ed} = \frac{F_{v,Ed}}{2} + \frac{M_{Ed}}{z} = \frac{877}{2} + \frac{1054}{8} = 439 + 132 = 570 \text{ kN}$$

In case of the fire situation, the maximum vertical design load can be calculated based on a load factor of 1 for the selfweight, $\psi_2=0,3$ for the imposed floor load and $\psi_1=0,2$ for the wind load. This leads to the following vertical load in case of fire.

$$N_{Ed,fire} = \frac{F_{v,Ed}}{2} + \frac{M_{Ed}}{z} = \frac{692}{2} + \frac{141}{8} = 346 + 18 = 364 \text{ kN}$$

This paragraph shows the method that is used to do the calculations concerning buckling for the maximum design load and the load in case of a fire situation, for 8 modules on top of each other. First, the effective second moment of inertia I_{eff} , that incorporates the shear effects of the cross-layers, will be calculated for both situations. Finally, the unity check for these two situations is shown for different building heights, in terms of the number of modules on top of each other (n). This is done to get more insight in which verifications are decisive and of relevance with an increasing building height.

Calculation I_{eff}

Analogously to paragraph 4.6.2, the effective second moment of inertia for a CLT panel with a thickness of 142 mm is calculated below. Because the fibres of the two layers in the middle are in the same direction, the panel can be considered as a 5-layered element instead of a 6-layered element.

Layer	Build-up h [mm]	Area A [mm ²]	Eccentricity a [mm]	2nd moment of area I [mm ⁴]	gamma factor	
					γ	formula
1	27	27000	57,50	1,64E+06	0,88	$(1 + \pi^2 \cdot E_{0,mean} \cdot A_1 \cdot h_2 / (G_R \cdot b \cdot l^2))^{-1}$
2	17	17000	35,50	4,09E+05	0,88	$(1 + \pi^2 \cdot E_{0,mean} \cdot A_2 \cdot h_3 / 2 / (G_R \cdot b \cdot l^2))^{-1}$
3	54	54000	0	1,31E+07	1,00	-
4	17	17000	35,50	4,09E+05	0,88	$(1 + \pi^2 \cdot E_{0,mean} \cdot A_4 \cdot h_3 / 2 / (G_R \cdot b \cdot l^2))^{-1}$
5	27	27000	57,50	1,64E+06	0,88	$(1 + \pi^2 \cdot E_{0,mean} \cdot A_5 \cdot h_4 / (G_R \cdot b \cdot l^2))^{-1}$

Table 41 - Calculation of gamma factors

The gamma factors are calculated using the $E_{0,mean} = 11000 \text{ N/mm}^2$, $G_R = 60 \text{ N/mm}^2$, $l_{buc} = 2,67 \text{ m}$, as the real values of the CLT. Using these factors, the effective second moment of inertia can be calculated as follows.

$$I_{y,eff} = I_1 + I_3 + I_5 + \gamma_1 \cdot A_1 \cdot a_1^2 + \gamma_3 \cdot A_3 \cdot a_3^2 + \gamma_5 \cdot A_5 \cdot a_5^2 = 1,73 \cdot 10^8 \text{ mm}^4$$

Similarly, this value can be calculated for the reduced cross-section of the wall panel after a 90 min. fire using a charring rate β_n of 0,70 mm/min. The remaining thickness of the panel is calculated below:

$$d_{eff} = d - (d_{char,n} + k_0 \cdot d_0) = d - (\beta_n \cdot t + k_0 \cdot d_0) = 142 - (0,70 \cdot 90 + 1 \cdot 7) = 72 \text{ mm}$$

The residual cross section of the CLT is that is left is (27-17-27-1), results in exactly one symmetric half of the original cross section, because the 1 mm that's left of the partly burned layer may not be considered in the verifications. The same method is used for the remaining 3-layered element to calculate the effective second moment of area, which results in the following.

$$I_{y,eff,fi} = I_1 + I_3 + \gamma_1 \cdot A_1 \cdot a_1^2 + \gamma_3 \cdot A_3 \cdot a_3^2 = 2,77 \cdot 10^7 \text{ mm}^4$$

The side wall of a module is modelled as a panel with a width of 1 m, with a hinged support at the top and the bottom of the panel. This implies that the buckling length (l_{buc}) is the same as the height of the timber wall, namely 2,67 m and 2,90 m in case of a module with a concrete and timber wall, respectively.

Buckling verification

First, the instability factor is calculated using the strength and stiffness values as well as the imperfection coefficient (β_c) of glued laminated timber (GL24c), that may be used according to the technical approvals concerning CLT.

- $f_{c,0,k} = 24 \text{ N/mm}^2$
- $E_{0,05} = 9100 \text{ N/mm}^2$
- $\beta_c = 0.1$

In Table 42 it is demonstrated how the instability factor is calculated for the original cross-section of the CLT wall ($t = 142 \text{ mm}$) for ultimate limit state verifications and for the reduced cross-section ($t = 71 \text{ mm}$) to perform verifications in case of a fire situation. The more instability, the lower the instability factor.

Parameter	Formula/symbol	ULS	Fire	
Net area	A_{net}	108000	54000	mm ²
Effective second moment of area	I_{eff}	1,76E+08	2,80E+07	mm ⁴
Radius of gyration	$i = \sqrt{\frac{I_{0,eff}}{A_{0,net}}}$	40	23	mm
Slenderness	$\lambda = \frac{l_{buc}}{i}$	66	116	-
Relative slenderness ratio	$\lambda_{rel} = \frac{\lambda}{\pi} \cdot \sqrt{\frac{f_{c,0,k}}{E_{0,05}}}$	1,07	1,90	-
Buckling coefficient	$k = 0,5 \cdot (1 + \beta_c \cdot (\lambda_{rel} - 0,3) + \lambda_{rel}^2)$	1,11	2,39	-
Instability factor	$k_c = \frac{1}{(k + \sqrt{k^2 - \lambda_{rel}^2})}$	0,71	0,26	-

Table 42 - Calculation of instability factor k_c

Once the instability factor is calculated, the verifications of the wall can be performed. Below in Table 43, this is done for the modular building with 8 modules on top of each other. The vertical design force is the design load N_{Ed} as calculated before on the lowest module wall for a one meter strip width at the end of the wall. The same holds for the fire situation. Apart from the different load combinations for the different design situations, more favourable partial factors hold for the fire situation.

Parameter	Formula/symbol	ULS	Fire	
Vertical force	N_{ed}	570	364	kN
Conversion coefficient	k_{fi}	1	1,15	-
Load duration factor	k_{mod}	0,8	1	-
Partial safety factor	γ_M	1,25	1	-
Design stress	$\sigma_{c,0,d} = \frac{N_{ed}}{A_{net}}$	5,28	6,73	N/mm ²
Design strength	$f_{c,0,d} = \frac{f_{c,0,k} \cdot k_{mod} \cdot (k_{fi})}{\gamma_M}$	15,36	27,60	N/mm ²
Unity check	$UC = \frac{\sigma_{c,0,d}}{k_c \cdot f_{c,0,d}}$	0,49	0,94	-

Table 43 - Verification of wall against buckling for n=8

The results of the unity checks are below 1 for both situations in case of 8 modules on top of each other, which means that the building meets with the requirements of buckling. To gain more insight in the susceptibility of the building to buckling, the unity-check results with increasing building height are presented in Figure 80. For the blue line, buckling check for the maximum vertical load in ultimate limit state, the non-linear effect of increased wind-moment, with building height is more visible since the wind load has a bigger portion on the vertical buckling design load (wind load reduced with ψ_1 factor of 0,2).

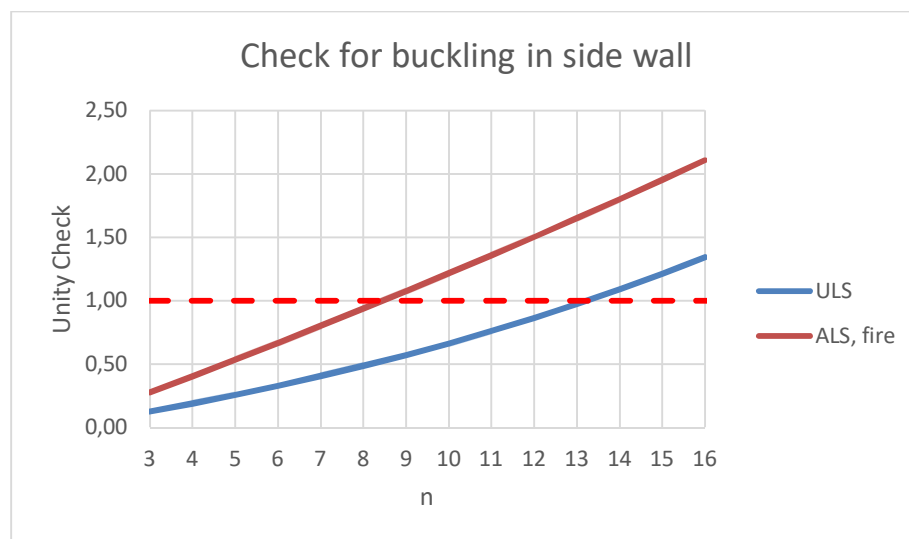


Figure 80 - Unity check for buckling of side wall with increasing building height

8 Conclusions and recommendations

The main goal of this research was to investigate the aspects and limits for stacking CLT modules to prove the structural feasibility of an innovative multi-storey building solution that has a multi-purpose applicability. This chapter deals with the conclusions that can be drawn to answer the research questions formulated to achieve the goal. First the sub research question will be answered after which the conclusions to the main question will be given.

- *Which practical and structural aspects play a role in multi-storey modular buildings made from timber?*

Multi-storey (cross-laminated) timber buildings have been successfully applied in several modern projects over the last 10 years, including one with CLT modules stacked in layers of 4 modules in height. Aspects that are proof of potential, are high building speed and sustainability ratings. Research resulted in the following critical structural aspects for multi-storey modular timber buildings.

- Deformations and connections

Due to the high strength to weight ratio of timber, the control of horizontal deformations is a critical aspect which needs to be addressed by appropriate design of the connections.

- Fire safety

Dutch legislation requires a fire resistance of 120 minutes, which can in general be decreased to 90 minutes by the use of a sprinkler installation. Unprotected timber, as a combustible material, needs to be designed with an additional 'sacrificing' thickness, to allow for charring of the cross-section.

- Inaccuracies and imperfections

Inaccuracies and imperfections due to the manufacturing process as well as during installation of modules, need to be accounted for by considering additional notional horizontal forces.

- 2nd order effects

With increasing modular height and deformation, the vulnerability to 2nd order effects need to be investigated and if so, incorporated by a magnification factor.

- Robustness

The robustness of multi-storey modular structures needs to be addressed to prevent progressive collapse. The inter-modular connections need to have sufficient resistance against tying forces.

- *What are the properties and calculation methods of cross-laminated timber elements?*

The main beneficial properties of using CLT as a building material are the high and accurate degree of prefabrication to allow for high building speed, high dimensional stability. Due to the high strength and stiffness properties in multiple directions to achieve diaphragm action, CLT elements are particularly suitable for applications in cellular and modular buildings. The material properties and calculation methods for CLT are currently not covered by the Eurocode. Therefore, the calculation methods presented are based on literature and form a guideline to verify CLT structures.

- *Which connection types are suitable for an application in the CLT modules and how can the modules be connected to each other?*
 - *What practical issues are of importance for the connections?*
 - *What is the strength and stiffness of the connections when applied in CLT?*

Screwed connections are commonly used and very suitable to connect CLT elements to each other, due to simplicity and low cost and high strength and stiffness if designed properly. To connect CLT to concrete, glued-in rods are very suitable, due to high strength and stiffness. Both are hidden connections which is beneficial from an esthetical viewpoint as well as the protection against fire.

- Screws

Investigation into screws revealed relatively high axial compared to lateral strength and stiffness's, so crossed screw pairs are advisable. Realistic strength and stiffness values for CLT elements are based on a recent published k-factor method which is based on axial withdrawal and incorporates the effects of screw angle, gaps in CLT and the system effect of penetrating multiple layers.

- Glued-in rods

For glued-in rods it became clear that they should be dimensioned to ensure ductile failure of the rod. Glued-in rods are currently not covered by the Eurocode, so the strength resistance is based on DIN 1052 and stiffness values as input for the finite element modelling are based on reference research.

- Inter-modular connections

There is no standard connection available to connect individual modules to each other. Therefore an option could be a custom T-shaped angle profile with pins are used, which account for implications considering the stacking sequence of the modules.

- *How can a universally applicable cross-laminated timber module be designed for which the stability can be guaranteed in order to ensure a self-supporting system of modules?*

To prevent high compression stresses perpendicular to the grain, continuous walls can be used to achieve a balloon type behaviour. By applying an internal stabilization wall, open façades are created and horizontal loads can be taken. In stacking the modules on top of each other, elastomer bearing strips should be placed between the contact area of the side walls and the concrete floor to transfer and distribute the bearing loads and to minimize transfer of sound and vibrations.

- *What are the properties and what is a suitable modelling design to set up a useful finite element model of a building configuration consisting of CLT modules?*

The properties and suitable modelling design for a useful finite element model of a CLT modular building depend on the required accuracy and the finite element program used (in this case AxisVM). The finite element model made, is based on a linear elastic calculation method. AxisVM doesn't allow the input of a complete stiffness matrix for in-plane and out-of-plane stiffness's. Next to that, the shear stiffness is automatically calculated, which doesn't match the real CLT stiffness. Therefore, the bearing mechanism which is decisive for the deformation should be determined for every element individually to define fictitious stiffness's for realistic deformation results. Despite other finite

element packages might be more suitable for modelling CLT by inputting the total stiffness matrix, a useful model is obtained for determining force distributions and displacements.

- *What is the force distribution in a modular CLT building and what are the deformations that result from wind forces?*

The interaction between the CLT side walls and the deformation of the podium beams, revealed the development of an arch-effect in the CLT side walls due to the high in-plane CLT stiffness. This effect is very beneficial in preventing tension stresses between the modules, since the inter-modular connections are not designed for tension.

From the deformation results following from the finite element modelling, it can be concluded that the horizontal deformation is only relevant for wind directed parallel to the building, involving the stabilization wall. The contributions of the mechanisms responsible for this deformation are elaborated and expressed in percentages. The major contribution (75%) is rotation of the stabilization wall, due to bending of the concrete floor and the ceiling. Based on this modelling method in AxisVM for an 8 x 8 composition an effective concrete stiffness of 16000 N/mm² would be needed to achieve compliance with the maximum horizontal deformation requirements.

After calculating the 2nd order effects based on the investigated modular configuration and a pure shear deformation profile, it appeared that the magnification factor is below 1,1 and thus, 2nd order effects do not have to be taken into account according to the standards. For modular configurations higher than 8 modules, additional loads as a result of 2nd order effects have to be accounted for.

- *What are the governing resistance capacities of CLT modules and which maximum modular height can be achieved for the designed modules?*

- Horizontal resistance stabilization wall

For the resistance of the stabilization wall, the lateral shear strength of the glued-in rods is the governing failure mechanism. Subsequently, a maximum modular height in terms of minimum number of modules next to each other for a certain modular height, can be read from Figure 78.

- Buckling resistance of the side wall

Calculations concerning buckling behaviour of the side walls, based on vertical loads concentrated at a one meter strip at the end of the side wall, reveal that the fire situation is critical for a 142 mm thick wall and 8 modules on top of each other is the maximum modular height.

After answering the sub questions the following main research question can be answered.

- ***What is the structural behaviour of a cross-laminated timber module system, how can it be designed and is it possible to construct a 'self-supporting' system of modules for a tall timber building?***

First of all, yes, it is possible to construct a 'self-supporting' system of modules for a tall timber building. How it can be designed has been shown by the basic case design configuration of 8 modules in height and 8 modules in width. This design is based on high strength and stiffness connections using glued-in rods and crossed screw pairs and continuous walls to prevent high compression stresses perpendicular to the grain. The structural behaviour of a cross-laminated timber module system, can be characterized by the very strong and stiff in-plane behaviour of CLT elements and the following behaviour for different wind directions.

- Parallel wind direction

High rotation of the stabilization walls, largely due to bending in the concrete floor and ceiling.

- Perpendicular wind direction

Prevention of tensile stresses between the modules due to the arch effect of side walls in relation to the podium structure.

Limits

To end with, the investigation into the aspects that limit the maximum height and minimum slenderness for a modular cross laminated timber building, as was the main goal, resulted in the following aspects found:

- Fire safety

Based on the used method for calculation of buckling stresses located in a one meter strip at the end of the side walls, the fire situation limits the modular height at 8 storeys for the used wall thickness and CLT layer build-up.

- Connections

Based on this module design, the lateral GIR resistance governs the resistance capacity against wind parallel to the building.

- Deformations

Based on this module design and modelling technique, deformations mainly due to bending in the floor and ceiling elements, limits the slenderness for 8 modules in height to 8 modules in width.

Recommendations

This chapter deals with the improvements that can be made if the following aspects are further investigated.

- The influence of using a rib (strip with increased thickness) under the concrete slab on the decrease of rotation of the stabilization wall as a result of parallel wind forces. Possibly non-linear finite element modelling can be applied to investigate this effect. Other improvements implying non-linear modelling are stated in paragraph 7.1.6.
- In this research the podium structure is assumed to be infinitely stiff, except for the podium beams. To incorporate the horizontal stiffness and the stiffness of the foundation piles more information is needed but more detailed deformation behaviour could be obtained.
- Further research can be performed on the building costs of this construction method compared to other modular buildings, other timber buildings or to conventional building solutions. In order to proof the success of this building type, cost effectiveness plays a major role.
- In this study, modules with prefabricated concrete floors have been investigated, due to the increased sound and vibration performance and positive effects of self-weight. Further research can be put into the possibilities and implications of using a CLT floor in the modules.
- Concerning the sound and vibration performance, a research study or tests would be helpful to proof the required minimum levels of transmission.
- More research has to be done to investigate the effect of fire onto the connection system. Possibly the position of the glued-in rods and/or screws should move more to the outside of the module. One can argue whether this consideration would be helpful, other than complying with the requirements set by legislation when progressive collapse is not considered. This brings up to the next aspect of further research, namely, what are the capacities of the inter-modular connections in relation to progressive collapse. How can the inter-modular connections be designed to provide the robustness to carry the vertical loads of modules if a corner or internal module burns down.
- In this study the modules are designed and verified based on maximum load in the bottom modules. There is potential to optimise the modules, since the loads are smaller with increasing building height.

9 References

- Abrahamsen, R.B., and K.A. Malo. 2014. *Structural design an assembly of "Treet"- A 14-storey timber residential building in Norway*. World Conference on Timber Engineering.
- American Wood Council. 2001. *Details for conventional wood frame construction*. Washington: American Forest & Paper Association.
- Arch daily. 2016. *Architecture Daily*. 19 May. <http://www.archdaily.com/787698/50-modular-timber-apartments-ppa-architectures>.
- Barber, D., and R. Gerard. 2015. "Summary of the fire protection foundation report - fire safety challenges of tall wood buildings." *Fire Science Reviews* 1-15.
- Bathon, L., and O. Bletz. 2008. "In holz eingeklebte Verbindungsmittel aus Metall." *Holzbau* Issue 2 13-18.
- Bogensperger, T., G. Silly, and G. Schickhofer. 2012. *Comparison of methods of approximate verification procedures for cross laminated timber*. Research Report, Graz: holz.bau forschungs gmbh.
- Bogensperger, T., M. Augustin, and G. Schickhofer. 2011. "Properties of CLT-Panels Exposed to Compression Perpendicular to their Plane." *CIB-W18 Meeting 44*. Alghero, Italy: Holz.bau forschungs gmbh.
- Bogensperger, T., M. Augustin, and G. Schickhofer. 2011. *Properties of CLT-Panels Exposed to Compression Perpendicular to their Plane*. Graz: Institute for Timber Engineering and Wood Technology TU Graz.
- Bogensperger, T., T. Moosbrugger, and G. Silly. 2010. "Verification of CLT-plates under loads in plane." Riva del Garda, Italy: WCTE.
- Brandner, R. 2013. *Production and Technology of Cross Laminated Timber (CLT)*. A state-of-the-art Report, Graz, Austria: Institute of Timber Engineering and Wood Technology, Graz University of Technology.
- Brandner, R., and G. Schickhofer. 2014. "Properties of Cross Laminated Timber (CLT) in Compression Perpendicular to Grain." *1st INTER-Meeting*. Bath.
- Brandner, R., G. Flatscher, A. Ringhofer, G. Schickhofer, and A. Thiel. 2016. "Cross laminated timber (CLT): overview and development." *European Journal of Wood and Wood Products* 1-21.
- Brandner, R., P. Dietsch, J. Dröscher, M. Schulte-Wrede, H. Kreuzinger, M. Sieder, G. Schickhofer, and S. Winter. 2015. "Shear properties of Cross Laminated Timber (CLT) under in-plane load: Test Configuration and Experimental Study." *2nd INTER-Meeting*. Sibenik.
- Brandner, R., T. Bogensperger, and G. Schickhofer. 2013. *In plane Shear Strength of Cross Laminated Timber (CLT): Test Configuration, Quantification and influencing Parameters*. Graz: Graz University of Technology, Competence Centre holz.bau forschungs gmbh.

- Brandt, G.A., J.J. Blok, H.P. Houtman, E.A. Zwaanswijk, L. Zwetheul, L. Verboom, and A.J. Jeurdink. 2014. *Klemconstructies op palen Stubeco studiecel A 1 2/2*. Gouda: Studievereniging Uitvoering Betonconstructies (Stubeco).
- Breunese, A., and I.J. van Straalen. 2014. "Lecture sheets CIE 5131: Fire safety design." Delft: TNO and Efectis.
- Breunese, A.J., and J. Maljaars. 2015. *Fire Safety Design Course reader CIE5131*. Delft: Delft University of Technology.
- Brinck, T. 2013. "Wolkenkrabbers van hout. Mooi en duurzaam?" *Wattisduurzaam.nl*, 17 July.
- Buchanan, A. 2000. "Fire performance of timber construction." *Progress in Structural Engineering and Materials* Issue 3 278-289.
- Buchanan, A.H., and D.J. Barber. 1996. "Fire resistance of epoxied steel rods in glulam timber." *NZ Timber Design Journal* 12-18 Issue 2 Volume 5.
- Campbell-Dollaghan, K. 2016. "Can Timber Skyscrapers Really Help Save The Planet?" *Fastcodesign*, 18 May.
- CEN/TC 124. 3013. "EN 16351." Brussels: European committee for standardization.
- Chans, D.O., J.E. Cimadevila, and E.M. Gutiérrez. 2013. "Withdrawal strength of threaded steel rods glued with epoxy in wood." *International Journal of Adhesion & Adhesives* Issue 44 115-121.
- Crielaard, R. 2015. *Self-extinguishment of cross-laminated timber*. Master thesis report, TU Delft.
- Deutsches Institut für Bautechnik. 2010. "European Technical Approval ETA-10/0241." *LenoTec*. Berlin: Finnforest Merk GmbH.
- Dias, A.M.P.G. 2005. "Mechanical behaviour of timber-concrete joints." Dissartation, Delft.
- DIN 1052. . "Entwurf, Berechnung und Bemessung von Holzbauwerken - Allgemeine Bemessungsregeln und Bemessungsregeln für den Hochbau." Berlin: Deutsches Institut für Normung.
- Dundar, C., and I.F. Kara. 2007. "3D analysis of RC frames using effective-stiffness models." Adana, Turkey: Department of Civil Engineering, Cukurova University.
- Espinoza, O., V.R. Trujillo, M.F.L. Mallo, and U. Buehlmann. 2016. "Cross-Laminated Timber: Status and Research Needs in Europe." *BioResources* 11, 281-295.
- Flaig, M., and H. J. Blaß. 2013. "Shear strength and shear stiffness of CLT-beams loaded in plane." *CIB-W18/46-12-3*. Vancouver, Canada.
- Flatscher, G., K. Bratulic, and G. Schickhofer. 2014. "Screwed joints in cross laminated timber structures." Quebec: World Conference on timber engineering.

- Frangi, A. 2013. "Tragverhalten und Bemessung von Verbindungen im Brandfall." *Internationales Holzbau-Forum*. Zürich: ETH Zürich.
- Frangi, A., M. Fontana, and M. Knobloch. 2007. "Fire Design Concepts for Tall Timber Buildings." *Structural Engineering International* 148-155.
- Frangi, A., M. Fontana, M. Knobloch, and G. Bochicchio. 2008. "Fire behaviour of Cross-Laminated Solid Timber Panels." *Fire safety science* 9. Zurich: Trees and Timber Institute CNR-IVALSA.
- Frangi, A., M. Knobloch, and M. Fontana. 2010. "Fire design of timber-concrete composite slabs with screwed connections." *Journal of structural engineering ASCE* 219-228.
- Frühwald, A. 2002. University of Hamburg. Centre for Wood Science and Technology.
- Gavric, I., M. Fragiaco, and A. Ceccotti. 2015. "Cyclic Behavior of CLT Wall Systems: Experimental Tests and Analytical Prediction Models." *Journal of Structural Engineering* Volume 141, Issue 11.
- Getzner. 2015. *Solid timber apartment building by Meickl*. Case study report, Bürs, Austria: Getzner Engineering a quiet future.
- Gonzales, E., T. Tannert, and T. Vallee. 2016. "The impact of defects on the capacity of timber joints with glued-in rods." *International Journal of Adhesion & Adhesives* Issue 65 33-40.
- Green, M.C. 2012. *The case for tall wood buildings*. Vancouver: mgb Architecture and Design.
- Halfen. 2015. "Deha spherical head lifting anchor system." Langenfeld, Germany: Halfen.
- Hoenderkamp, J.C.D. 2002. "Critical loads of lateral load resisting structures for tall buildings." *The Structural Design of Tall Buildings* 221-232.
- Hoenderkamp, J.C.D. 2002. "Kritische belastingen van stabiliteitselementen." *Bouwen met Staal* 46-52.
- Hummel, J., G. Flatscher, W. Seim, and G. Schickhofer. 2013. "CLT Wall Elements Under Cyclic Loading - Details for Anchorage and Connection." *European Conference on Cross Laminated Timber (CLT) - Focus Solid Timber Solutions*. Graz: University of Bath. 152-165.
- Inter-CAD Kft. 2015. "User's Manual AxisVM13 Finite Element Analysis & Design Program." Budapest: Inter-CAD Kft.
- Jiang, X., K. Tanaka, and M. Inoue. 2012. "Strength properties of GIR (Glued-in-Rod) Joint System Subjected to Shearing and Tensile Force." *International Conference on Biobase Material Science and Engineering*. Changsha, China: IEEE. 297-301.
- Jöbstl, R., and G. Schickhofer. 2007. "Comparative examination of creep of GLT- and X-Lam-slabs in Bending." *Timber Structures*. Working Commission W18.
- Jöbstl, R.A., T. Bogensperger, G. Schickhofer, and G. Jeitler. 2008. "In-plane shear strength of cross laminated timber." St. Andrews, Canada: CIB-W18/41-12-3.

- Jorissen, A., and A.J.M. Leijten. 2008. "Tall Timber Buildings in The Netherlands." *Structural Engineering International* 133-136.
- Karacabeyli, E., and B. Douglas. 2013. *CLT Handbook*. Pointe-Claire: FPInnovations.
- KLH Massivholz GmbH. 2012. *Bemessung nach Eurocode 5*. Katsch an der Mur: KLH.
- Knauf, M., M. Köhl, V. Mues, K. Olschofsky, and A. Früwald. 2015. "Modeling the CO₂-effects of forest management and wood usage on a regional basis." *Carbon Balance and Management*. Bielefeld: Springer. 12.
- Koets, R.J. 2012. *Hoogbouw met Cross Laminated Timber*. Afstudeerrapport, Eindhoven: Technische Universiteit Eindhoven.
- Kollár, L.P. 2008. "Second Order Effects on Building Structures - an Approximate Evaluation." *Creating and Renewing Urban Structures*. Chicago: 17th Congress of Iabse. 1-8.
- Larsen, H.J., and J. Munch-Andersen. 2011. "The sad storey of glued-in bolts in Eurocode 5." *Proceedings of the CIB-W18 A review of meetings I-43*. Danish Timber Information. Part 6: Essays 51-55.
- Lawrence, A. 2014. "Recommendations for the Design of Complex Indeterminate Timber Structures." In *Materials and Joints in Timber Structures; Recent developments of Technology*, by S. Aicher, H. Reinhardt and H. Garrecht, 129-134. Stuttgart: Springer.
- Lawson, M., R. Ogden, and C. Goodier. 2014. *Design in Modular Construction*. Boca Raton: CRC Press.
- Lawson, R., and J. Richards. 2010. "Modular design for high-rise buildings." *Structures and Buildings* 163 Issue SB3 151-164.
- Lawson, R., M. Byfield, S. Popo-Ola, and P. Grubb. 2008. "Robustness of light steel frames and modular construction." *Structures & Buildings* 161 Issue SB1 3-16.
- MERK Timber GmbH. 2013. "LENO Cross Laminated Timber (CLT)." Aichach, Germany: Merk Timber GmbH.
- Moneo, S. 2015. *Associations weigh in on wood building*. 23 April. <http://journalofcommerce.com/Associations/News/2015/4/Associations-weigh-in-on-wood-building-1007098W/>.
- NEN. 2012. *Convenant high-rise buildings*. Delft: Nederlands normalisatie instituut.
- New Steel Construction. 2016. "Hybrid modular systems using a steel-framed podium." *NSC*. 5 January. <http://www.newsteelconstruction.com/wp/hybrid-modular-systems-using-a-steel-framed-podium/>.
- Nijse, R. 2013. *Dictaat Draagconstructies I*. Delft: TU Delft, Faculteit Bouwkunde.

- Parida, G., H. Johnsson, and M. Fragiaco. 2013. "Provisions for Ductile Behavior of Timber-to-Steel Connections with Multiple Glued-In Rods." *Journal of Structural Engineering - ASCE* 1438-1477.
- Park, J-S., A.H. Buchanan, and J-J. Lee. 2006. "Fire Performance of Laminated Veneer Lumber (LVL) with Glued-in Steel Rod Connections." *Journal of Fire Sciences* 27-46.
- Porteous, J., and A. Kermani. 2013. *Structural Timber Design to Eurocode 5*. West Sussex: John Wiley & Sons.
- Ravenshorst, G.J.P. 2014. "Lecture sheets: CIE 5124 Timber Structures II." *Fire Safety in Timber Buildings*. Delft: TU Delft.
- Ringhofer, A., R. Brandner, and G. Schickhofer. 2013. "Withdrawal resistance of self-tapping screws in unidirectional and orthogonal layered timber products." *Materials and Structures* Issue 48: 1435-1447.
- Ringhofer, A., R. Brandner, G. Flatscher, and G. Schickhofer. 2015. "Axial beanspruchte Holzschrauben in Vollholz, Brettschichtholz und Brettspertholz." *Bautechnik* Volume 92, Issue 11, 770-782.
- Rothoblaas. 2012. "European Technical Approval ETA-11/0030." *Self-tapping screws for use in timber structures*. Charlottenlund, Denmark: European Organisation for Technical Approvals.
- Rothoblaas. 2014. *Plates and connectors for wood*. Brochure, Cortaccia: Rothoblaas.
- Search. 2014. "Hotel Jakarta tender submission." Amsterdam.
- Serrano, E. 2009. "Limnologen - Experiences from an 8- storey timber building." 15. *Internationales Holzbau-Forum* 1-12.
- Seventh framework programme. 2015. *Report on structural guidance; Development of modular construction systems for high-rise residential buildings*. Grant agreement Modcons Deliverable D1.6, SCI.
- SOM. 2013. *Timber Tower Research Project*. Research report, Chicago: Skidmore, Owings & Merrill, LLP.
- SP. 2010. *Fire safety in timber buildings*. Stockholm: Joint Research Centre and CEN TC 250/SC5 Technical Research Institute of Sweden.
- SPAX self-tapping screws. 2012. "European Technical Approval ETA-12/0114." *Self-tapping screws for use in timber structures*. Charlottenlund, Denmark: European Organisation for Technical Approvals.
- Spickler, K. 2014. "5 myths about cross-laminated timber." *Building Design + Construction*, 20 Februari.

- Steiger, R., E. Serrano, M. Stepinac, V. Rajcic, C. O'Neill, D. McPolin, and R. Widmann. 2015. "Strengthening of timber structures with glued-in rods." *Construction and Building Materials* 90-105 Volume 97.
- Stepinac, M., V. Rajcic, F. Hunger, J-W. van de Kuilen, R. Tomasi, and E. Serrano. 2013. "Comparison of design rules for glued-in-rods and design rule proposal for implementation in european standards." Vancouver: International council for research and innovation in building and construction.
- Thiel, A., and G. Schickhofer. 2010. "CLT designer - A software tool for designing CLT elements: 1D-plate-design." Graz: World conference on timber engineering.
- Thompson, Weber. 2013. "Tall wood buildings have a promising future with CLT." *Weber Thompson*. 19 June. <http://www.weberthompson.com/blog/2013/06/tall-wood-buildings-have-a-promising-future-with-clt/>.
- Thustochowicz, G. 2011. *Stabilising System for Multi-Storey Beam and Post Timber Buildings*. Doctoral Thesis, Luleå Sweden: Luleå University of Technology.
- Thustochowicz, G., E. Serrano, and R. Steiger. 2011. "State-of-the-art review on timber connections with glued-in steel rods." *Materials and Structures* Volume 44, Issue 5, pp 997-1020.
- Tomasi, R. 2012. "Research into glued-in rods at University of Trento." Wroclaw, Poland: Cost actions FP1004 & FP1101.
- Trada. 2009. *Case Study: Stadthaus, Murray Grove, London*. Buckinghamshire: Trada Technology Ltd.
- Tropical Timber. 2011. *Tropical Timber & Co Environment*. http://www.tropicaltimberco.com/page_143.htm.
- Uibel, T., and H. Blaß. 2007. *Joints with Dowel Type Fasteners in CLT Structures*. Karlsruhe: Karlsruhe Institute of Technology.
- Uibel, T., and H.J. Blaß. 2007. "Edge joints with dowel type fasteners in cross laminated timber." *Working Commission W18-Timber Structures*. Bled, Slovenia: International Council for Research and Innovation in Building and Construction.
- Unterwieser, H., and G. Schickhofer. 2013. "Characteristic Values and Test Configurations of CLT with Focus on Selected Properties." In *Focus solid timber solutions - European conference on cross laminated timber (CLT)*, by R. Harris, A. Ringhofer and G. Schickhofer, 53-73. Bath: University of Bath.
- Wallner-Novak, M., J. Koppelhuber, and K. Pock. 2014. *Cross-Laminated Timber Structural Design - Basic design and engineering principles according to Eurocode*. Graz: ProHolz Austria.
- Watts, A., and L. Helm. 2015. "Cross-laminated Timber: the Future of Building?" *Seattle Business*.
- Will+Perkins. 2014. *Survey of international tall wood buildings*. Vancouver: Forestry Innovation Investment.

Xu, B.H., A. Bouchaïr, and P. Racher. 1012. "Analytical study and finite element modelling of timber connections with glued-in rods in bending." *Construction and Building Materials* Issue 34 337-345.